# AN INVESTIGATION OF BLOWING AS A METHOD OF INCREASING THE MAXIMUM LIFT OF A DOUBLE-WEDGE AIRFOIL

Thesis by

John W. Bacon, Jr.

In Partial Fulfillment of the Requirements

for the Degree of Aeronautical Engineer

California Institute of Technology

Pasadena, California

June, 1949

## ACKNOWLEDGMENTS

The author wishes to express his appreciation to Mr. Henry T. Nagamatsu for his interest and guidance throughout these investigations.

Appreciation and gratitude are expressed to Mr. Peter Kyropolus for his unfailing generosity with equipment under his cognizance and to the men in the GALCIT machine shop for their good suggestions and assistance in the modifications necessary to adapt the model to the 10-foot wind tunnel.

Thanks is to be given to all the members of the GALCIT 10-foot wind tunnel crew who accomplished a major part of the running, computing, plotting, typing and blacklining of the report. Special thanks is given to Louis Schmidt and Ted Pounder for technical assistance, to Lewis Balthasar for assistance beyond the duties of his job, and to Barbara Killian who did most of the work on the figures.

The donation by Robert Bacon of a week-end of his time to fill in on the running crew is also acknowledged.

TABLE OF CONTENTS


| Part | Title | Page |
|---|---|---|
| | Index of Figures . . . . . | 1 |
| I. | Summary. . . . . | 5 |
| II. | Introduction . . . . . | 6 |
| III. | Notation . . . . . | 8 |
| IV. | Description of Experimental Set-Up . . . . . | 10 |
| V. | Test Procedure . . . . . | 12 |
| VI. | Experimental Results . . . . . | 13 |
| VII. | Accuracy . . . . . | 15 |
| VIII. | Conclusion . . . . . | 16 |
| IX. | References . . . . . | 17 |
| X. | Index of Runs. . . . . | 18 |

# INDEX OF FIGURES

## General

Page

Model Sketches

1. Three-View Sketch of Model . . . . . 27

2. Schematic Sketch of Air System and Method of Model Support . . . 28

## Experimental Results

Reynolds Number Effects

3. Reynolds Number Effects, Configuration S . . . . . 29

4. " " " , " " + $F_N$ . . . . . 30

5. " " " , " " + $F_S$ . . . . . 31

6. " " " , " " + $F_N$ + $F_S$ . . . . . 32

Maximum Lift Investigation with Blowing

15% Chord Slot Position

Wing Alone

7. Maximum Lift, Configuration $S_{15}$ + $B^2$ . . . . . 33

8. " " , " " + $B^4$ . . . . . 34

9. " " , " " + $B^7$ . . . . . 35

10. " " , " " + " . . . . . 36

11. " " , " " + " . . . . . 37

12. " " , " " + " . . . . . 38

Nose Flap

13. Maximum Lift, Configuration $S_{15}$ + $F_N$ + $B^2$ . . . . . 39

14. " " , " " + " + $B^4$ . . . . . 40

15. " " , " " + " + " . . . . . 41

## INDEX OF FIGURES (Cont'd)


Page

16. Maximum Lift, Configuration $S_{15} + F_N + B^7$ . . . . . 42
17. " " , " " + " + " . . . . . 43
18. " " , " " + " + " . . . . . 44
19. " " , " " + " + " . . . . . 45

Combined Flaps

20. Maximum Lift, Configuration $S_{15} + F_N + F_S + B^2$ . . . . . 46
21. " " , " " + " + " + $B^4$ . . . . . 47
22. " " , " " + " + " + " . . . . . 48
23. " " , " " + " + " + $B^7$ . . . . . 49
24. " " , " " + " + " + " . . . . . 50
25. " " , " " + " + " + " . . . . . 51
26. " " , " " + " + " + " . . . . . 52

25% and 35% Chord Slot Position

Wing Alone

27. Maximum Lift, Configuration $S_{25} + B^2$ . . . . . 53
28. " " , " " + $B^4$ . . . . . 54
29. " " , " " + $B^7$ . . . . . 55
30. " " , " $S_{35} + B^2$ . . . . . 56
31. " " , " " + $B^4$ . . . . . 57

Flaps

32. Maximum Lift, Configuration $S_{25 \text{ or } 35} + F_N + B$ . . . . . 58
33. " " , " " + $F_S$ + " . . . . . 59
34. " " , " " + $F_N + F_S + B$ . . . . . 60

## INDEX OF FIGURES (Cont'd)

Page

Flap Effectiveness

35. Nose Flap Effectiveness without Blowing, Configuration $S_{15} + F_N$ . 61

36. " " " with Blowing, Configuration $S_{35} + F_N + B$. 62

37. Split " " without Blowing, Configuration $S_{15} + F_S$ . 63

38. " " " " " , " " + " . 64

39. Combined Flap Effectiveness without Blowing, Configuration $S_{15} + F_N + F_S$ . . . . . 65

40. Combined Flap Effectiveness with Blowing, Configuration $S_{15} + F_N + F_S + B$ . . . . . 66

41. Combined Flap Effectiveness with Blowing, Configuration $S_{35} + F_N + F_S + B$ . . . . . 67

Flap Build-Up

42. Nose Flap Build-Up, Configuration $S_{15}$ . . . . . 68

43. Split " " , " " . . . . . 69

44. Combined Flap Build-Up, Configuration $S_{15}$ . . . . . 70

Blowing Effectiveness

45. Blowing Effectiveness, Configuration $S_{15} + B$. . . . . 71

46. " " , " $S_{25 \text{ and } 35} + B$ . . . . . 72

47. " " , " $S_{15} + F_N + B$ . . . . . 73

48. " " , " $S_{25 \text{ and } 35} + F_N + B$. . . . . 74

49. " " , " $S + F_S + B$ . . . . . 75

50. " " , " $S_{15} + F_N + F_S + B$. . . . . 76

51. " " , " $S_{25 \text{ and } 35} + F_N + F_S + B$ . . 77

## INDEX OF FIGURES (Cont'd)

Page

Tuft Investigation

52. Tuft Photographs, Configuration $S_{15}$ + Tufts . . . . . 78
53. " " , " " + B + Tufts . . . . . 79
54. " " , " " + $F_N^{150}$ + Tufts. . . . . 80
55. " " , " " + $F_N^{120}$ + B + Tufts. . . . . 81
56. " " , " " + $F_S^{70}$ + Tufts . . . . . 82
57. " " , " " + " + B + Tufts . . . . . 83
58. " " , " " + $F_N^{140}$ + $F_S^{70}$ + Tufts. . . . . 84
59. " " , " " + $F_N^{120}$ + $F_S^{60}$ + B + Tufts. . . 85

Model Photos

1. Top View Showing Model. . . . . 86
2. Front View Showing Model Mounted in Tunnel. . . . . 86
3. Side " " " " " " . . . . . 86
4. Front " " End Plates and Tail Sting with Wing Removed. . 86
5. " " " Air Supply Outside Tunnel. . . . . 86
6. Rear " " " " " " . . . . . 86

## I. SUMMARY

This report presents the results of an investigation of boundary layer energization by blowing as a method of increasing the maximum lift coefficient for supersonic airfoils operating at low subsonic speeds.

The model used was a double wedged airfoil with end plates and a spanwise slot located at the 15%, 25% or 35% chord position. Air was blown back over the wing from this slot producing a considerable increase in maximum lift for most configurations. Blowing proved to be most effective in increasing the maximum lift when used with the nose flap, fairly effective with combined flaps and wing alone, but ineffective with the split flap.

## II. INTRODUCTION

The data presented in this report were obtained in the three-dimensional test section of the GALCIT* 10-foot wind tunnel during the periods August 21, 1948 to August 22, 1948, October 28, 1948 to November 6, 1948, December 27, 1948 to December 31, 1948 and February 7, 1949 to February 8, 1949.

The problem under consideration was that of obtaining greater maximum lift coefficients for supersonic airplanes at low speeds. Although the sharp leading edge of the double wedge or circular arc airfoil profiles is desirable for supersonic speeds, these same airfoils at subsonic speeds have a very low value of maximum lift coefficient. This low lift coefficient presents a serious problem particularly in landing the transonic and supersonic airplanes. As a result, there is a great need for devices to raise this maximum lift coefficient. The available lift increments from the use of leading edge and trailing edge flaps is fairly well known but in many cases insufficient.

Boundary layer control is one possible device. It is a generally accepted fact that suction is a more efficient method of boundary layer control than blowing. As a result, a great deal of work has been and is being done on suction, and very little on blowing. On the other hand, with the turbo-jet engine as a potential source of blowing air, the blowing method of boundary layer control is well worth further investigation.

W. Schwier at Goettingen (Ref. 1) has done considerable work on blowing over deflected flaps on an NACA 23012-64 airfoil that gave a good resulting

*Guggenheim Aeronautical Laboratory, California Institute of Technology

increase in maximum lift coefficient. A. D. Pollock and F. F. Reck (Ref. 2) did the initial work on blowing from a spanwise slot of a double wedge airfoil in the California Institute of Technology-Merrill Wind Tunnel (24" x 48"). This thesis is a continuation of the work started by Pollock and Reck using the same model in the GALCIT 10-foot wind tunnel.

The aim of this work was to determined the Reynolds number effects and to learn as much about boundary layer energization by blowing as possible within the limitations of the model. It was hoped to find how lift coefficient varied with variations in volumetric flow coefficients, and what was the optimum blowing pressure and chordwise slot location.

## III. NOTATION

### Definition of Tests

P = Polar test; pitch angle varied, yaw angle = $0^{\circ}$; lift, drag and pitching moment data are taken.

Tuft Pict. = Photographs of flow over upper surface of wing as shown by floss tufts.

### Definition of Angular Measurements

$\alpha$ = Angle of attack of wing chord line relative to equivalent free air windstream.

$\psi$ = Angle of yaw of model plane of symmetry relative to wind tunnel axis.

### Definition of Coefficients

$C_L$ = Lift coefficient = $\frac{\text{lift}}{qS}$ ($C_L$ is positive when it tends to lift the airplane)

$C_{L_\tau}$ = Tare lift coefficient = $\frac{\text{tare lift}}{qS}$

$C_D$ = Drag coefficient = $\frac{\text{drag}}{qS}$ ($C_D$ is positive when it acts in the direction of the relative wind)

$C_{D_\tau}$ = Tare drag coefficient = $\frac{\text{tare drag}}{qS}$

$C_m$ = Pitching moment coefficient = $\frac{\text{pitching moment}}{qSc}$ ($C_m$ is positive when it tends to raise the nose)

$C_{m_\tau}$ = Tare pitching moment coefficient = $\frac{\text{tare pitching moment}}{qSc}$

For $C_m$ the following notation is used:

$( )_{c/4}$ = Moments referred to the 1/4 MAC (mean aerodynamic chord) position

$C_Q$ = Volumetric flow coefficient = $\frac{Q}{VS}$

R = Reynolds Number = $\frac{\rho cV}{\mu}$

For the foregoing coefficients use:

S = Projected wing area = 0.695 $ft^2$

$c$ = Mean aerodynamic chord = 0.42 ft

$b$ = Wing span = 1.67 ft

$q$ = Dynamic pressure averaged over model span ($\rho V^2/2$, lbs/ft$^2$)

$V$ = Average windstream velocity $\sqrt{\frac{2q}{\rho}}$ , ft/sec

$V_S$ = Air velocity in slot considering pressure energy isentropically converted to velocity (at atmospheric pressure)

$\rho$ = Mass density of air

$Q$ = Quantity of airflow through slot, ft$^3$/sec (at $\rho$ = 0.00219 $\frac{\text{slugs}}{\text{ft}^3}$)

$\mu$ = Absolute viscosity of air = $3.726 \times 10^{-7}$ $\frac{\text{lb weight x sec}}{\text{ft}^2}$

(for T = 15°C, h = 760 mm)

| Model Notation | Notation | Figure No. | Photo No. |
|---|---|---|---|
| S | = Wing as tested with end plates and tail sting, subscript indicates chordwise position of slot in 1% chord | 1 | 1,2,3 |
| S-W | = End plates and tail sting with wing removed as used in determining tares | | 4 |
| W | = Wing 10% thick double wedge airfoil | 1 | 1,2,3 |
| s | = Blowing slot sealed | | |
| $F_N$ | = Nose flap, 10% chord made from 20 gage sheet steel, attached to the model with screws and tape, superscript denotes angle of deflection as defined on Figure 1 | 1 | |
| $F_S$ | = Split flap, 20% chord, made from 20 gage sheet steel, attached to the model with screws and tape, superscript denotes angle of deflection as defined on Figure 1 | 1 | |
| B | = Blowing through slot, superscript denotes slot gap in thousandths of an inch, subscript indicates absolute pressure (psi.) inside wing | | |
| Tufts | = Short lengths of floss attached to the upper surface of the wing by scotch tape to indicate direction of airflow | 52-59 | |

## IV. DESCRIPTION OF EXPERIMENTAL SET-UP

### A. Description of the Model

The model was a double wedge airfoil with a rectangular profile and small end plates to increase the effective aspect ratio (cf. photo 1). It was constructed with 0.10 inch phospher-bronze plates soldered and screwed to the ribs and the end plates. The model surface was sealed except at the spanwise slot which could be set at the 15%, 25% and 35% chord position. Air was taken into the model through the end plates and directed back over the wing by the slot. The initial intention was that the model would be run at sufficient internal pressure to assure a Mach number of one at the slot and consequently, an even spanwise distribution of flow. The slot gap was adjusted by inserting shims along the slot in line with the slot lip hold-down screws. A great deal of the time and effort was expended to get an even spanwise distribution of flow from the slot. Under pressure, the slot lip bulged somewhat between the hold-down screws, and the shims blocked a small portion of the gap; therefore, the resulting flow was not perfectly even. The model also tended under pressure to bulge out between the ribs and thus changed the airfoil section by a small amount.

### B. Description of Air Supply System

Air from the building pressure lines was conducted into a settling tank, past a pressure gage and a thermometer, through a rotometer flow gage and into the wind tunnel through the breather slot aft of the working section (cf. photos 5 and 6). Inside the tunnel the air went upstream on each side of the model and through a soft rubber hose enclosed in a

fine wire coil to a tee fitting which attached on one side to the support bayonet and on the other side lead through a special swivel coupling into the model end plate (cf. photos 2 and 3). The piping was of sufficient size relative to the mass flow that there was no pressure drop detected when a pressure gage was inserted at the wing. There were two sets of aluminum gaskets which were alternately inserted at the end plate, the one set to cut off the flow of air into the model, the other set to allow free passage of the air. The pressure was found to be most easily controlled by setting the air supply control valve (Fig. 2) a little above the desired flow and making final adjustments with a bleed valve at the settling tank. By leaving some sag in the flexible rubber hoses, the effect of pressure in the line on the balance zeros was small. In fact, the lift and pitching moment zero readings seldom varied from pressure off to pressure on; the drag, however, varied plus or minus ten balance points. Thus, it was necessary to insert the solid gaskets to cut off the flow and zero the balances with pressure in the lines for runs that involved blowing.

## V. TEST PROCEDURE

Force and moment data were obtained from polar runs. To save testing time, only the range of angles near the maximum lift were taken for the maximum lift investigations. The first set of data was for Reynolds number effects and flap effectiveness to determine the optimum flap settings. The majority of the remaining runs were made on the most promising configurations at various volumetric flow coefficients. The variations in volumetric flow coefficients were obtained by varying the blowing pressure, slot width and tunnel dynamic pressure. The run schedule was prepared to give data that would show the relation between the maximum lift coefficient and the blowing coefficient as well as make possible the determination of the optimum blowing pressure and slot location.

GALCIT standard procedures were used throughout in regard to tunnel calibration, rigging, operation and data reduction. The reduction of the rotometer data was accomplished as outlined in Ref. 3. The span of the model was so small relative to the tunnel diameter that the wind tunnel wall corrections were negligible. Tares were obtained from runs made with the end plates, tail sting and all plumbing in place but with the wing removed. The force and moment coefficients obtained in these tare runs were subtracted from the model coefficients determined from the polar runs. Consequently, all final force and moment coefficients apply to the wing alone.

As an aid to subsequent investigators, a complete index of runs is included and all runs plotted appear in the figures.

## VI. EXPERIMENTAL RESULTS

The experimental results appear in Figures 3 through 59.

Since the Reynolds number effects show very little variation in the maximum lift coefficient on Figures 3 to 6, Reynolds number changes have been neglected throughout this report.

The individual results of the high lift investigations appear in Figures 7 to 41. The maximum lift points from these figures were used to make up the blowing effectiveness plots.

The increments in lift available from flaps and then from combined flaps and blowing are shown in the flap build-up plots, Figures 42 to 44. The runs shown on these figures were made for a full range of angle of attack from zero lift to stall to give a complete picture of the results of flaps and blowing.

The plots of volumetric flow coefficients versus the maximum lift coefficient, Figure 45, 47, 49 and 50, give the effectiveness of blowing on the various configurations. The interesting result here is that the relation of blowing coefficient to lift coefficient has an approximately constant slope.

| Configuration | $C_{L_{max}}$ $C_Q=0$ | $\Delta C_{L_{max}}$ $C_Q=0$ | $C_{L_{max}}$ $C_Q=0.0100$ | $\Delta C_{L_{max}}$ $C_Q=0.0100$ | $\frac{dC_L}{dC_Q}$ |
|---|---|---|---|---|---|
| Wing Alone ($S_{15}$) | 0.76 | 0 | 1.19 | 0.43 | 43 |
| Nose Flap ($S_{15}+F_N$) | 1.11 | 0.35 | 2.13 | 1.37 | 102 |
| Split Flap ($S_{15}+F_S$) | 1.63 | 0.87 | 1.79 | 1.03 | 16 |
| Combined Flaps ($S_{15}+F_N+F_S$) | 2.02 | 1.26 | 2.63 | 1.87 | 61 |

A cross plot of maximum lift coefficient versus pressure coefficient with volumetric flow coefficient as a parameter was attempted to show the effect of pressure. The variation of maximum lift coefficient with pressure, however, was of the same order of magnitude as the scatter in the data, and no reliable solution was found.

Figures 46, 48 and 51 show that although the 25 and 35% chord positions are less effective than the 15% slot location, the difference in effectiveness is quite small. The jet from each slot evidently induces a flow over the wing ahead of the slot such that the combination of induction and blowing for each slot produces the same delay of separation at the same volumetric flow coefficient.

The tuft investigations, Figures 52 through 59, reveal two distinct methods of stall. The addition of nose flap causes a separation that starts at the leading edge and moves progressively aft as the angle of attack increases; whereas with the split flap separation starts at the leading edge but then has an abrupt separation progressing from the trailing edge. Where the blowing delays the progress of separation with a nose flap, it has little effect on the abrupt stall of the split flap. The wing alone and combined flap configurations are evidently a combination of the above stall phenomena.

## VII. ACCURACY

In connection with the above results, it is important to know the accuracy of the data. Past experience has indicated that the following limits of scatter are obtained at the GALCIT 10-foot tunnel on a wing of five square feet area at a tunnel dynamic pressure of 50 pounds/sq. ft.:

| | | |
|---|---|---|
| Lift coefficient | = | $\pm$ 0.005 |
| Drag " | = | $\pm$ 0.0001 |
| Pitching moment coefficient | = | $\pm$ 0.001 |

Assuming a linear relation of area and dynamic pressure, the following limits of accuracy are estimated for this model:

| | | |
|---|---|---|
| Lift coefficient | = | $\pm$ 0.05 |
| Drag " | = | $\pm$ 0.001 |
| Pitching moment coefficient | = | $\pm$ 0.01 |

For the blowing runs, the effect of pressure in the line on drag as explained in Section III, page 8, could cause an error in the drag coefficient of plus or minus 0.001 in addition to the above error. Thus, the drag error with blowing would be $\pm$ 0.002.

The model had some surface roughness and some minor variations in cross section due to the internal pressure that caused additional unestimable errors.

The volumetric discharge coefficient is estimated to be accurate to $\pm$ 0.0001.

## VIII. CONCLUSION

Boundary layer control by blowing as a means of increasing the maximum lift of supersonic wings at low subsonic speeds shows sufficient promise to make further investigation worthwhile. The next logical step on this project would be to make a larger model, preferably one for a two-dimensional working section, of sufficient size to obtain more accurate results.

These preliminary investigations led to the following results:

1. There is an approximate linear relation between the amount of blowing and the maximum lift for each configuration.

2. Blowing is most effective with the nose flap, fairly effective with combined flaps and wing alone and ineffective with the split flap.

3. There is very little variation of maximum lift coefficient with pressure in the range of pressures tested.

4. The difference in effectiveness of the 15, 25 and 35% chordwise location of the slot is quite small with the 15% chord position proving to be the most effective.

## IX. REFERENCES

1. Schwier, W. - Lift Increase by Blowing out Air: Tests on Airfoil of 12% Thickness Using Various Types of Flap. GER No. 219.

2. Lt. Comdr. A. D. Pollock, Jr., U.S.N. and Lt. Comdr. F. F. Reck, U.S.N.- A Study of Methods to Increase the Lift of Supersonic Airfoils at Low Speeds. (C.I.T. Thesis 1947.)

3. Fischer & Porter Company - Theory of the Rotometer, Catalog Section 98-Y

## X. INDEX OF RUNS

| Run | Configuration | Test | $q, \frac{lb}{ft^2}$ | Figure Number |
|---|---|---|---|---|
| 1 | $S_{15}$ + S | P | 60 | 3 |
| 2 | " | " | " | ",38,42,43,44 |
| 3 | " | " | 15 | " |
| 4 | " | " | 30 | " |
| 5 | " | " | 45 | " |
| 6 | " + $B^{7}_{44.7}$ | " | " | 10 |
| 7 | " + " | " | 60 | 9,10 |
| 8 | " + $B^{7}_{34.7}$ | " | " | " |
| 9 | " + $B^{7}_{24.7}$ | " | " | " |
| 10 | " + $B^{7}_{44.7}$ | " | 15 | 10 |
| 11 | " + " | " | 30 | " |
| 12 | " + $F_S^{60}$ | " | 60 | 37 |
| 13 | " + $F_S^{70}$ | " | " | 5,37 |
| 14 | " + $F_S^{80}$ | " | " | 37 |
| 15 | " + $F_S^{70}$ | " | 45 | 5 |
| 16 | " + " | " | 15 | " |
| 17 | " + " | " | 30 | " |
| 18 | " + $F_N^{150}$ | " | 60 | 4,35 |
| 19 | " + $F_N^{140}$ | " | " | 35 |
| 20 | " + $F_N^{160}$ | " | " | " |
| 21 | " + $F_N^{150}$ | " | 15 | 4 |
| 22 | " + " | " | 30 | " |
| 23 | " + " | " | 45 | " |

## X. INDEX OF RUNS (Cont'd)

| Run | Configuration | Test | q, $\frac{lb}{ft^2}$ | Figure Number |
|---|---|---|---|---|
| 24 | $S_{15} + F_N^{150} + F_S^{70}$ | P | 60 | 39 |
| 25 | " + $F_N^{160}$ + " | " | " | " |
| 26 | " + $F_N^{140}$ + " | " | " | 6,39 |
| 27 | " + $F_N^{130}$ + " | " | " | 39 |
| 28 | " + $F_N^{140}$ + $F_S^{80}$ | " | " | " |
| 29 | " + " + $F_S^{60}$ | " | " | " |
| 30 | " + " + $F_S^{70}$ | " | 15 | 6 |
| 31 | " + " + " | " | 30 | " |
| 32 | " + " + " | " | 45 | " |
| 33 | " + " + " + $B^7_{44.7}$ | " | 60 | 40 |
| 34 | " + $F_N^{150}$ + " + " | " | " | " |
| 35 | " + $F_N^{130}$ + " + " | " | " | 25,26,40 |
| 36 | " + $F_N^{120}$ + " + " | " | " | 40 |
| 37 | " + $F_N^{130}$ + $F_S^{60}$ + " | " | " | " |
| 38 | " + " + $F_S^{50}$ + " | " | " | " |
| 39 | " + " + $F_S^{80}$ + " | " | " | " |
| 40 | " + " + $B^7_{44.7}$ | " | " | 19 |
| 41 | " + " + " | " | 15 | " |
| 42 | " + " + " | " | 30 | " |
| 43 | " + " + " | " | 45 | " |
| 44 | " + " + $F_S^{70}$ + $B^7_{44.7}$ | " | 15 | 26 |
| 45 | " + " + " + " | " | 30 | " |
| 46 | " + " + " + " | " | 45 | " |

## X. INDEX OF RUNS (Cont'd)

| Run | Configuration | Test | $q, \frac{lb}{ft^2}$ | Figure Number |
|---|---|---|---|---|
| 47 | $S_{15} + F_N^{130} + F_S^{70} + B_{24.7}^7$ | F | 60 | 25 |
| 48 | " + " + " + $B_{34.7}^7$ | " | " | " |
| 49 | " + $F_S^{70}$ + $B_{44.7}^7$ | " | " | Not Used |
| 50 | " - W | " | -- | Tares |
| 51 | $S_{35}$ - " | " | -- | " |
| 52 | " + $B_{39.7}^7$ | " | 60 | 36 |
| 53 | " + $F_N^{130}$ + $B_{39.7}^7$ | " | " | " |
| 54 | " + $F_N^{140}$ + " | " | " | " |
| 55 | " + $F_N^{120}$ + " | " | " | " |
| 56 | " + $F_N^{130}$ + " | " | " | " |
| 57 | " + " + $F_S^{70}$ + $B_{39.7}^7$ | " | " | 41 |
| 58 | " + $F_N^{140}$ + " + " | " | " | " |
| 59 | " + $F_N^{150}$ + " + " | " | " | " |
| 60 | " + $F_N^{140}$ + " + " | " | " | " |
| 61 | " + $F_S^{70}$ + $B_{39.7}^7$ | " | " | " |
| 62 | " + $B_{44.7}^2$ | " | " | 30 |
| 63 | " + " | " | 45 | " |
| 64 | " + " | " | 30 | " |
| 65 | " + $F_N^{130}$ + $B_{44.7}^2$ | " | " | 32 |
| 66 | " + $F_N^{140}$ + $F_S^{70}$ + $B_{44.7}^2$ | " | 60 | 34 |
| 67 | " + $F_S^{70}$ + $B_{44.7}^2$ | " | " | 33 |
| 68 | " + $B_{39.7}^2$ | " | " | 30 |
| 69 | " + $B_{34.7}^2$ | " | " | " |

## X. INDEX OF RUNS (Cont'd)

| Run | Configuration | Test | $q, \frac{lb}{ft^2}$ | Figure Number |
|---|---|---|---|---|
| 70 | $S_{35} + B^4_{44.7}$ | P | 60 | 31 |
| 71 | " + " | " | 45 | " |
| 72 | " + " | " | 30 | " |
| 73 | " + $B^4_{39.7}$ | " | 60 | " |
| 74 | " + $B^4_{34.7}$ | " | " | " |
| 75 | " + $F_N^{130} + B^4_{44.7}$ | " | " | 32 |
| 76 | " + $F_N^{140} + F_S^{70} + B^4_{44.7}$ | " | " | 34 |
| 77 | " + $F_S^{70} + B^4_{44.7}$ | " | " | 33 |
| 78 | $S_{25} + B^4_{44.7}$ | " | " | 28 |
| 79 | " + " | " | 45 | " |
| 80 | " + " | " | 30 | " |
| 81 | " + $B^4_{39.7}$ | " | 60 | " |
| 82 | " + $B^4_{34.7}$ | " | " | " |
| 83 | " + $F_N^{130} + B^4_{44.7}$ | " | " | 32 |
| 84 | " + $F_N^{140} + F_S^{70} + B^4_{44.7}$ | " | " | 34 |
| 85 | " + $F_S^{70} + B^4_{44.7}$ | " | " | 33 |
| 86 | " + $B^2_{44.7}$ | " | " | 27 |
| 87 | " + " | " | 45 | " |
| 88 | " + " | " | 30 | " |
| 89 | " + $B^2_{39.7}$ | " | 60 | " |
| 90 | " + $B^2_{34.7}$ | " | " | " |
| 91 | " + $F_N^{130} + B^2_{44.7}$ | " | " | 32 |
| 92 | " + $F_N^{140} + F_S^{70} + B^2_{44.7}$ | " | " | 34 |

## X. INDEX OF RUNS (Cont'd)

| Run | Configuration | Test | $q, \frac{lb}{ft^2}$ | Figure Number |
|---|---|---|---|---|
| 93 | $S_{25} + F_S^{70} + B_{44.7}^{2}$ | P | 60 | 33 |
| 94 | " $+ B_{44.7}^{7}$ | " | " | 29 |
| 95 | " + " | " | 45 | " |
| 96 | " + " | " | 30 | " |
| 97 | " $+ B_{39.7}^{7}$ | " | 60 | " |
| 98 | " $+ B_{34.7}^{7}$ | " | " | " |
| 99 | " $+ F_N^{130} + B_{44.7}^{7}$ | " | " | 32 |
| 100 | " $+ F_N^{140} + F_S^{70} + B_{44.7}^{7}$ | " | " | 34 |
| 101 | " $+ F_S^{70} + B_{44.7}^{7}$ | " | " | 33 |
| 102 | $S_{15} + F_N^{150}$ | " | 60 | 42 |
| 103 | " $+ F_N^{140} + B_{44.7}^{7}$ | " | 30 | " |
| 104 | " + " $+ F_S^{40}$ | " | 60 | 44 |
| 105 | " + " $+ F_S^{50}$ | " | " | " |
| 106 | " + " $+ F_S^{60}$ | " | " | " |
| 107 | " + " $+ F_S^{70}$ | " | " | " |
| 108 | " $+ F_N^{130}$ + " $+ B_{44.7}^{7}$ | " | 30 | " |
| 109 | " + " $+ F_S^{160} + B_{44.7}^{7}$ | " | " | " |
| 110 | " + " $+ F_S^{50}$ + " | " | " | " |
| 111 | " + " $+ F_S^{40}$ + " | " | " | " |
| 112 | " $+ F_S^{40}$ | " | 60 | 38 |
| 113 | " $+ F_S^{50}$ | " | " | " |
| 114 | " $+ F_S^{60}$ | " | " | " |
| 115 | " $+ F_S^{70}$ | " | " | " ,43 |

## X. INDEX OF RUNS (Cont'd)

| Run | Configuration | Test | $q, \frac{lb}{ft^2}$ | Figure Number |
|---|---|---|---|---|
| 116 | $S_{15} + F_S^{70} + B^7_{44.7}$ | P | 30 | 43 |
| 117 | " + $F_S^{60}$ + " | " | " | " |
| 118 | " + $F_S^{50}$ + " | " | " | " |
| 119 | " + $F_S^{40}$ + " | " | " | " |
| 120 | " + Tufts | Tuft Pict. | " | 52 |
| 121 | " + $B^7_{44.7}$ + Tufts | " " | " | 53 |
| 122 | " + $F_N^{150}$ + " | " " | " | 54 |
| 123 | " + $F_N^{140}$ + $B^7_{44.7}$ + Tufts | " " | " | Not Used |
| 124 | " + " + $F_S^{70}$ + Tufts | " " | " | " " |
| 125 | " + $F_N^{130}$ + " + $B^7_{44.7}$ + Tufts | " " | " | " " |
| 126 | " + $F_S^{70}$ + Tufts | " " | " | 56 |
| 127 | " + " + $B^7_{44.7}$ + Tufts | " " | " | 57 |
| 128 | " + $B^7_{44.7}$ | P | 60 | 11 |
| 129 | " + " | " | 40 | " |
| 130 | " + " | " | 20 | " |
| 131 | " + $B^7_{39.7}$ | " | 60 | " |
| 132 | " + $B^7_{34.7}$ | " | " | " |
| 133 | " + $B^7_{24.7}$ | " | " | " |
| 134 | " + $F_N^{130}$ + $B^7_{44.7}$ | " | " | 18 |
| 135 | " + " + " | " | 40 | " |
| 136 | " + " + " | " | 20 | " |
| 137 | " + " + $B^7_{39.7}$ | " | 60 | " |
| 138 | " + " + $B^7_{34.7}$ | " | " | " |

## X. INDEX OF RUNS (Cont'd)

| Run | Configuration | Test | $q, \frac{lb}{ft^2}$ | Figure Number |
|---|---|---|---|---|
| 139 | $S_{15} + F_N^{130} + B^7_{24.7}$ | P | 60 | Not Used |
| 139A | " + " + " | " | " | 18 |
| 140 | " + " + $F_S^{60} + B^7_{44.7}$ | " | " | 24 |
| 140A | " + " + " + " | " | " | Not Used |
| 141 | " + $F_N^{140}$ + " + " | " | 60 | " " |
| 142 | " + $F_N^{130}$ + " + " | " | 40 | 24 |
| 143 | " + " + " + " | " | 20 | " |
| 144 | " + " + " + $B^7_{39.7}$ | " | 60 | " |
| 145 | " + " + " + $B^7_{34.7}$ | " | " | " |
| 146 | " + " + " + $B^7_{24.7}$ | " | " | " |
| 147 | " + " + $B^7_{39.7}$ | " | 40 | 17 |
| 148 | " + " + " | " | 20 | " |
| 149 | " + " + $B^7_{34.7}$ | " | 40 | " |
| 150 | " + " + " | " | 20 | " |
| 151 | " + " + $B^2_{44.7}$ | " | 60 | Not Used |
| 152 | " + $F_N^{140}$ + " | " | " | 13 |
| 153 | " + $F_N^{150}$ + " | " | " | Not Used |
| 154 | " + $F_N^{140}$ + " | " | 40 | 13 |
| 155 | " + " + " | " | 20 | " |
| 156 | " + " + $F_S^{60} + B^2_{44.7}$ | " | 60 | 20 |
| 157 | " + " + " + " | " | 40 | " |
| 158 | " + " + " + " | " | 20 | " |
| 159 | " + $B^2_{44.7}$ | " | 60 | 7 |
| 160 | " + " | " | 40 | " |

## X. INDEX OF RUNS (Cont'd)

| Run | Configuration | Test | $q, \frac{lb}{ft^2}$ | Figure Number |
|---|---|---|---|---|
| 161 | $S_{15} + B^{2}_{44.7}$ | P | 20 | 7 |
| 162 | " + $F_N^{140}$ + $B^{4}_{44.7}$ | " | 60 | Not Used |
| 163 | " + $F_N^{130}$ + " | " | " | 15 |
| 164 | " + " + " | " | 40 | " |
| 165 | " + " + " | " | 20 | " |
| 166 | " + " + $B^{4}_{39.7}$ | " | 60 | Not Used |
| 167 | " + $F_N^{140}$ + $B^{4}_{34.7}$ | " | " | 15 |
| 168 | " + " + $B^{4}_{24.7}$ | " | " | " |
| 169 | " + $F_N^{130}$ + $F_S^{60}$ + $B^{4}_{44.7}$ | " | " | 22 |
| 170 | " + $F_N^{140}$ + " + " | " | " | Not Used |
| 171 | " + $F_N^{130}$ + " + " | " | 40 | 22 |
| 172 | " + " + " + " | " | 20 | " |
| 173 | " + " + " + $B^{4}_{39.7}$ | " | 60 | " |
| 174 | " + " + " + $B^{4}_{34.7}$ | " | " | " |
| 175 | " + " + " + $B^{4}_{24.7}$ | " | " | " |
| 176 | " + $F_N^{140}$ + $B^{4}_{39.7}$ | " | " | 15 |
| 177 | " | " | " | Not Used |
| 178 | " + $B^{7}_{44.7}$ | " | " | 12 |
| 179 | " + " | " | 50 | " |
| 180 | " + " | " | 40 | " |
| 181 | " + " | " | 30 | " |
| 182 | " + " | " | 20 | " |
| 183 | " + $F_N^{120}$ + $F_S^{60}$ + $B^{7}_{44.7}$ | " | " | 23 |

## X. INDEX OF RUNS (Cont'd)

| Run | Configuration | Test | $q, \frac{lb}{ft^2}$ | Figure Number |
|---|---|---|---|---|
| 184 | $S_{15} + F_N^{120} + F_S^{60} + B^7_{44.7}$ | P | 30 | 23 |
| 185 | " + " + " + " | " | 40 | " |
| 186 | " + " + " + " | " | 50 | " |
| 187 | " + " + $B^7_{44.7}$ | " | " | 16 |
| 188 | " + " + " | " | 40 | " |
| 189 | " + " + " | " | 30 | " |
| 190 | " + " + " | " | 20 | " |
| 191 | " + $B^4_{44.7}$ | " | " | 8 |
| 192 | " + " | " | 30 | " |
| 193 | " + " | " | 40 | " |
| 194 | " + " | " | 45 | " |
| 195 | " + " | " | 50 | " |
| 196 | " + " | " | 60 | " |
| 197 | " + $F_N^{120} + F_S^{60} + B^4_{44.7}$ | " | 20 | 21 |
| 198 | " + " + " + " | " | 30 | " |
| 199 | " + " + $B^4_{44.7}$ | " | " | 14 |
| 200 | " + " + " | " | 20 | " |
| 201 | " + " + $F_S^{60} + B^4_{44.7}$ | " | 40 | 21 |
| 202 | " + " + $B^4_{44.7}$ | " | 15 | 14 |
| 203 | " + " + $B^7_{44.7}$ | Tuft Pict. | 30 | Not Used |
| 203A | " + " + " | " " | " | 55 |
| 204 | " + " + $F_S^{60} + B^7_{44.7}$ | " " | " | Not Used |

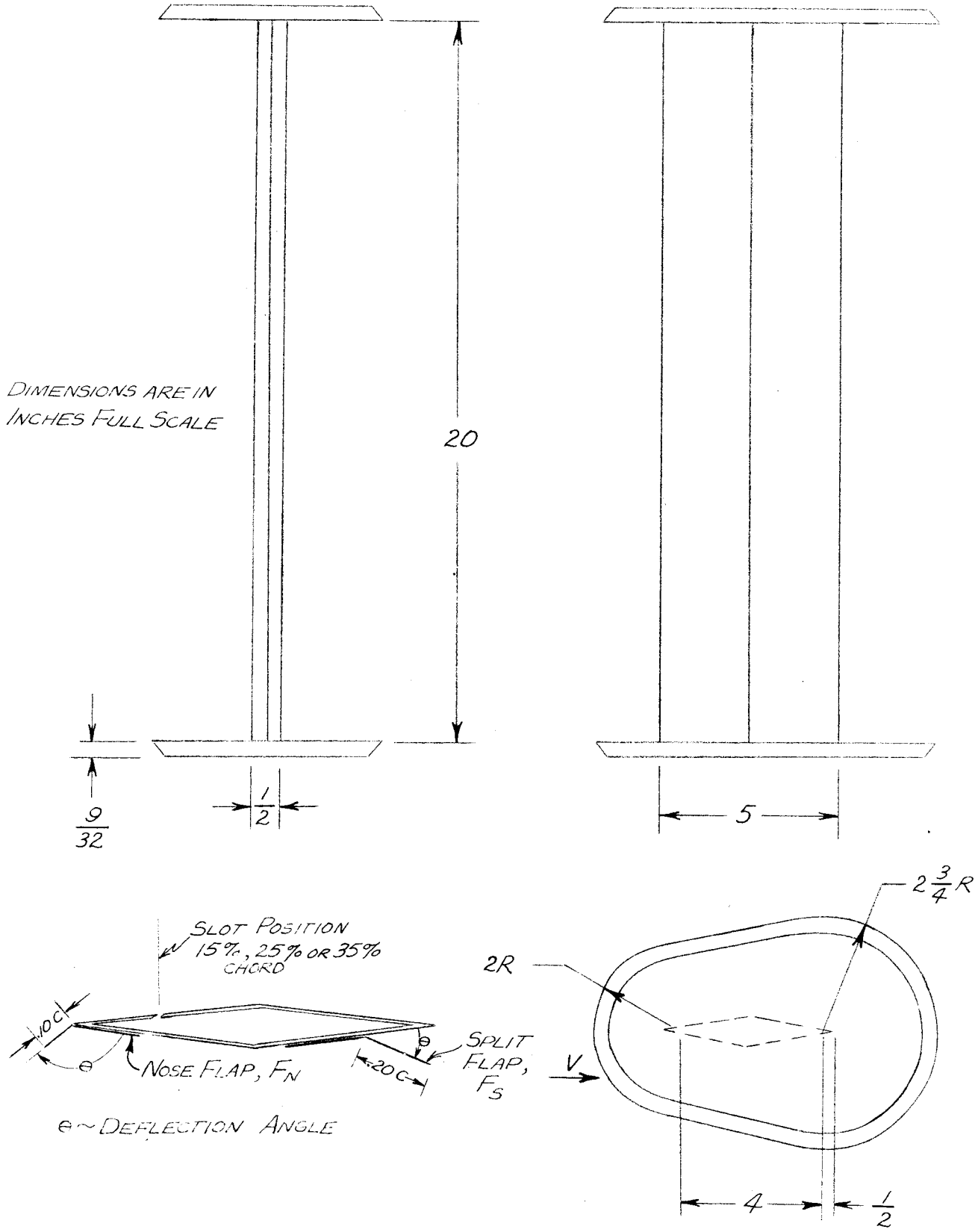


THREE VIEW SKETCH OF MODEL

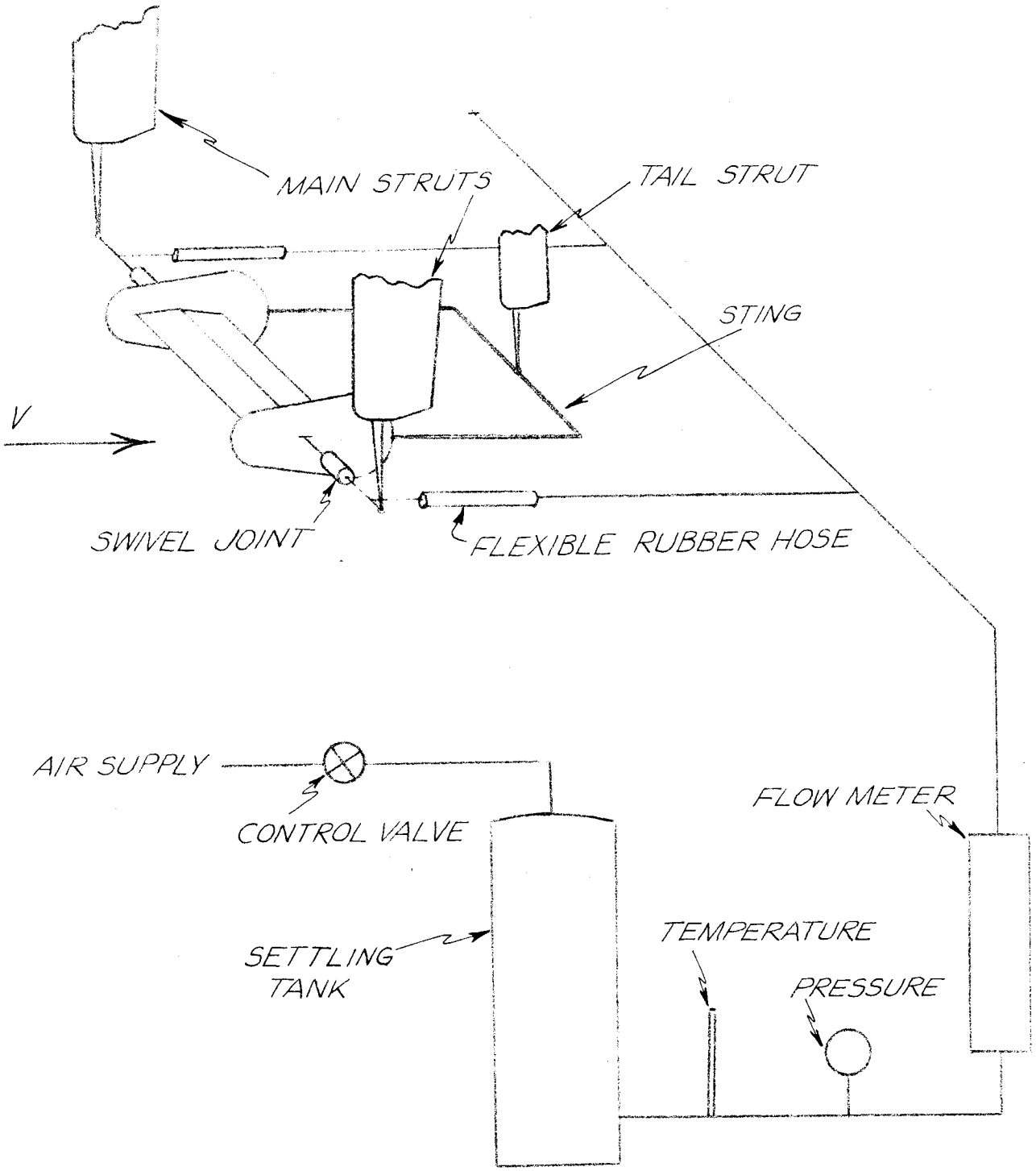


SCHEMATIC SKETCH OF AIR SYSTEM
AND METHOD OF MODEL SUPPORT

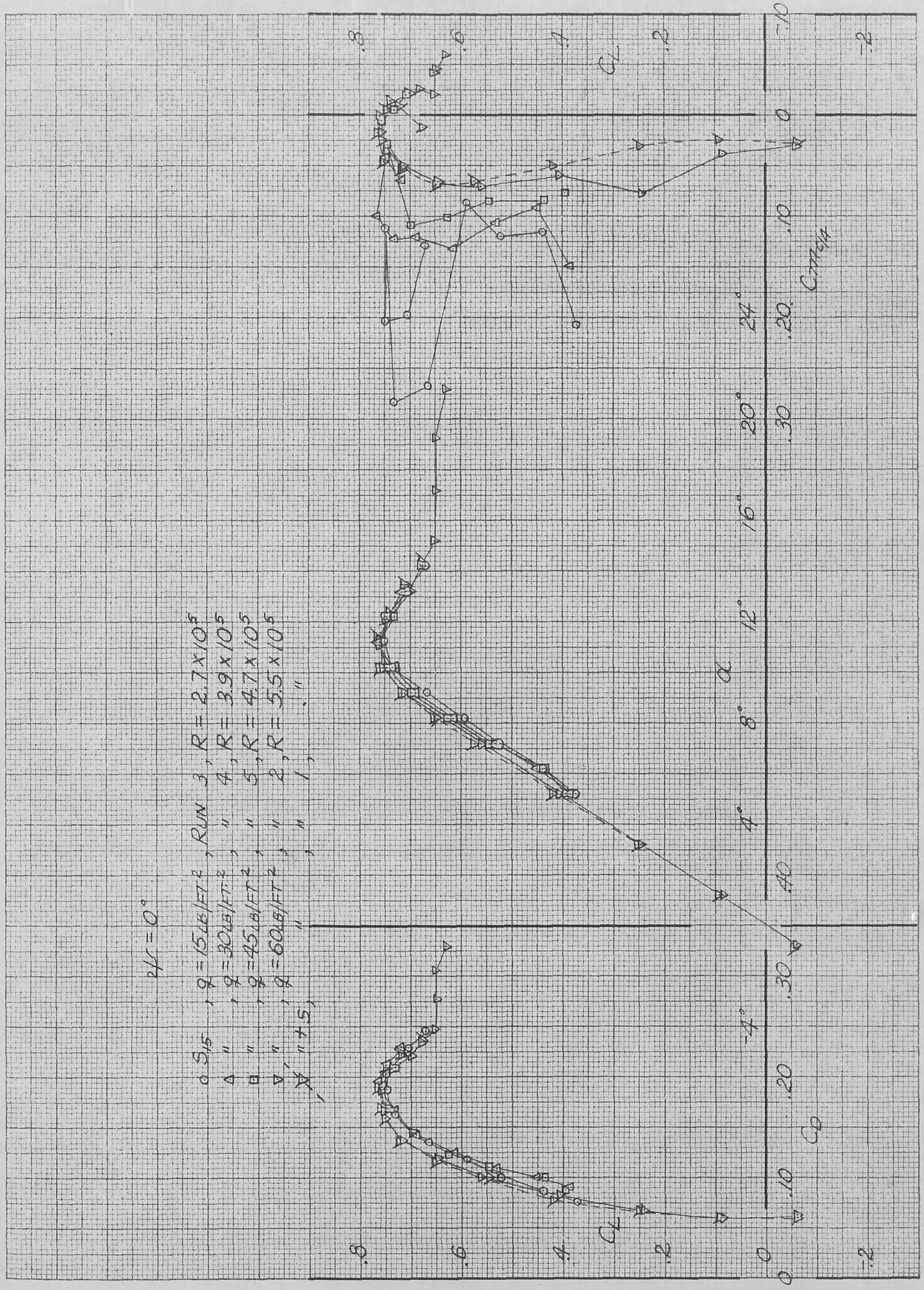


REYNOLDS NUMBER EFFECTS, CONFIGURATION S

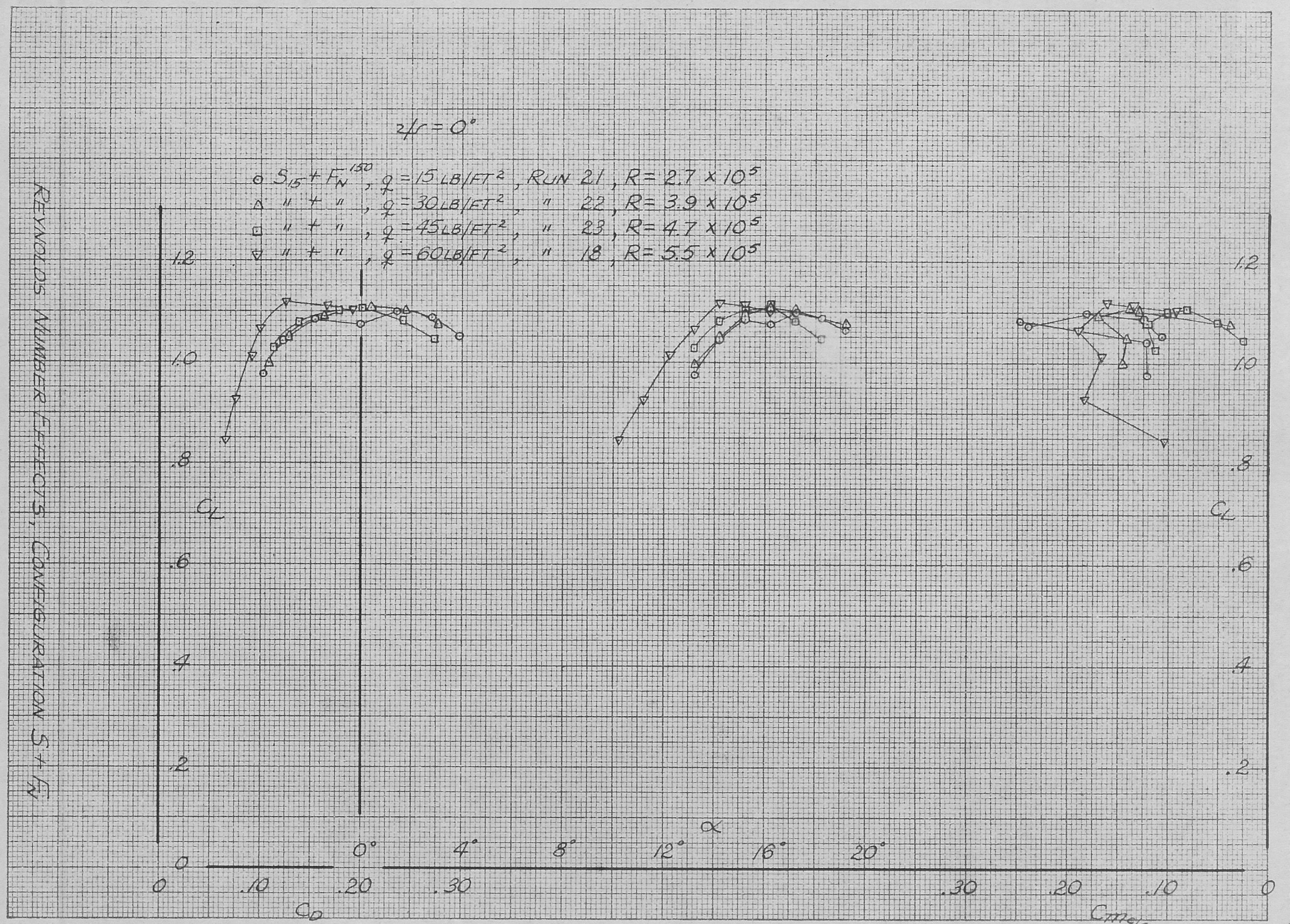
REYNOLDS NUMBER EFFECTS, CONFIGURATION S+F_N
i_f = 0°
○ S_15 + F_N^150, q = 15 LB/FT², RUN 21, R = 2.7 x 10^5
△ " + ", q = 30 LB/FT², " 22, R = 3.9 x 10^5
□ " + ", q = 45 LB/FT², " 23, R = 4.7 x 10^5
▽ " + ", q = 60 LB/FT², " 18, R = 5.5 x 10^5
C_L
1.2
1.0
.8
.6
.4
.2
0
α
0°
4°
8°
12°
16°
20°
0
.10
.20
.30
C_D
.30
.20
.10
0
C_m c/4

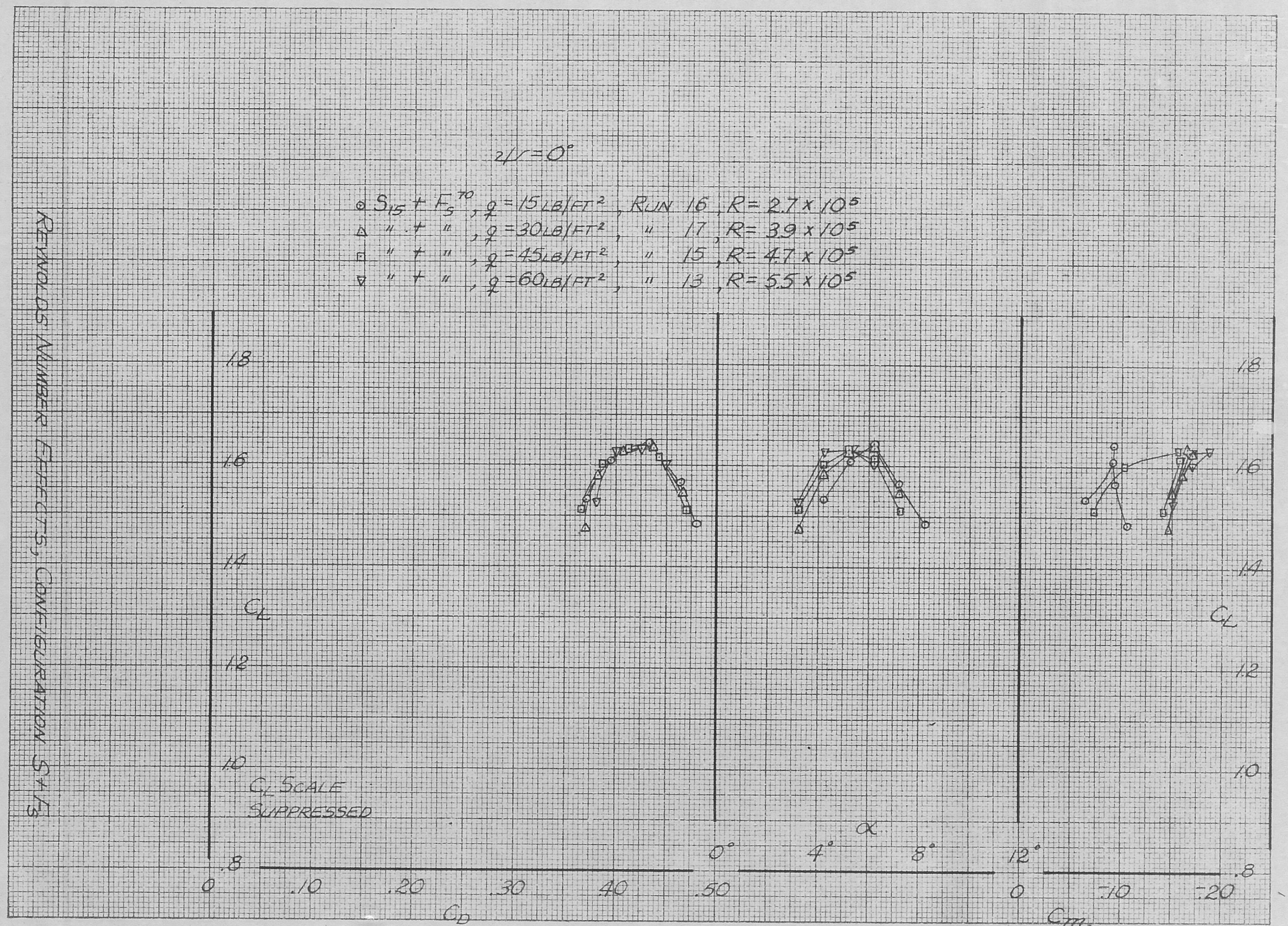
$\delta_f = 0°$
⊙ $S_{15} + F_5^{70}$, $q = 15$ LB/FT², RUN 16, $R = 2.7 \times 10^5$
△ " + ", $q = 30$ LB/FT², " 17, $R = 3.9 \times 10^5$
□ " + ", $q = 45$ LB/FT², " 15, $R = 4.7 \times 10^5$
▽ " + ", $q = 60$ LB/FT², " 13, $R = 5.5 \times 10^5$
REYNOLDS NUMBER EFFECTS, CONFIGURATION $S + F_5$
$C_L$
1.8
1.6
1.4
1.2
1.0
.8
$C_L$ SCALE SUPPRESSED
0
.10
.20
.30
.40
.50
$C_D$
$\alpha$
0°
4°
8°
12°
0
-.10
-.20
$C_{m_{c/4}}$

$S_{15} + F_N^{140} + F_S^{70}$, $q = 15$ LB/FT², RUN 30, $R = 2.7 \times 10^5$
" + " + " , $q = 30$ LB/FT², " 31, $R = 3.9 \times 10^5$
" + " + " , $q = 45$ LB/FT², " 32, $R = 4.7 \times 10^5$
" + " + " , $q = 60$ LB/FT², " 26, $R = 5.5 \times 10^5$
$\beta = 0°$
$C_L$
$C_D$
$C_L$ SCALE FACTOR SUPPRESSED
$\alpha$, DEG
REYNOLDS NUMBER EFFECTS, CONFIGURATION $S + F_N + F_S$

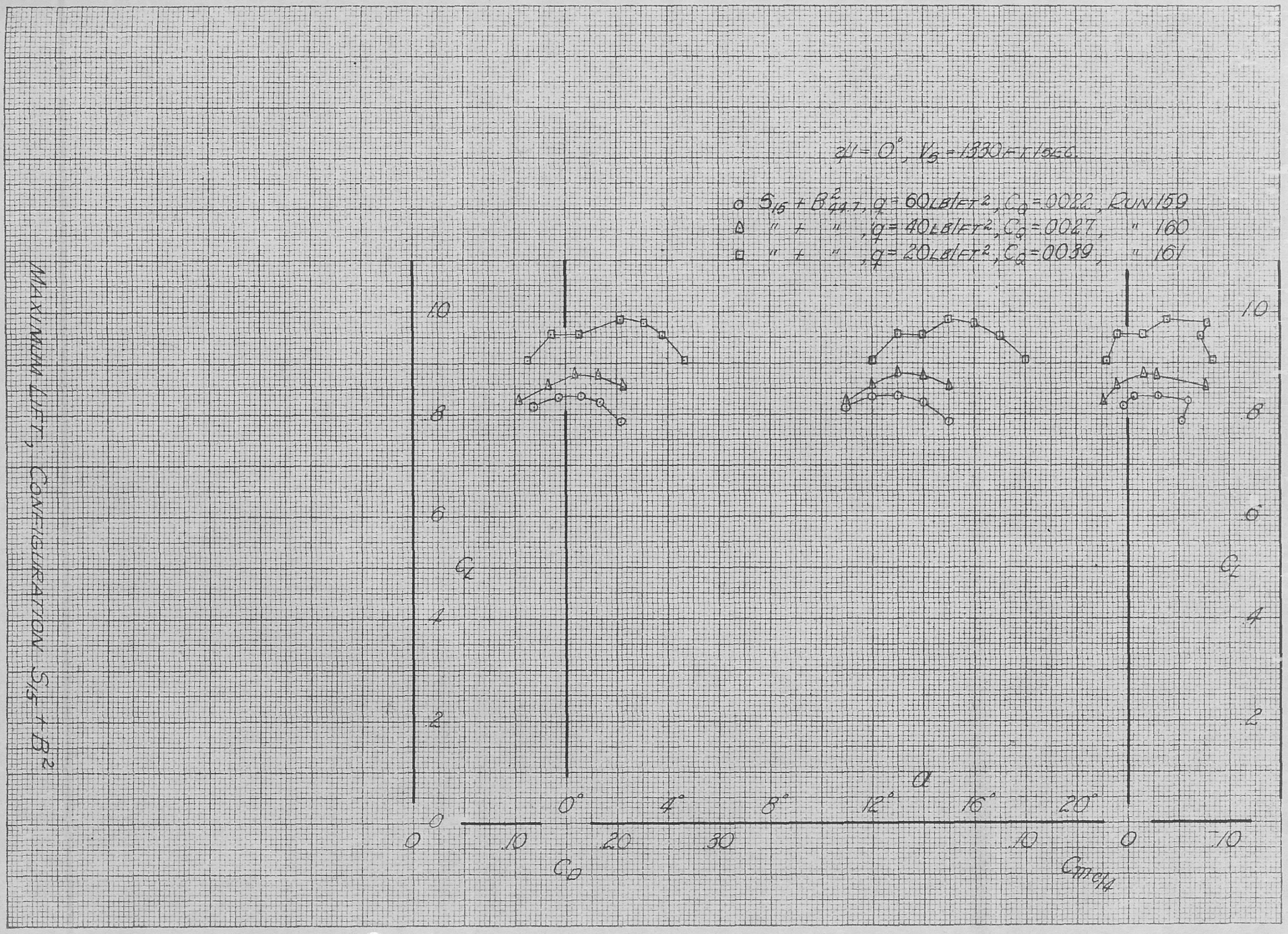
$\psi = 0°$, $V_s = 1330$ FT/SEC.
○ $S_{15} + B^2_{44.7}$, $q = 60$ LB/FT$^2$, $C_Q = .0022$, RUN 159
△ " + " , $q = 40$ LB/FT$^2$, $C_Q = .0027$, " 160
□ " + " , $q = 20$ LB/FT$^2$, $C_Q = .0039$, " 161
MAXIMUM LIFT, CONFIGURATION $S_{15} + B^2$
$C_L$
$C_D$
$C_{m_{c/4}}$
$\alpha$
0°
4°
8°
12°
16°
20°
0
2
4
6
8
10
20
30
10
0
10

PAGE 33
FIG. 7

$\phi_H = 0°$, $V_S = 1330$ FT/SEC

| | | | | |
|---|---|---|---|---|
| ○ | $S_{15} + B^{A}_{44.7}$, | $q = 60$ LB/FT$^2$, | $C_Q = .0043$, | RUN 196 |
| △ | " + " , | $q = 50$ LB/FT$^2$, | $C_Q = .0048$, | " 195 |
| □ | " + " , | $q = 45$ LB/FT$^2$, | $C_Q = .0050$, | " 194 |
| ▽ | " + " , | $q = 40$ LB/FT$^2$, | $C_Q = .0053$, | " 193 |
| ◇ | " + " , | $q = 30$ LB/FT$^2$, | $C_Q = .0061$, | " 192 |
| X | " + " , | $q = 20$ LB/FT$^2$, | $C_Q = .0076$, | " 191 |

MAXIMUM LIFT, CONFIGURATION $S_{15} + B^{A}_{44}$

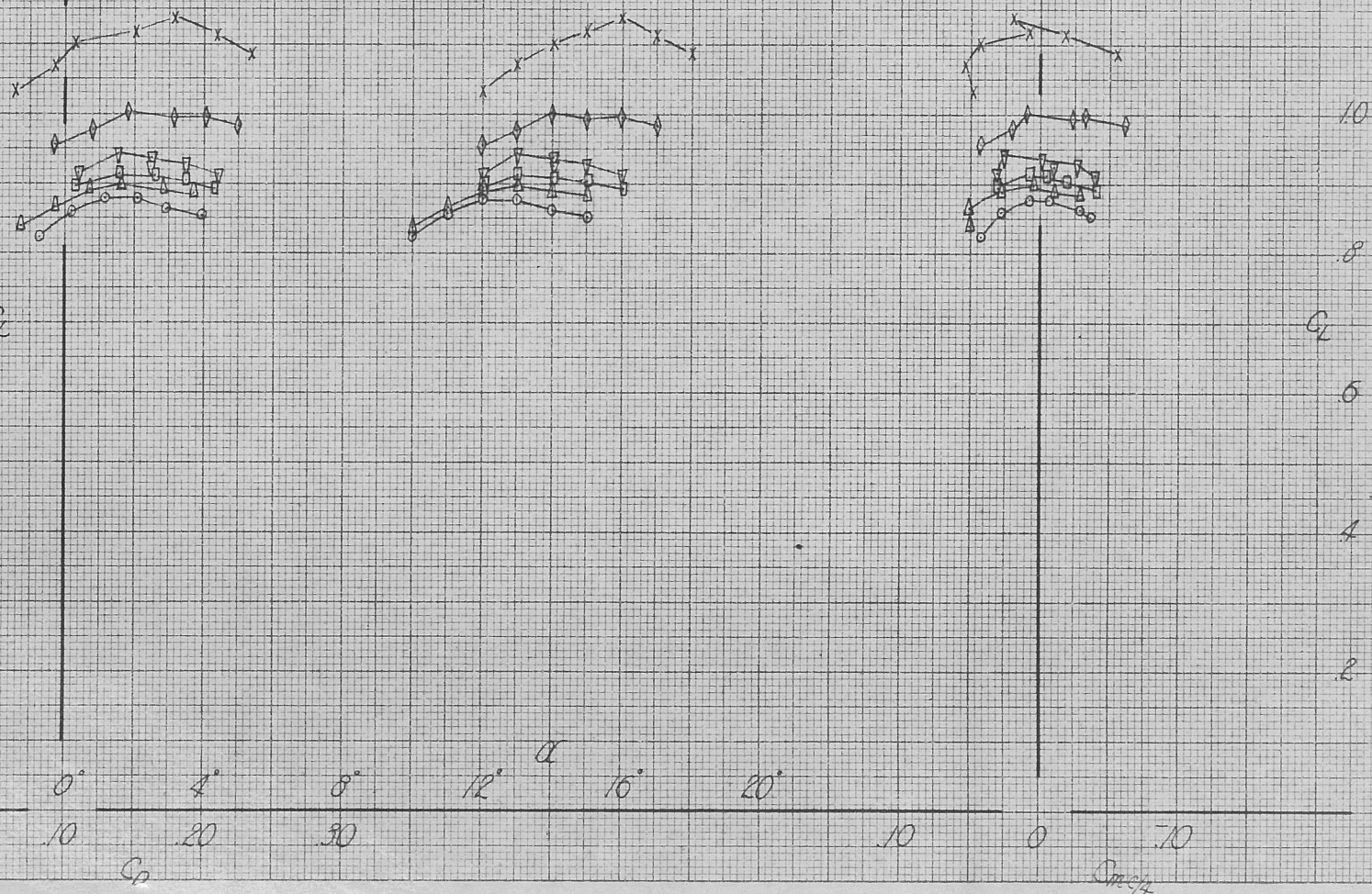


PAGE 34
FIG 8

MAXIMUM LIFT, CONFIGURATION $S_{15}+B^{7}$

$q = 60 LB/FT^2$, $i_t = 0°$

- o $S_{15} + B^{7}_{2,4,7}$, $C_Q = .0041$, $V_S = 910 FT/SEC$, RUN 9
- Δ " $+ B^{7}_{2,4,7}$, $C_Q = .0057$, $V_S = 1190 FT/SEC$, " 8
- □ " $+ B^{7}_{4,4,7}$, $C_Q = .0070$, $V_S = 1330 FT/SEC$, " 7

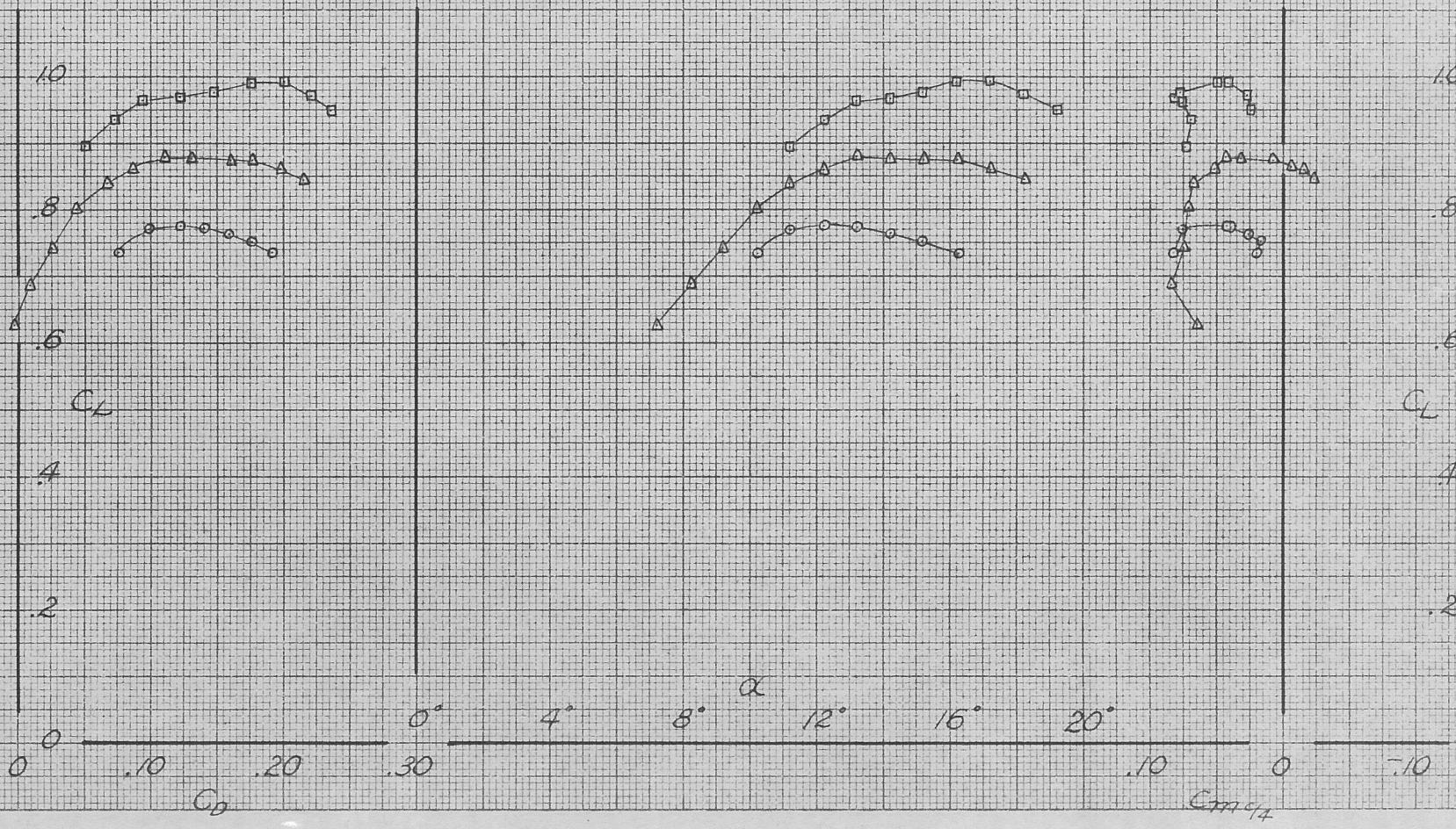

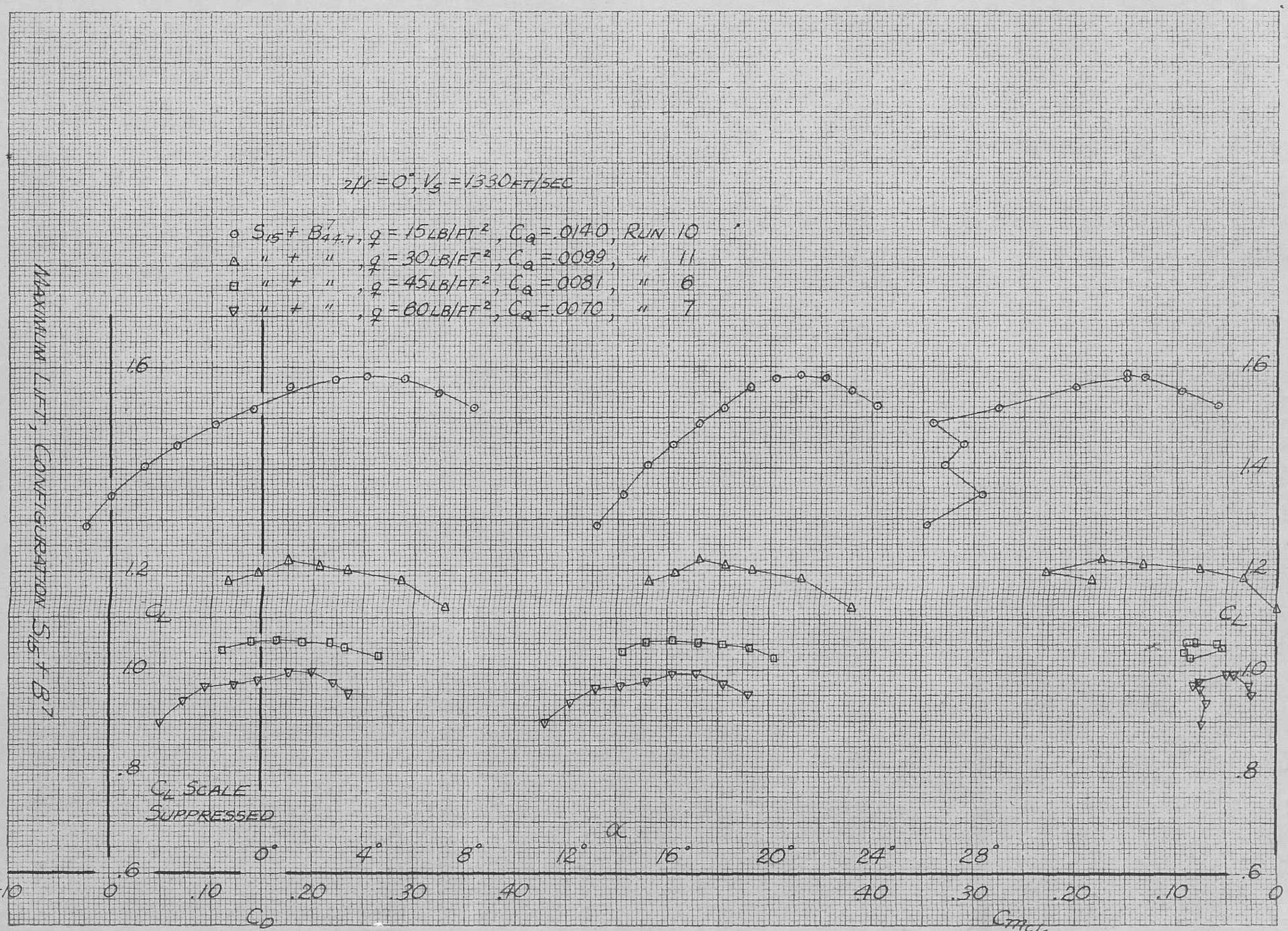
$z/r = 0°$, $V_s = 1330$ FT/SEC
○ $S_{15} + B^{7}_{4\,1.7}$, $q = 15$ LB/FT², $C_Q = .0140$, RUN 10
△ " + " , $q = 30$ LB/FT², $C_Q = .0099$, " 11
□ " + " , $q = 45$ LB/FT², $C_Q = .0081$, " 6
▽ " + " , $q = 60$ LB/FT², $C_Q = .0070$, " 7
MAXIMUM LIFT, CONFIGURATION $S_{15} + B^{7}$
$C_L$
1.6
1.4
1.2
1.0
.8
.6
$C_L$ SCALE SUPPRESSED
$\alpha$
0° 4° 8° 12° 16° 20° 24° 28°
-.10 0 .10 .20 .30 .40
$C_D$
.40 .30 .20 .10 0
$C_{m_{c/4}}$

MAXIMUM LIFT, CONFIGURATION $S_{15} + B_7$

$i_t = 0°$

- ⊙ $S_{15} + B^7_{24.1}$, $q = 60$ LB/FT$^2$, $C_Q = .0037$, $V_S = 910$ FT/SEC, RUN 133
- △ " $+ B^7_{34.1}$, " , $C_Q = .0053$, $V_S = 1190$ FT/SEC, " 132
- □ " $+ B^7_{29.1}$, " , $C_Q = .0061$, $V_S = 1250$ FT/SEC, " 131
- ▽ " $+ B^7_{44.1}$, " , $C_Q = .0070$, $V_S = 1330$ FT/SEC, " 128
- ◇ " $+$ " , $q = 40$ LB/FT$^2$, $C_Q = .0085$, " , " 129
- × " $+$ " , $q = 20$ LB/FT$^2$, $C_Q = .0121$, " , " 130

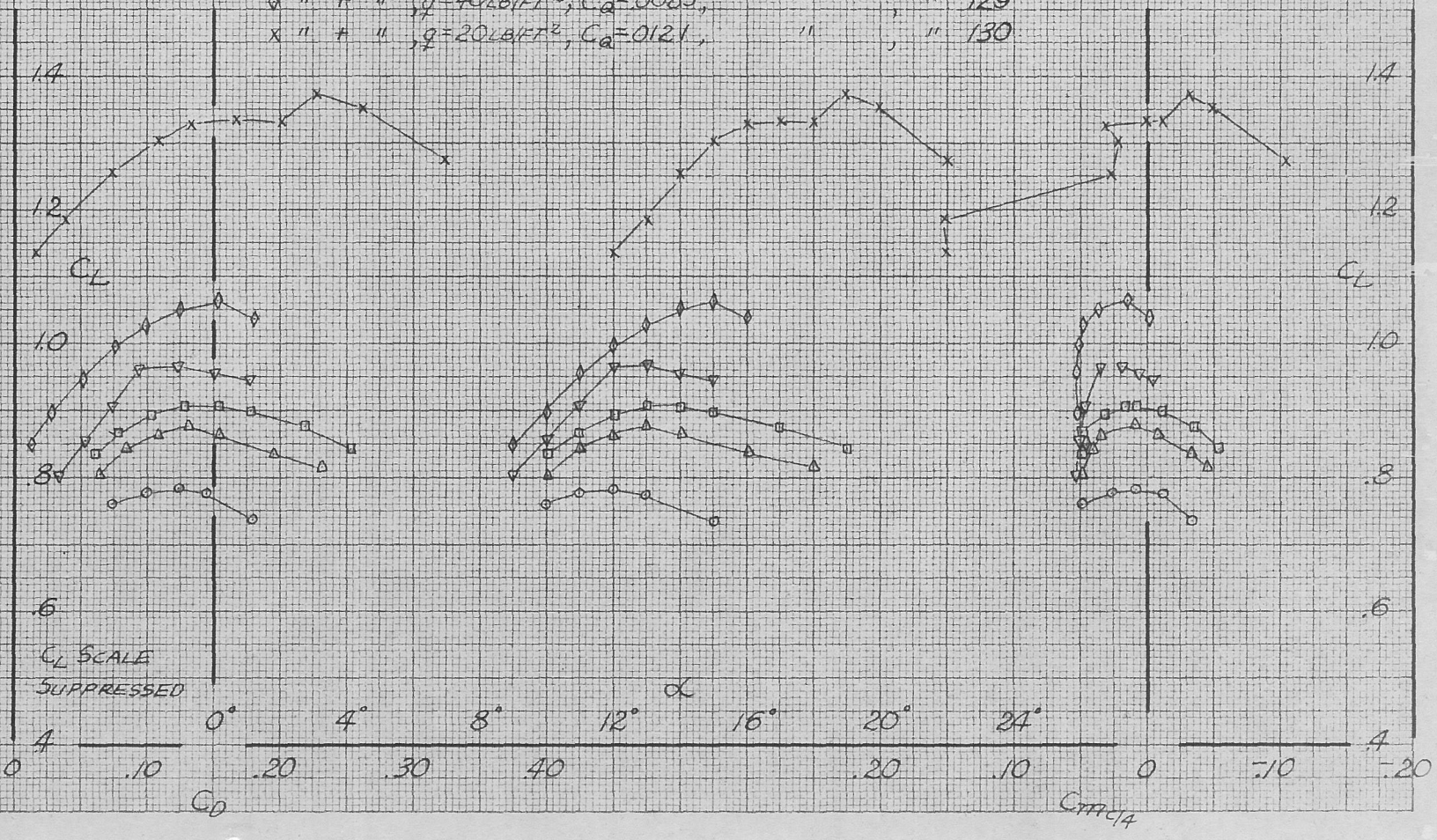


PAGE 37
FIG. 11

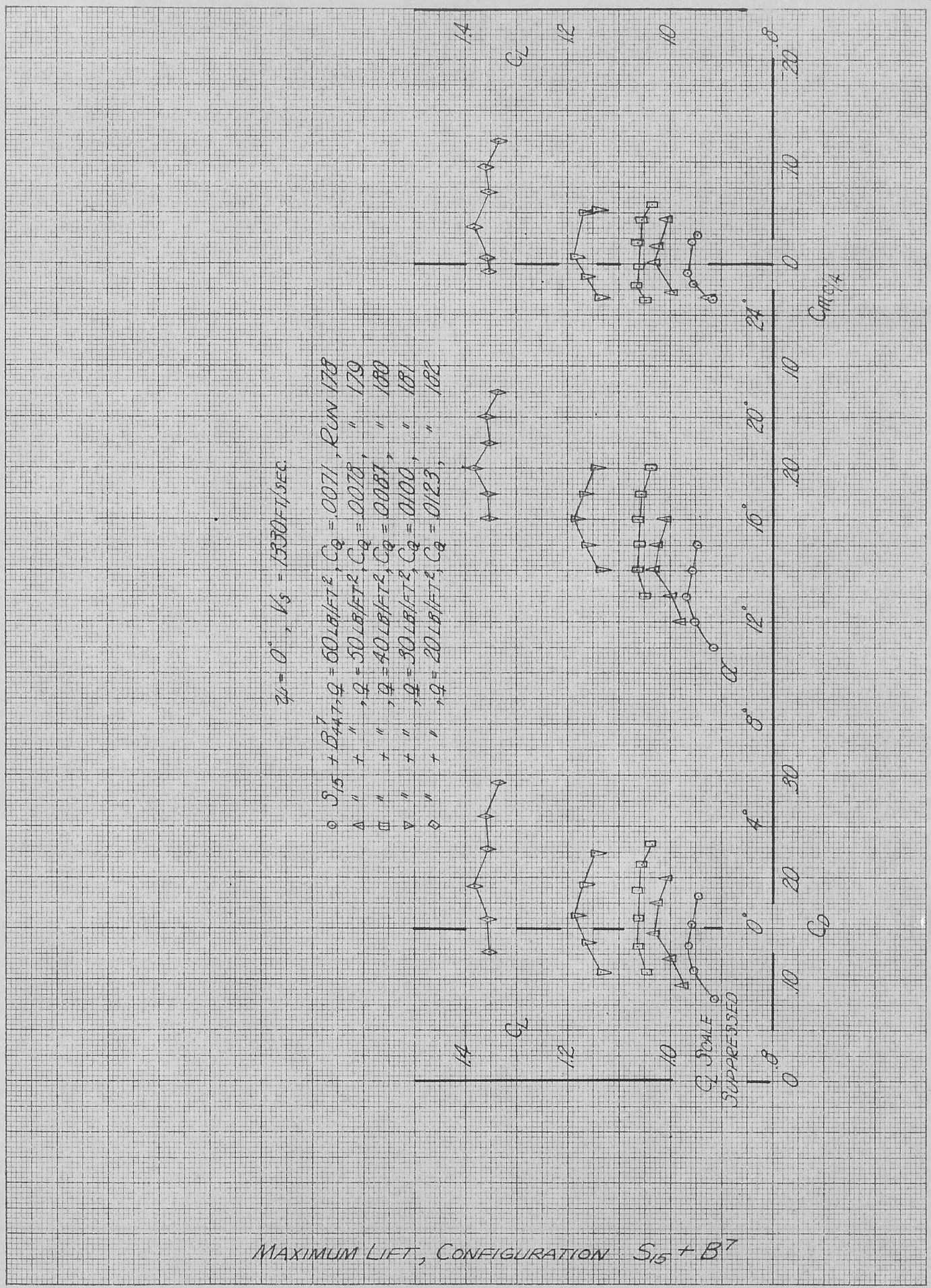


MAXIMUM LIFT, CONFIGURATION $S_{15} + B^7$

$\psi = 0°$, $V_S = 1330$ FT/SEC

○ $S_{15} + F_N^{140} + B^2_{44T}$, $q = 60$ LB/FT$^2$, $C_Q = .0022$, RUN 152
△ " + " + " , $q = 40$ LB/FT$^2$, $C_Q = .0027$, " 154
□ " + " + " , $q = 20$ LB/FT$^2$, $C_Q = .0039$, " 155

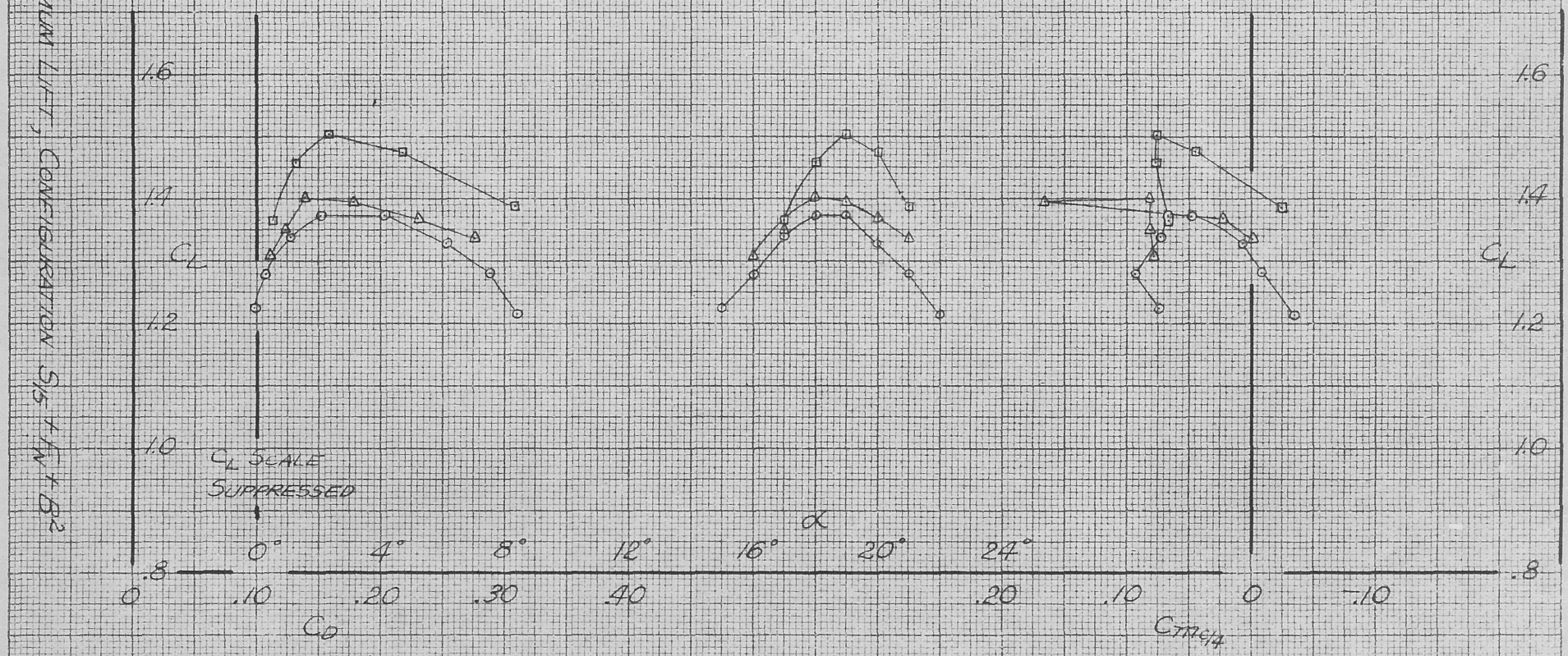


PAGE 39
FIG. 13

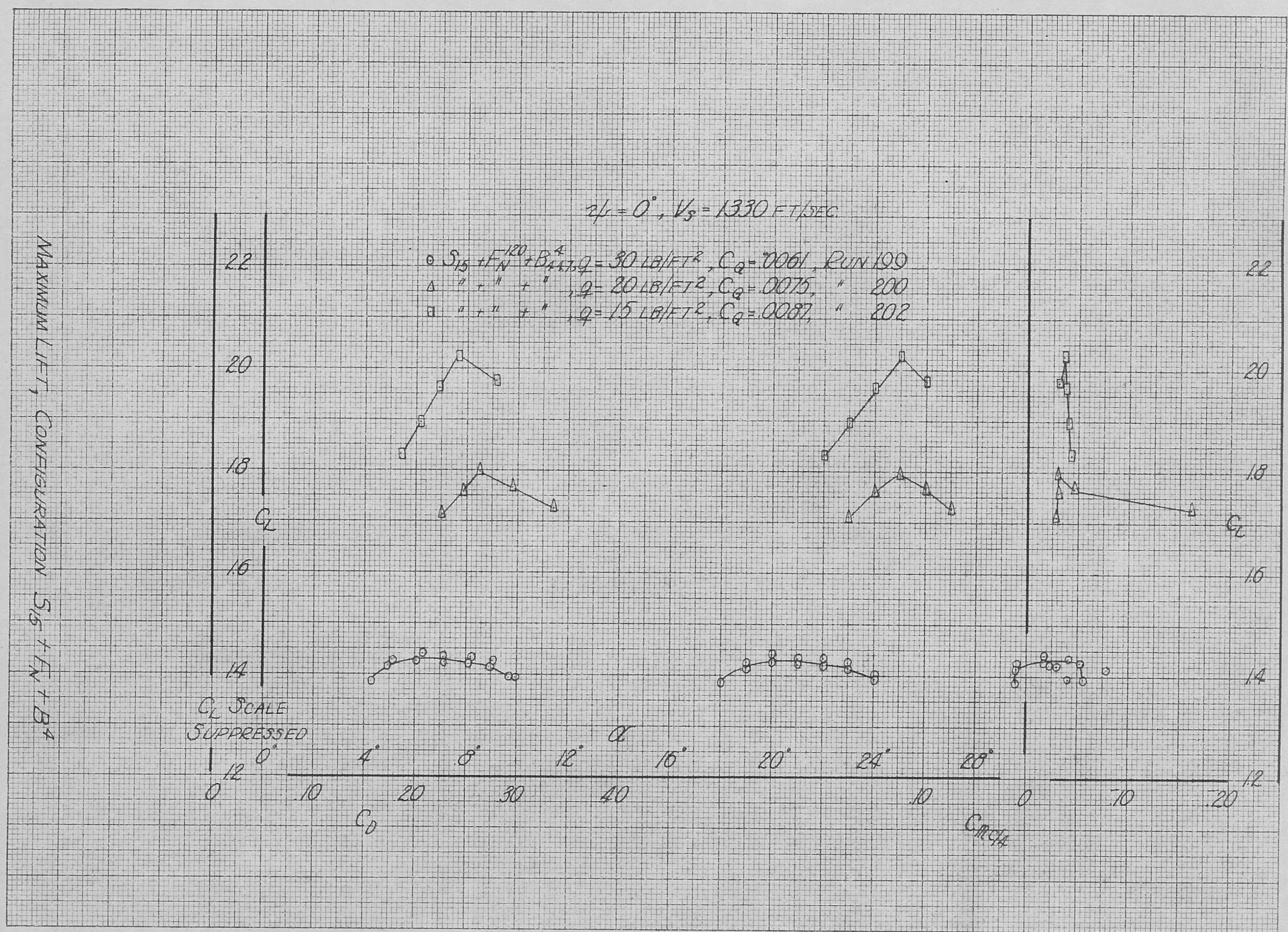


PAGE 40
FIG. 14

$S_{15}+F_N^{140}+B_{247}^{4}$, $q=60$ LB/FT$^2$, $C_a=.0024$, $V_s=910$ FT/SEC, RUN 168
" " " $B_{347}^{4}$, " $C_a=.0032$, $V_s=1190$ FT/SEC, " 167
" " " $B_{347}^{4}$, " $C_a=.0037$, $V_s=1250$ FT/SEC, " 116
" " " $B_{347}^{4}$, " $C_a=.0042$, $V_s=1330$ FT/SEC, " 163
" " " $B_{347}^{4}$, " $C_a=.0052$, " " 164
" " " " $q=40$ LB/FT$^2$, $C_a=.0052$, " " 165
" " " " $q=20$ LB/FT$^2$, $C_a=.0073$, " "
$\gamma\gamma=0°$
$\alpha$
$C_L$
$C_D$
$C_L$ SCALE SUPPRESSED
MAXIMUM LIFT, CONFIGURATION $S_{15}+F_N+B^4$

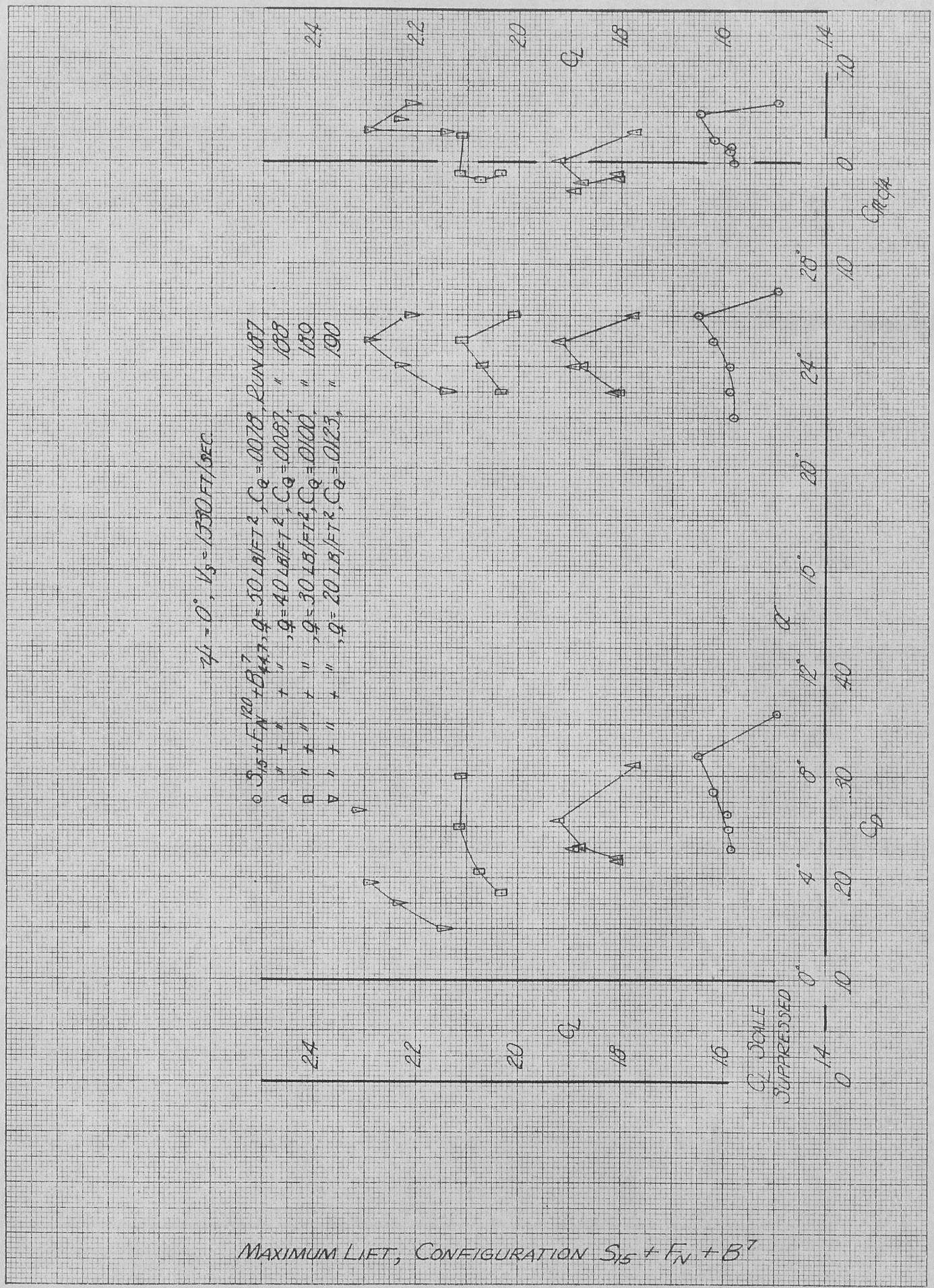


MAXIMUM LIFT, CONFIGURATION $S_{15}+F_N+B^7$

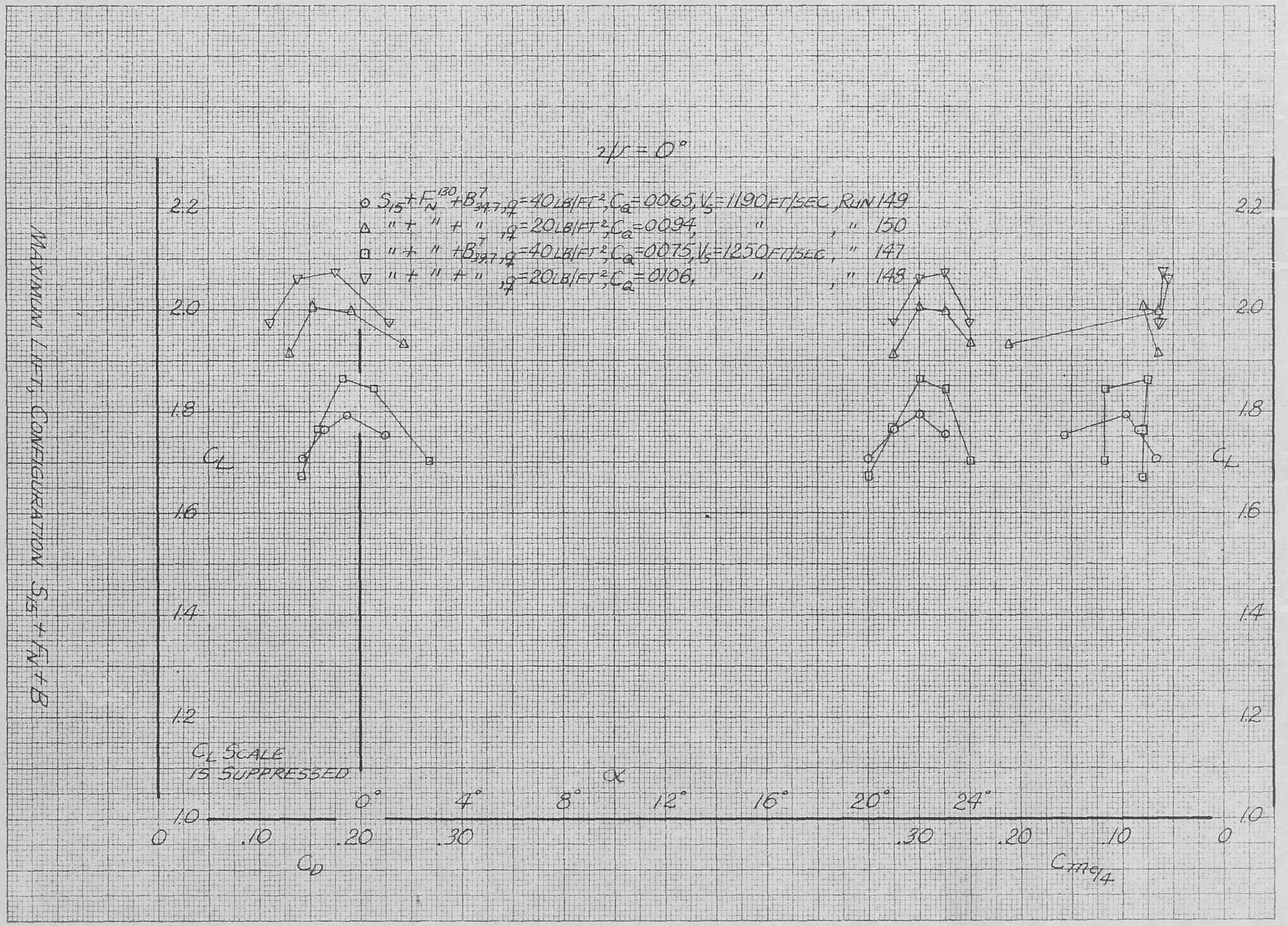


PAGE 83
FIG. 17

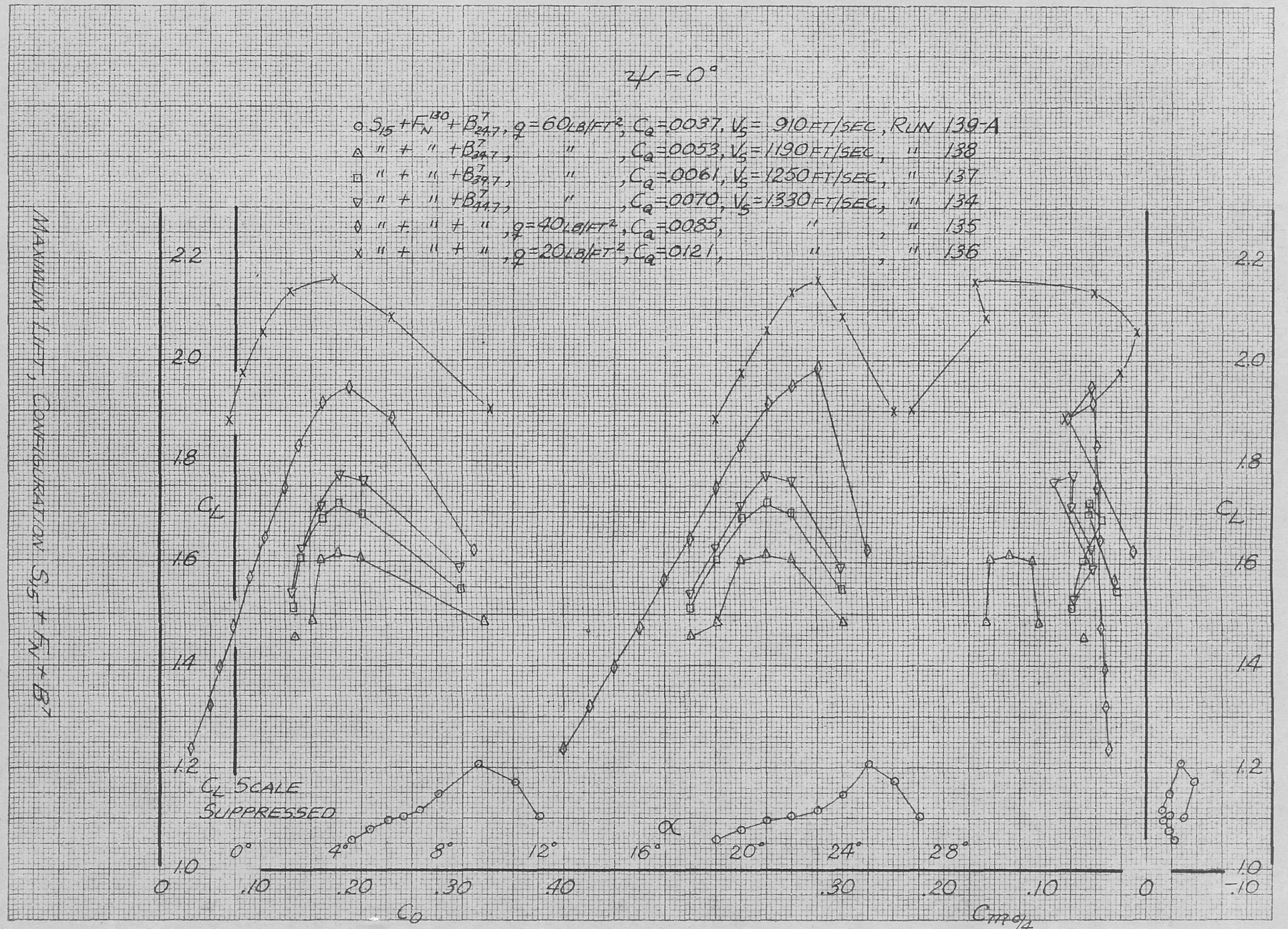


PAGE 44
FIG 18

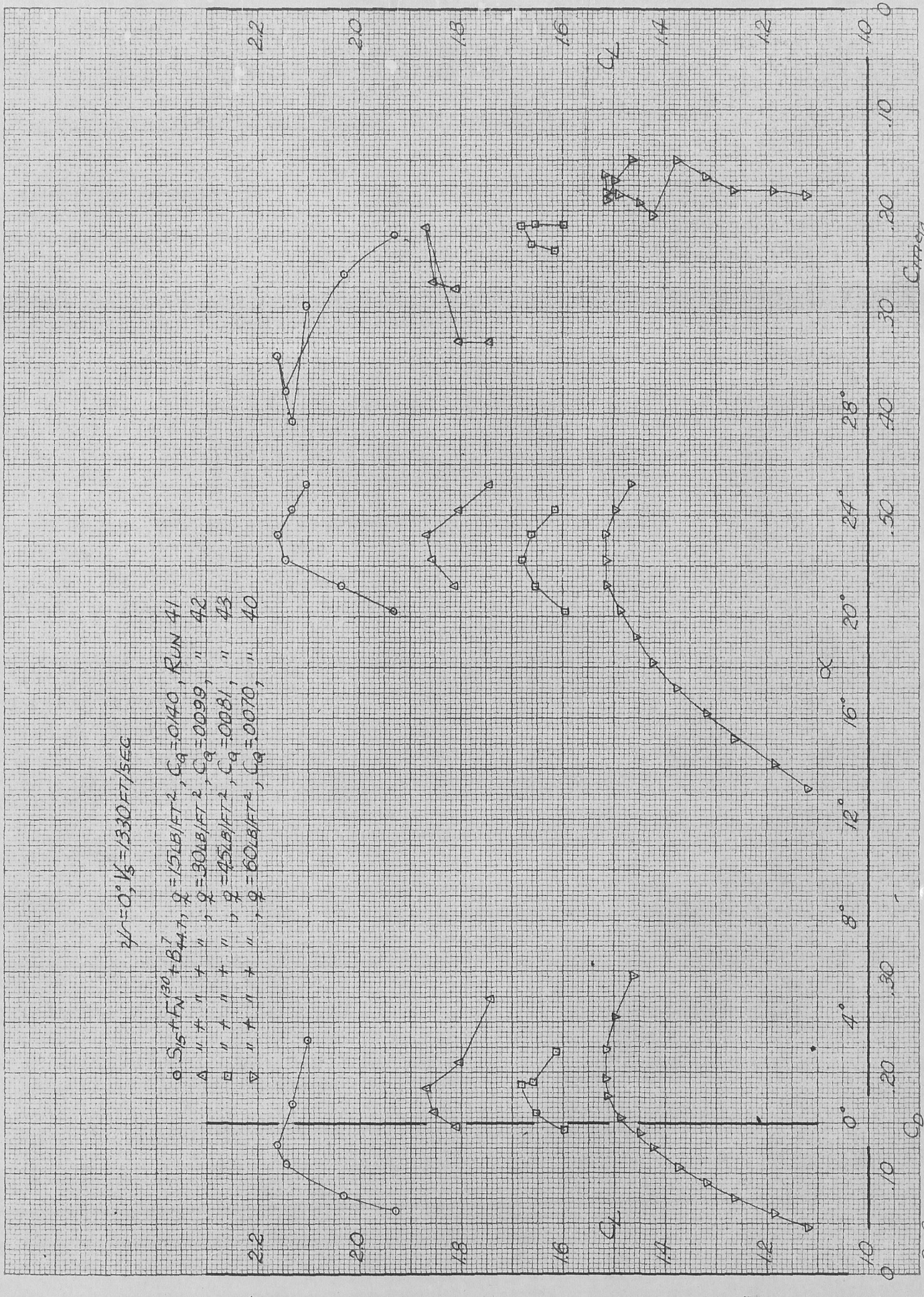


MAXIMUM LIFT, CONFIGURATION $S_{15}+F_N+B^7$

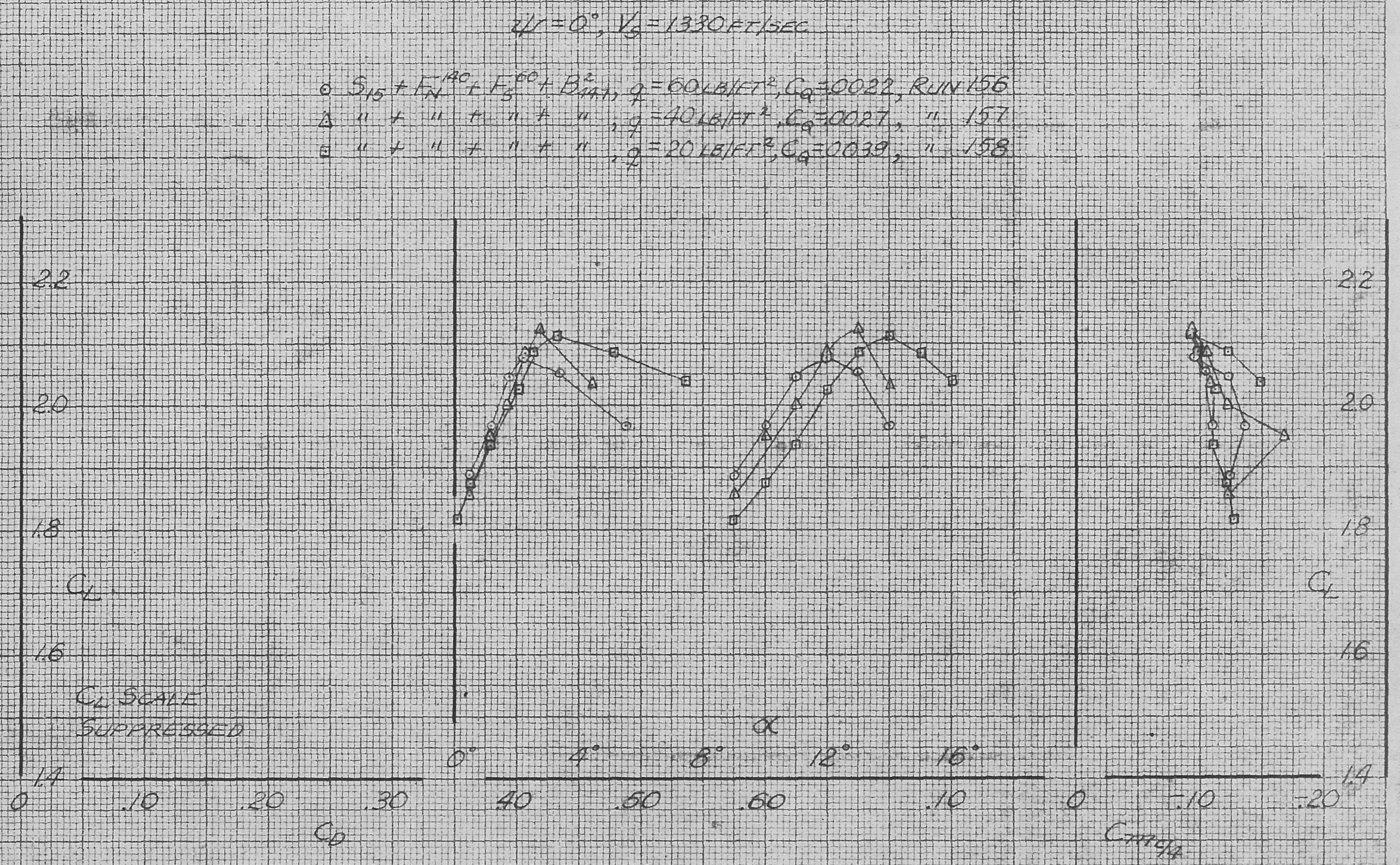


MAXIMUM LIFT, CONFIGURATION $S_{15} + F_M + F_S + B^2$

MAXIMUM L/ET, CONFIGURATION $S_{16} + F_N + F_S + B_4$

$\psi = 0°$, $V_S = 1330$ FT/SEC

○ $S_{16} + F_N^{120} + F_S^{60} + B_{447}^{A}$, $q = 40$ LB/FT$^2$, $C_Q = .0053$, RUN 201
△ " + " + " + " , $q = 30$ LB/FT$^2$, $C_Q = .0061$, " 198
□ " + " + " + " , $q = 20$ LB/FT$^2$, $C_Q = .0075$, " 197

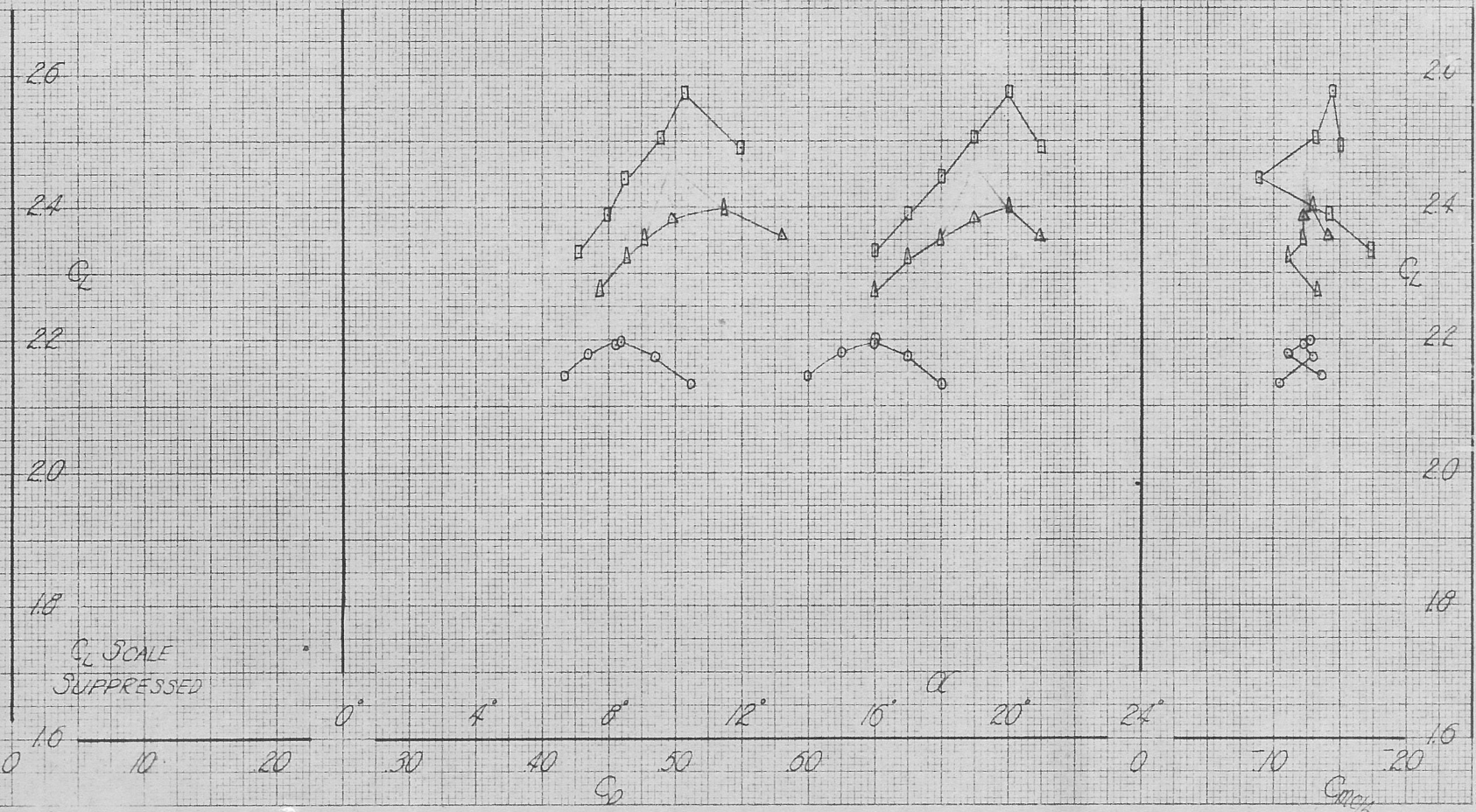


PAGE 47
FIG 21

MAXIMUM LIFT, CONFIGURATION $S_{15}+H_{2N}+F_5+B^4$
$C_L$ SCALE SUPPRESSED
$C_L$
$C_D$
$C_m$
$\alpha$
$\delta_e$
$\delta_e = 0°$ FOR ALL RUNS
○ $\delta_{F_{120}} + \delta_{F_{60}} + \delta_{F_{30}} + \delta_{N_{30}} + \delta_{N_{60}}$, $q = 60$ LBS/FT², $C_D = .0024$, $N_R = 910,000$, EQUALS
△ " + " + " + " + " + " , " = 80 " " , " = .0032, " = 1190 " , " 117
□ " + " + " + " + " + " , " = 100 " " , " = .0037, " = 1450 " , " 113
◇ " + " + " + " + " + " , " = 40 " " , " = .0042, " = 1300 " , " 109
▽ " + " + " + " + " + " , " = 20 " " , " = .0052, " = " " 111
× " + " + " + " + " + " , " = 10 " " , " = .0073, " = " " 112

MAXIMUM LIFT, CONFIGURATION $S_{15} + F_N + F_S + B_7$

$\psi = 0^\circ$, $V_\infty = 1330$ FT/SEC

○ $S_{15} + F_N^{120} + F_S^{60} + B_{447}^{7}$, $q = 50$ LB/FT$^2$, $C_Q = .0078$, RUN 186
△ " + " + " + ", $q = 40$ LB/FT$^2$, $C_Q = .0087$, " 185
□ " + " + " + ", $q = 30$ LB/FT$^2$, $C_Q = .0100$, " 184
▽ " + " + " + ", $q = 20$ LB/FT$^2$, $C_Q = .0123$, " 183

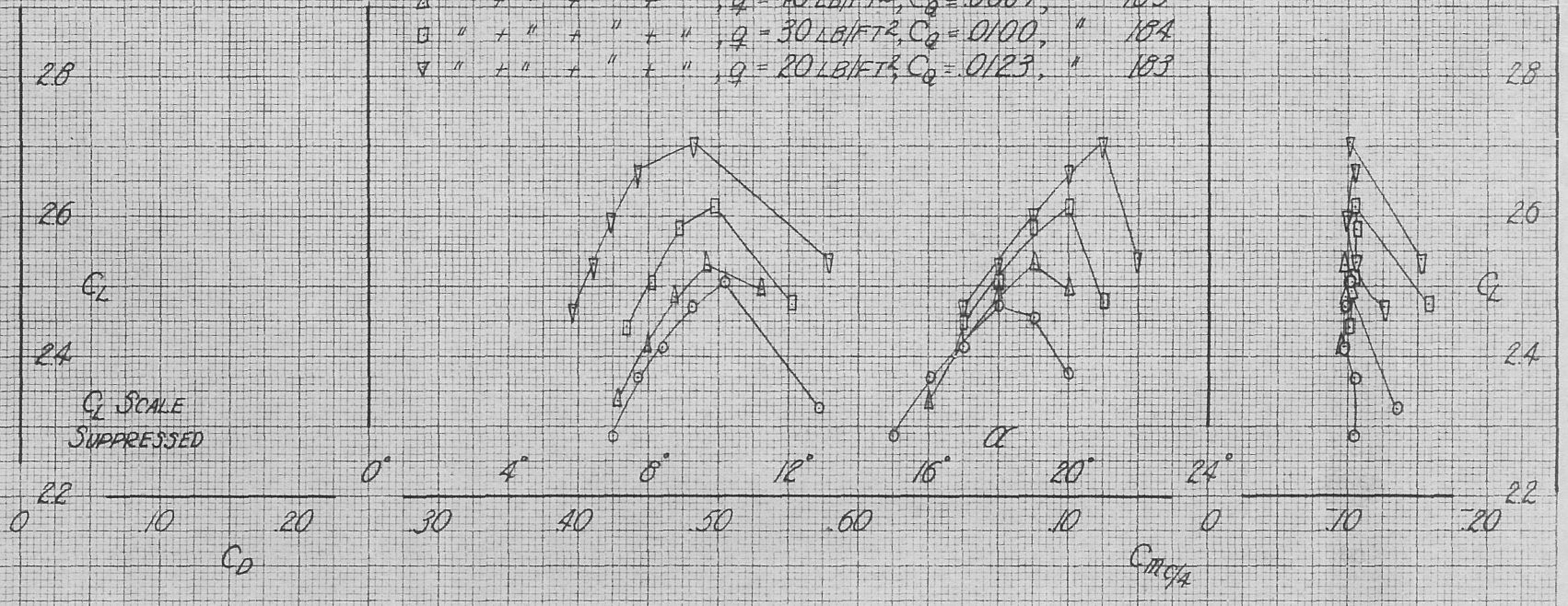

MAXIMUM LIFT, CONFIGURATION $S_{15}+F_N+F_S+B_7$

$\gamma/r = 0°$

- ⊙ $S_{15}+F_N^{130}+F_S^{60}+B_{247}^{7}$, $q = 60\ LB/FT^2$, $C_a = .0037$, $V_S = 910\ FT/SEC$, RUN 146
- △ " + " + " + $B_{347}^{7}$, " , $C_a = .0053$, $V_S = 1190\ FT/SEC$, " 145
- □ " + " + " + $B_{227}^{7}$, " , $C_a = .0061$, $V_S = 1250\ FT/SEC$, " 144
- ▽ " + " + " + $B_{147}^{7}$, " , $C_a = .0070$, $V_S = 1330\ FT/SEC$, " 140
- ◇ " + " + " + " , $q = 40\ LB/FT^2$, $C_a = .0085$, " , " 142
- × " + " + " + " , $q = 20\ LB/FT^2$, $C_a = .0121$, " , " 143

$C_L$ SCALE SUPPRESSED

$C_L$: 2.6, 2.4, 2.2, 2.0, 1.8

$C_D$: 0, .10, .20

$\alpha$: 0°, 4°, 8°, 12°, 16°, 20°, 24°

$C_L$: .26, 2.4, 2.2, 2.0, 1.8

$C_{m_{c/4}}$: 0, -.10, -.20

PAGE 5.0
FIG. 24

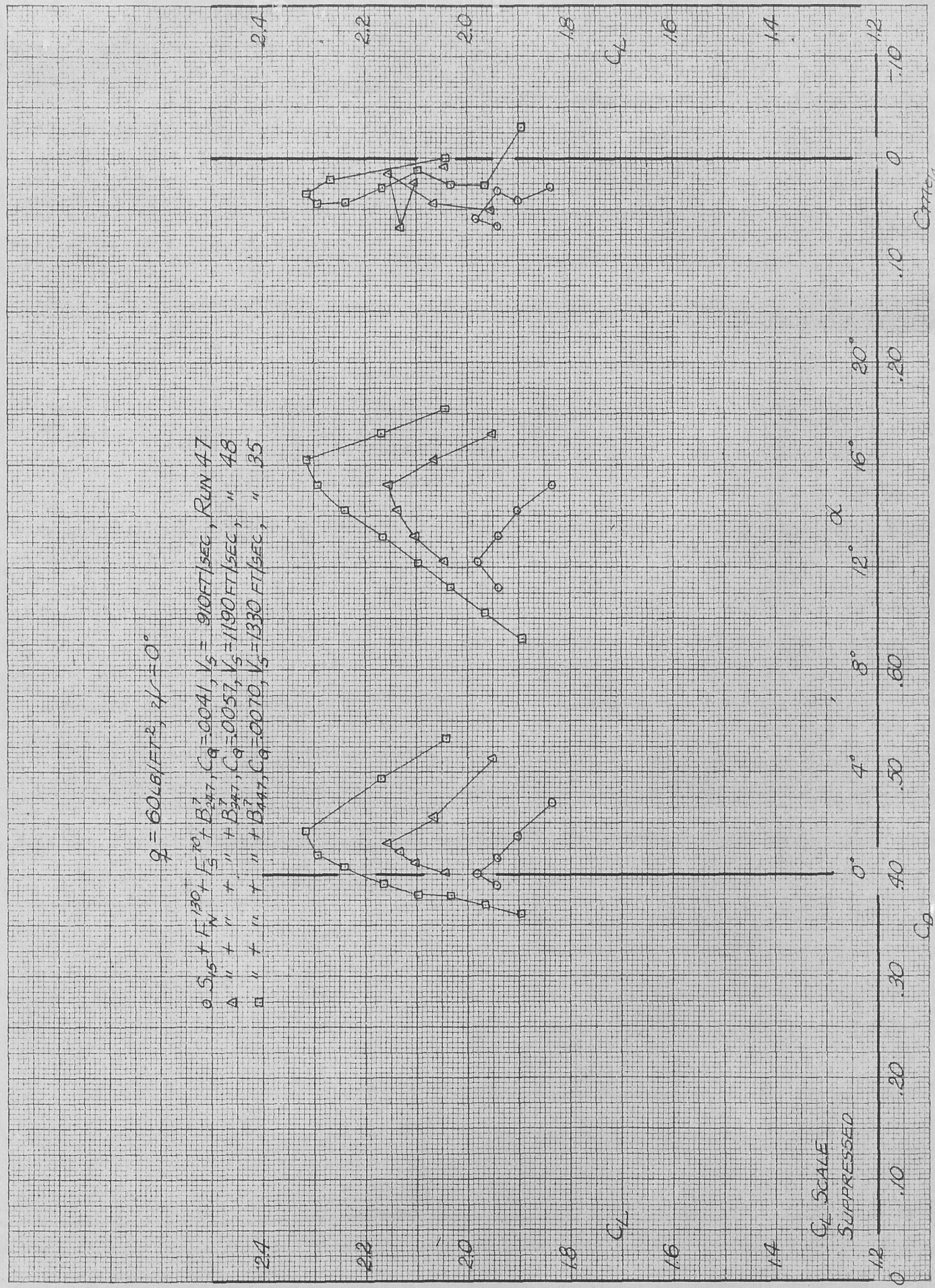


MAXIMUM LIFT, CONFIGURATION $S_{15} + F_N + F_S + B^7$

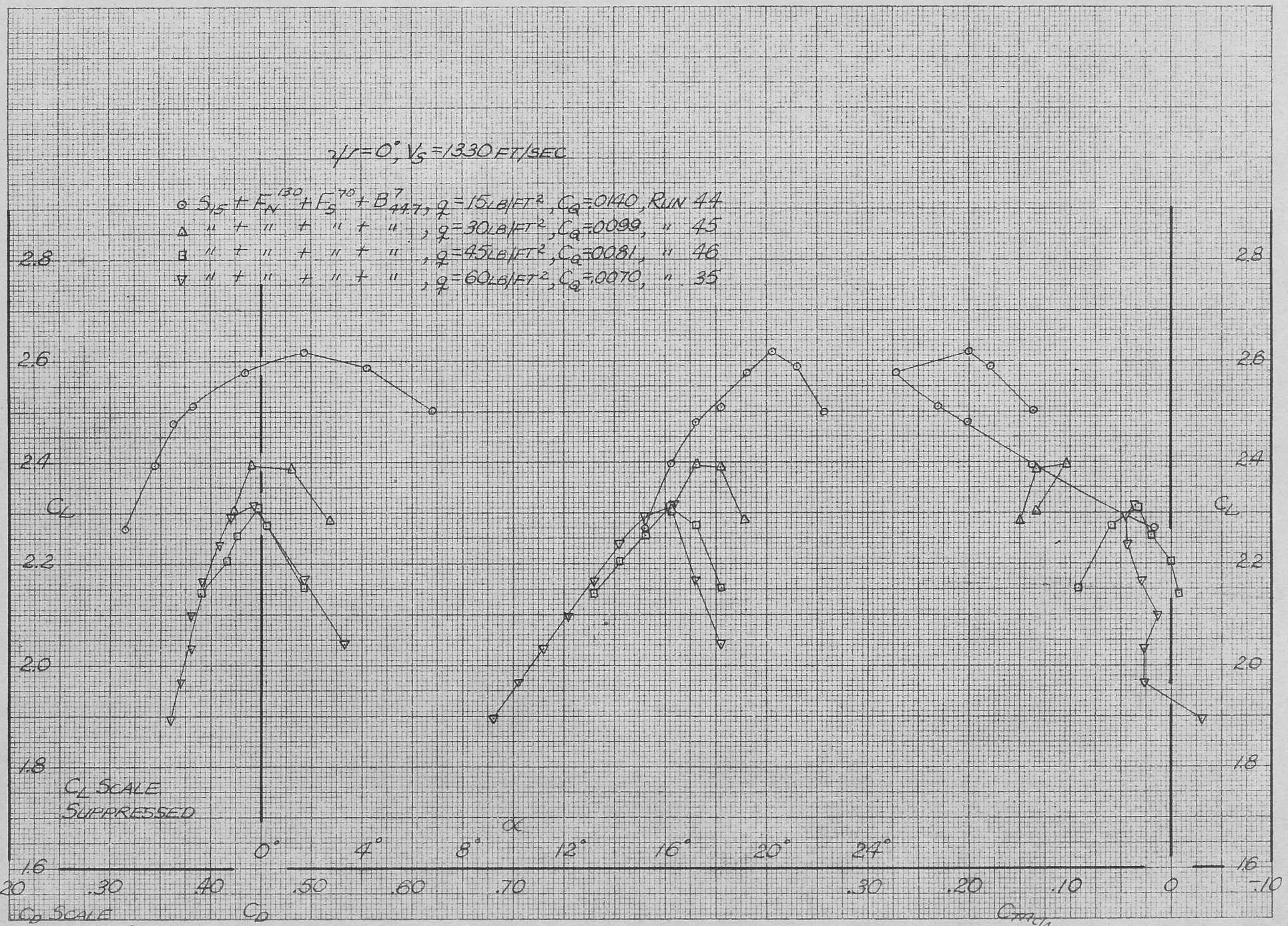


PAGE 52
FIG. 26

$i_t/r = 0°$

- ○ $S_{25} + B^2_{24.7}$, $q = 60$ LB/FT$^2$, $C_Q = .0014$, $V_S = 1190$ FT/SEC, RUN 90
- △ " $+ B^2_{39.7}$, " , $C_Q = .0015$, $V_S = 1250$ FT/SEC, " 89
- □ " $+ B^2_{44.7}$, " , $C_Q = .0017$, $V_S = 1330$ FT/SEC, " 86
- ▽ " + " , $q = 45$ LB/FT$^2$, $C_Q = .0019$, " , " 87
- ◇ " + " , $q = 30$ LB/FT$^2$, $C_Q = .0024$, " , " 88

MAXIMUM LIFT, CONFIGURATION $S_{25} + B^2$

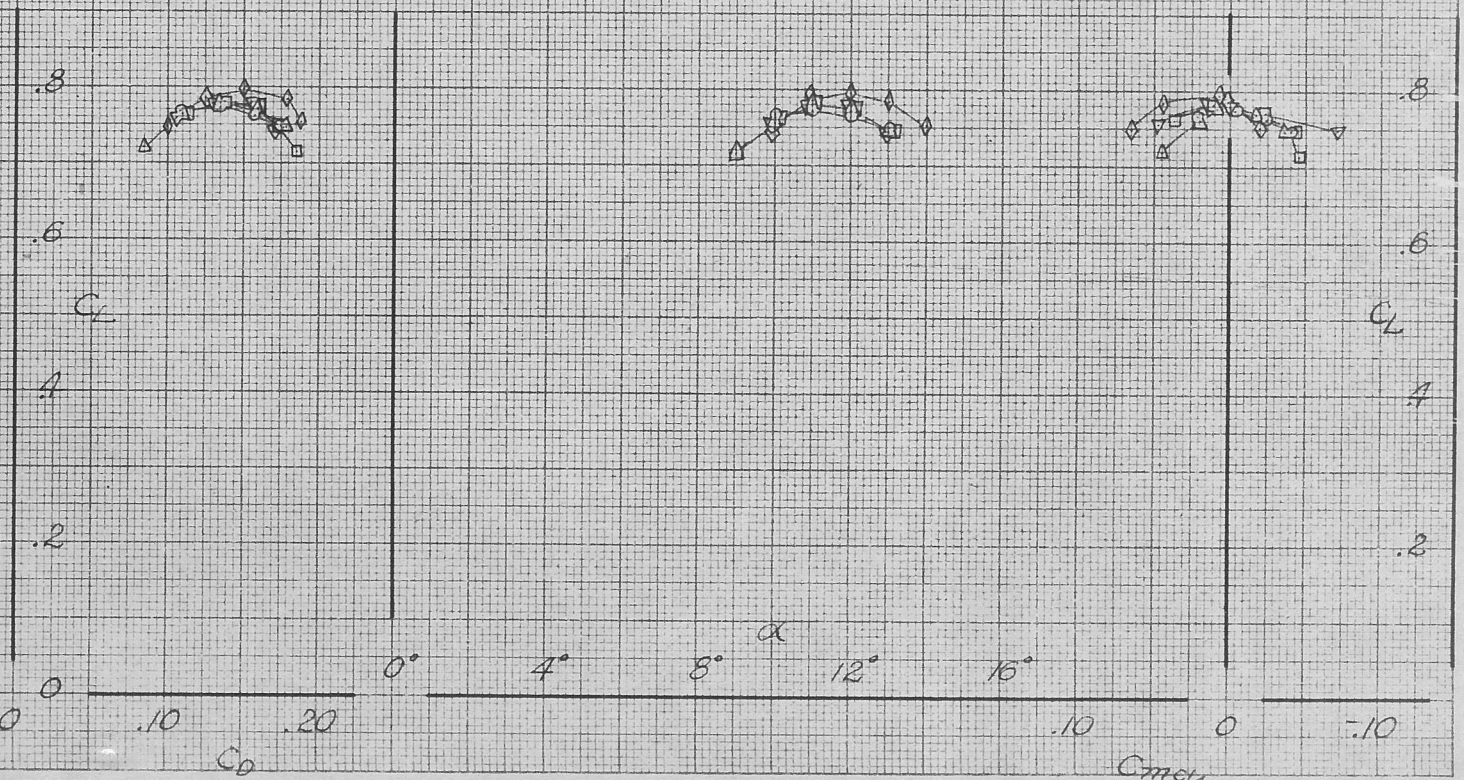

MAXIMUM LIFT, CONFIGURATION $S_{25} + B^4$

$i_t/r = 0°$

○ $S_{25} + B^{7}_{247}$, $q/r = 60$ LB/FT$^2$, $C_Q = .0047$, $V_S = 1190$ FT/SEC, RUN 98
△ " $+ B^{7}_{197}$, " , $C_Q = .0054$, $V_S = 1250$ FT/SEC, " 97
□ " $+ B^{7}_{147}$, " , $C_Q = .0060$, $V_S = 1330$ FT/SEC, " 94
▽ " + " , $q/r = 45$ LB/FT$^2$, $C_Q = .0069$, " , " 95
◇ " + " , $q/r = 30$ LB/FT$^2$, $C_Q = .0085$, " , " 96

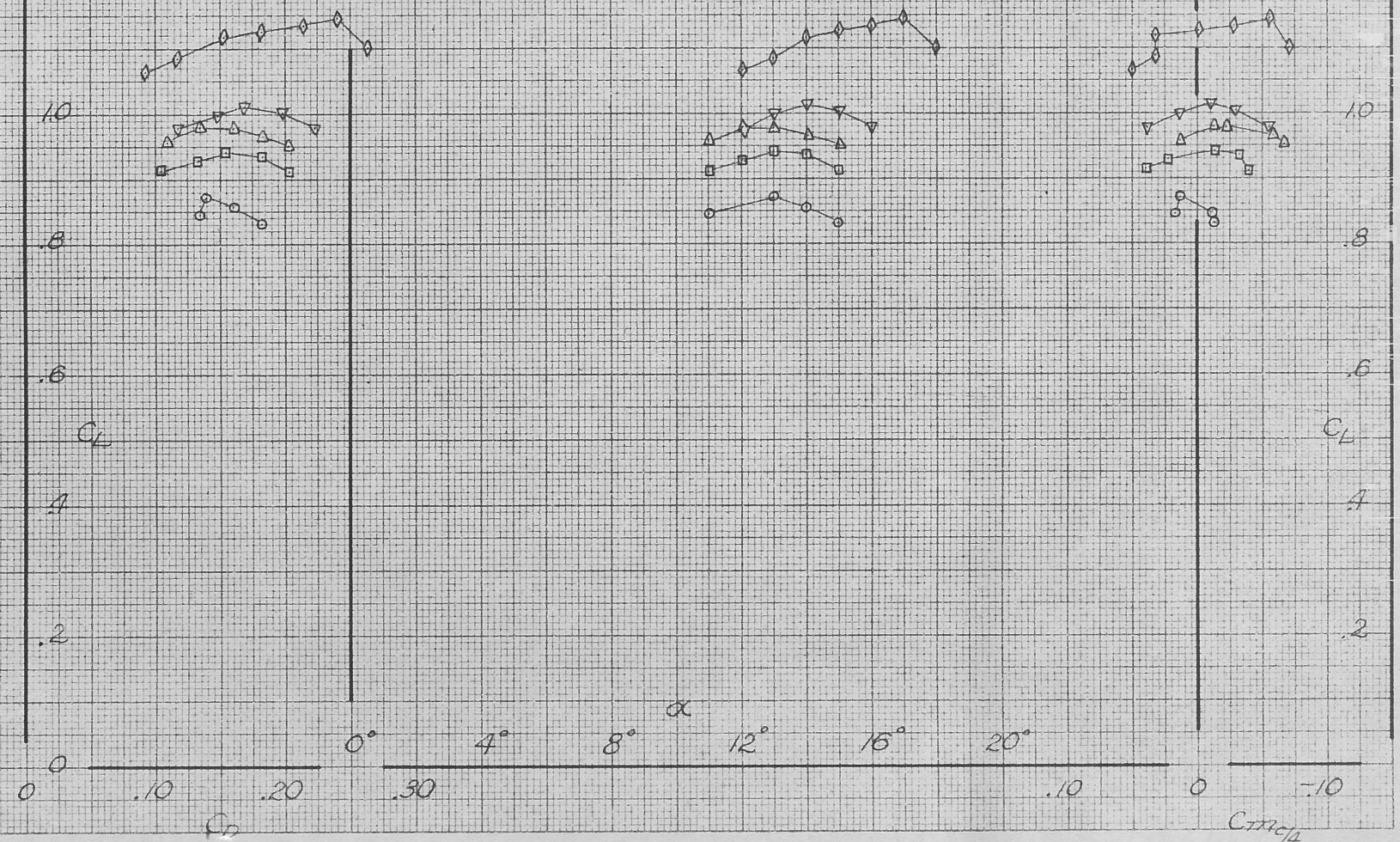


MAXIMUM LIFT, CONFIGURATION $S_{25} + B7$

$i_f = 0°$

- ○ $S_{35} + B^2_{347}$, $q = 60\ LB/FT^2$, $C_Q = .0030$, $V_S = 1190\ FT/SEC$, RUN 69
- △ " $+ B^2_{397}$, " , $C_Q = .0033$, $V_S = 1250\ FT/SEC$, " 68
- □ " $+ B^2_{447}$, " , $C_Q = .0036$, $V_S = 1330\ FT/SEC$, " 62
- ▽ " + " , $q = 45\ LB/FT^2$, $C_Q = .0041$, " , " 63
- ◇ " + " , $q = 30\ LB/FT^2$, $C_Q = .0051$, " , " 64

MAXIMUM LIFT, CONFIGURATION $S_{35} + B^2$

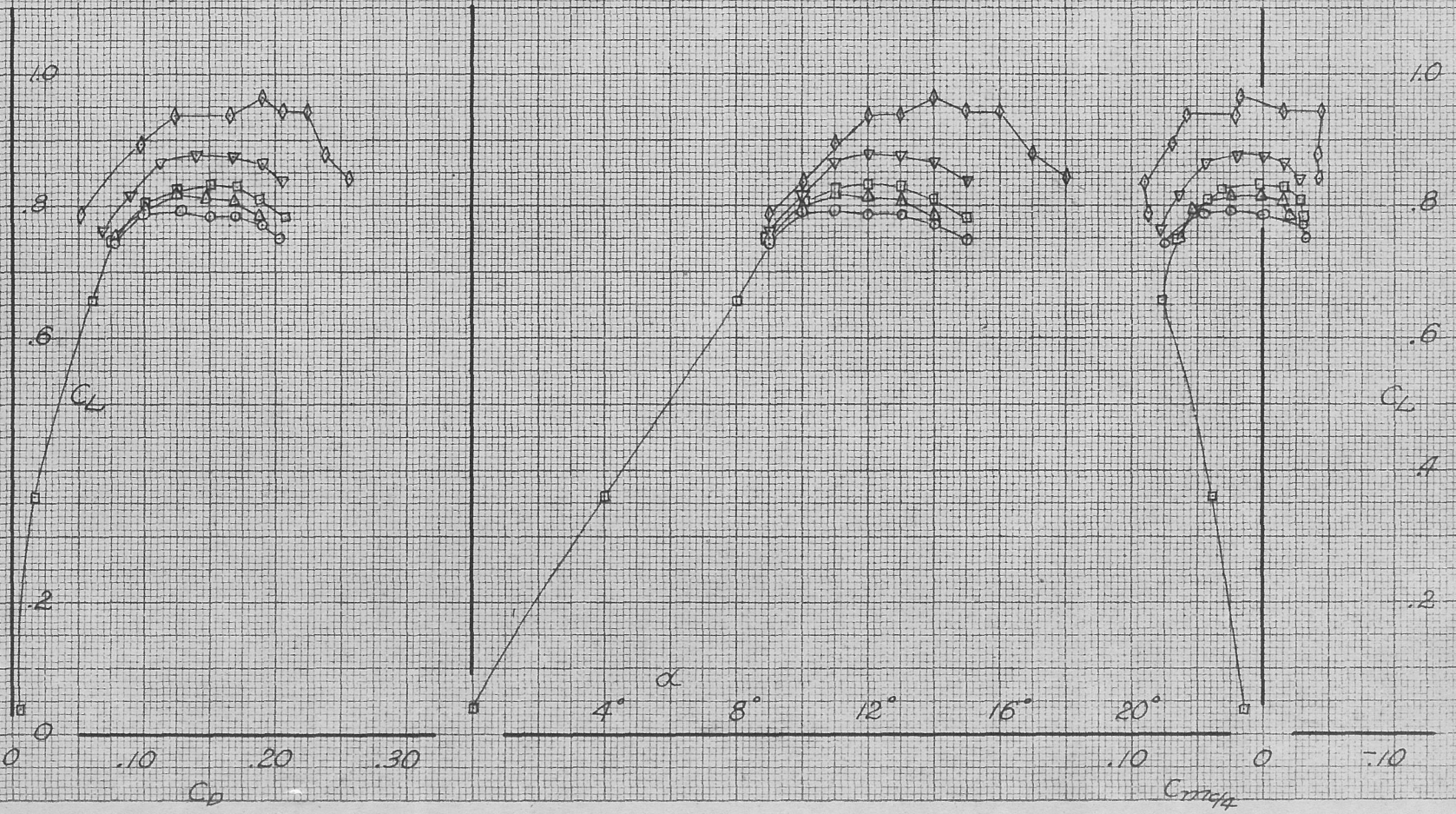

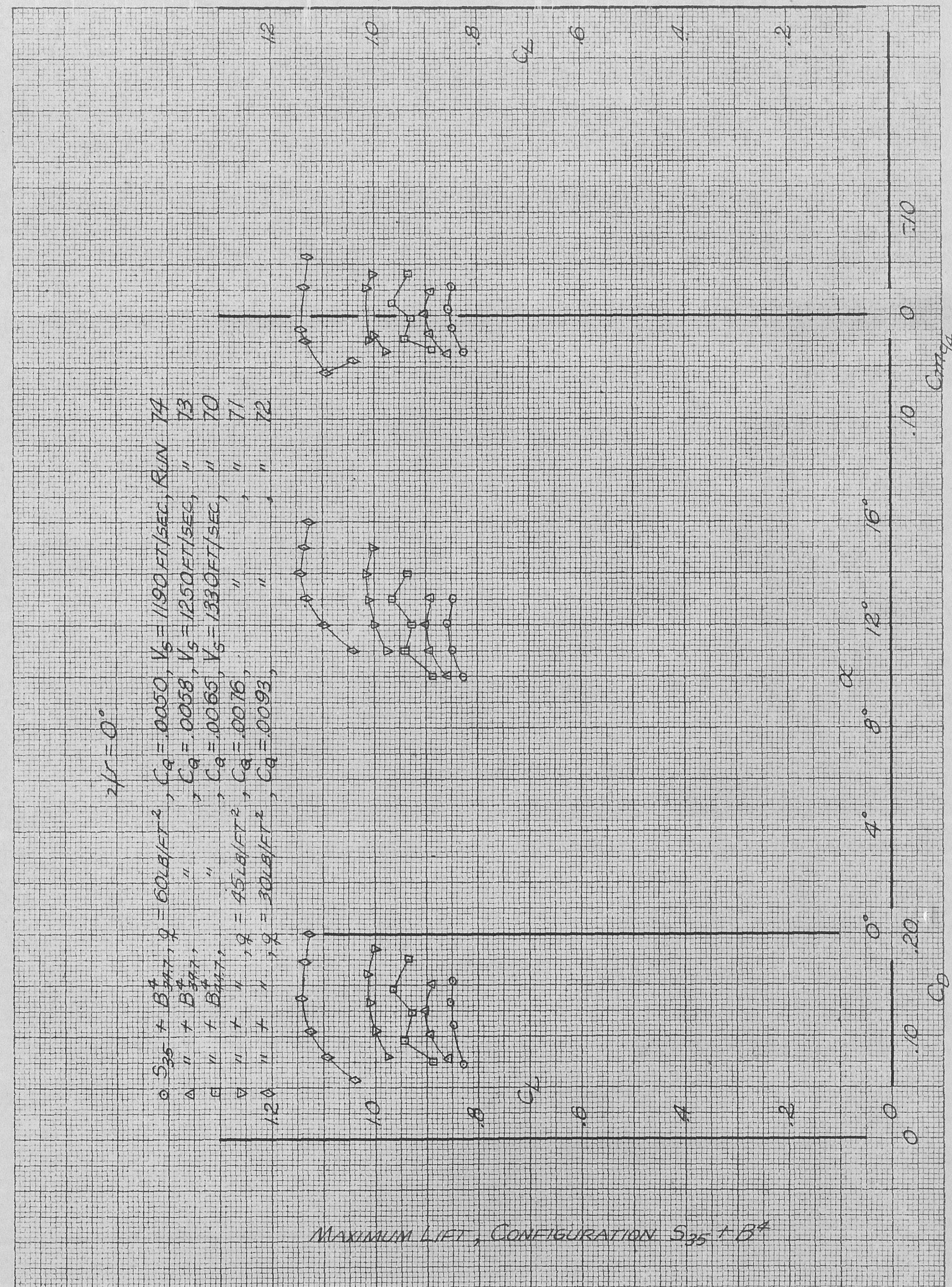


MAXIMUM LIFT, CONFIGURATION $S_{35} + B^4$

MAXIMUM LIFT, CONFIGURATION $S_{25}$ OR $S_{35} + F_N + B$

$\psi = 0°$, $q = 60$ LB/FT$^2$, $V_S = 1330$ FT/SEC

- ○ $S_{25} + F_5^{70} + B^2_{44.7}$, $C_a = .0017$, RUN 93
- △ " + " + $B^4_{44.7}$, $C_a = .0056$, " 85
- □ " + " + $B^7_{44.7}$, $C_a = .0060$, " 101
- ▽ $S_{35}$ + " + $B^2_{44.7}$, $C_a = .0036$, " 67
- ◇ " + " + $B^4_{44.7}$, $C_a = .0065$, " 77

MAXIMUM LIFT, CONFIGURATION, $S_{25}$ OR $S_{35} + F_5 + B$

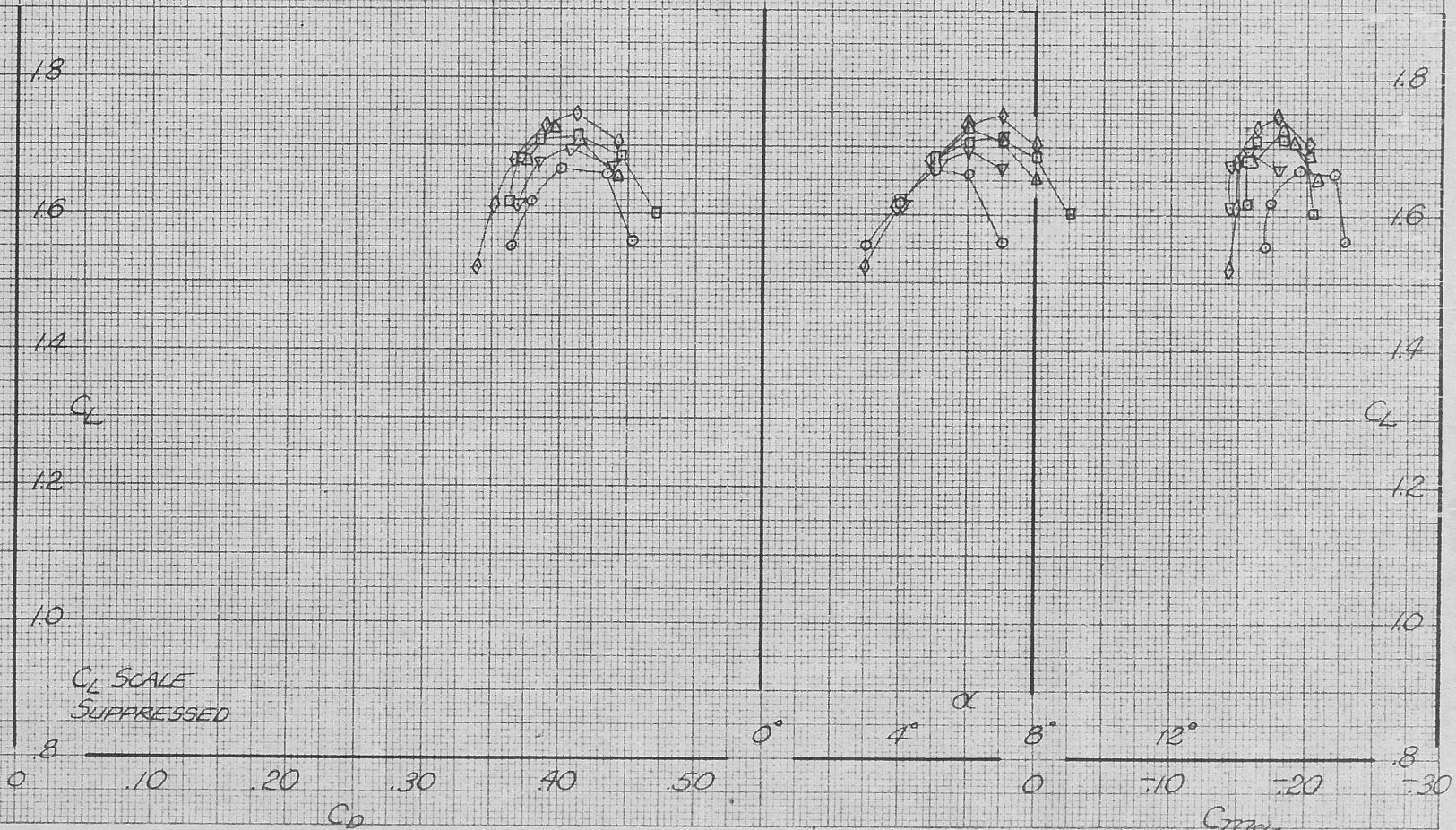

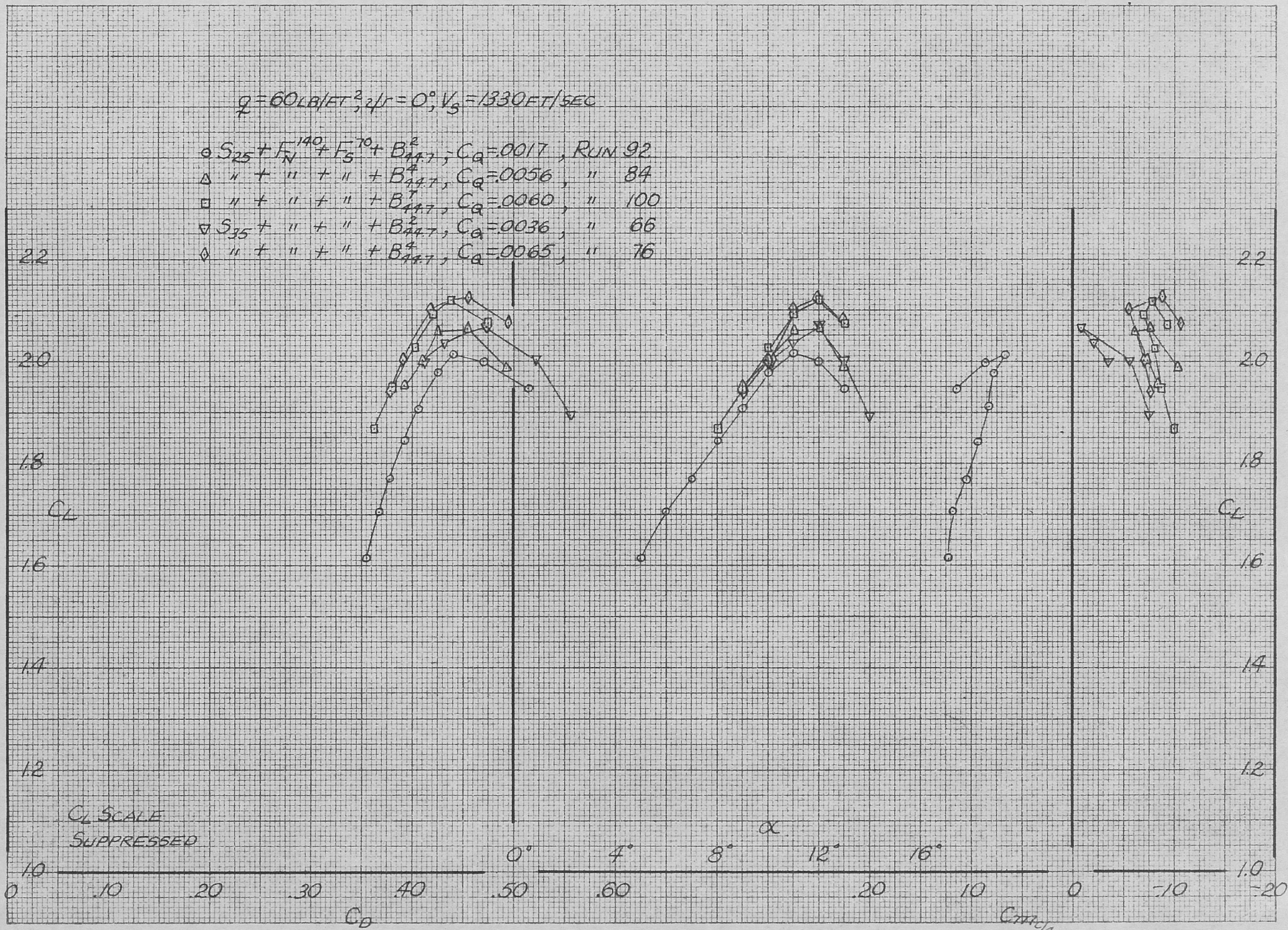


MAXIMUM LIFT, CONFIGURATION $S_{25}$ OR $S_{35}$ + $F_N$ + $F_S$ + B

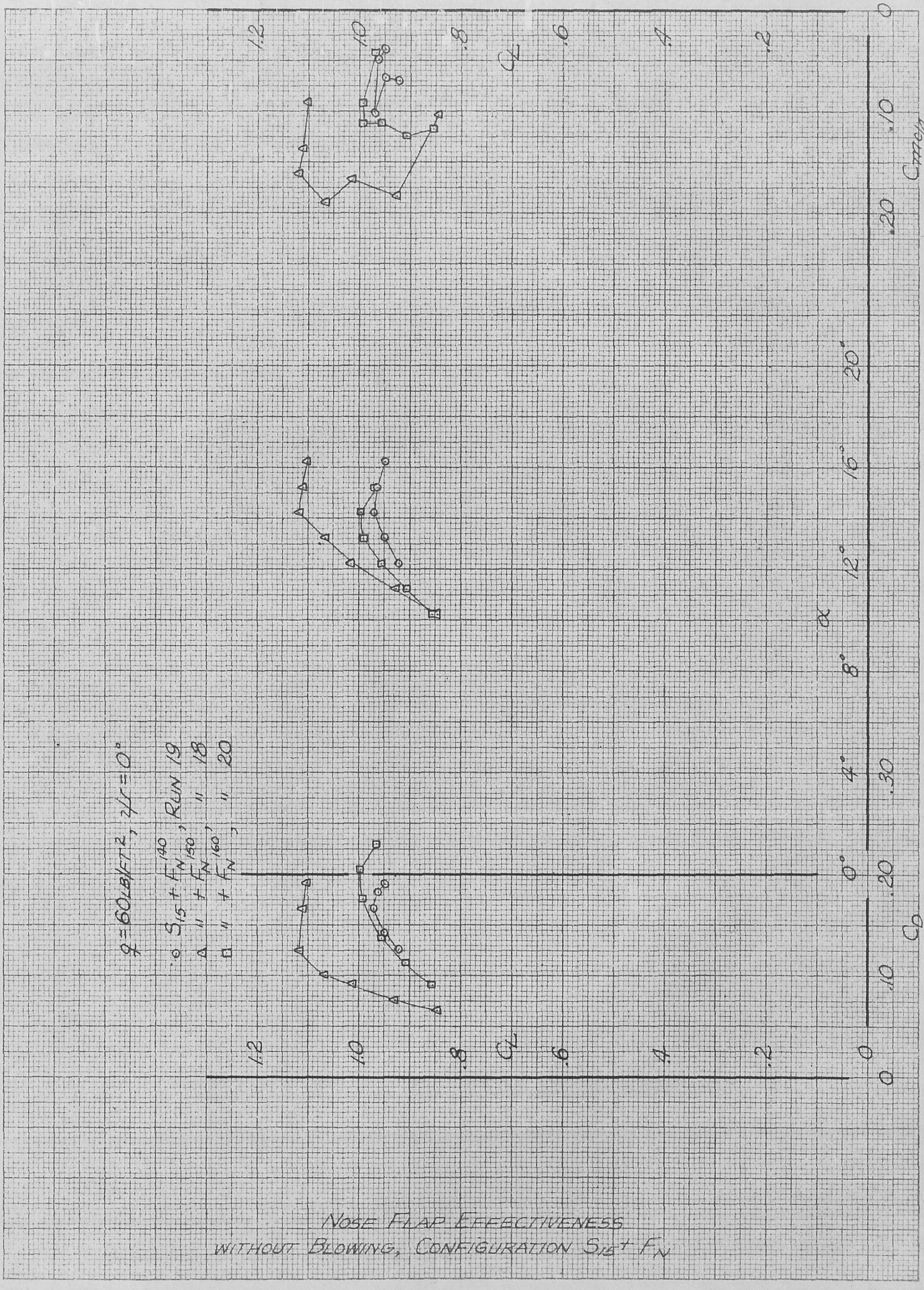


NOSE FLAP EFFECTIVENESS
WITHOUT BLOWING, CONFIGURATION SLS + FN

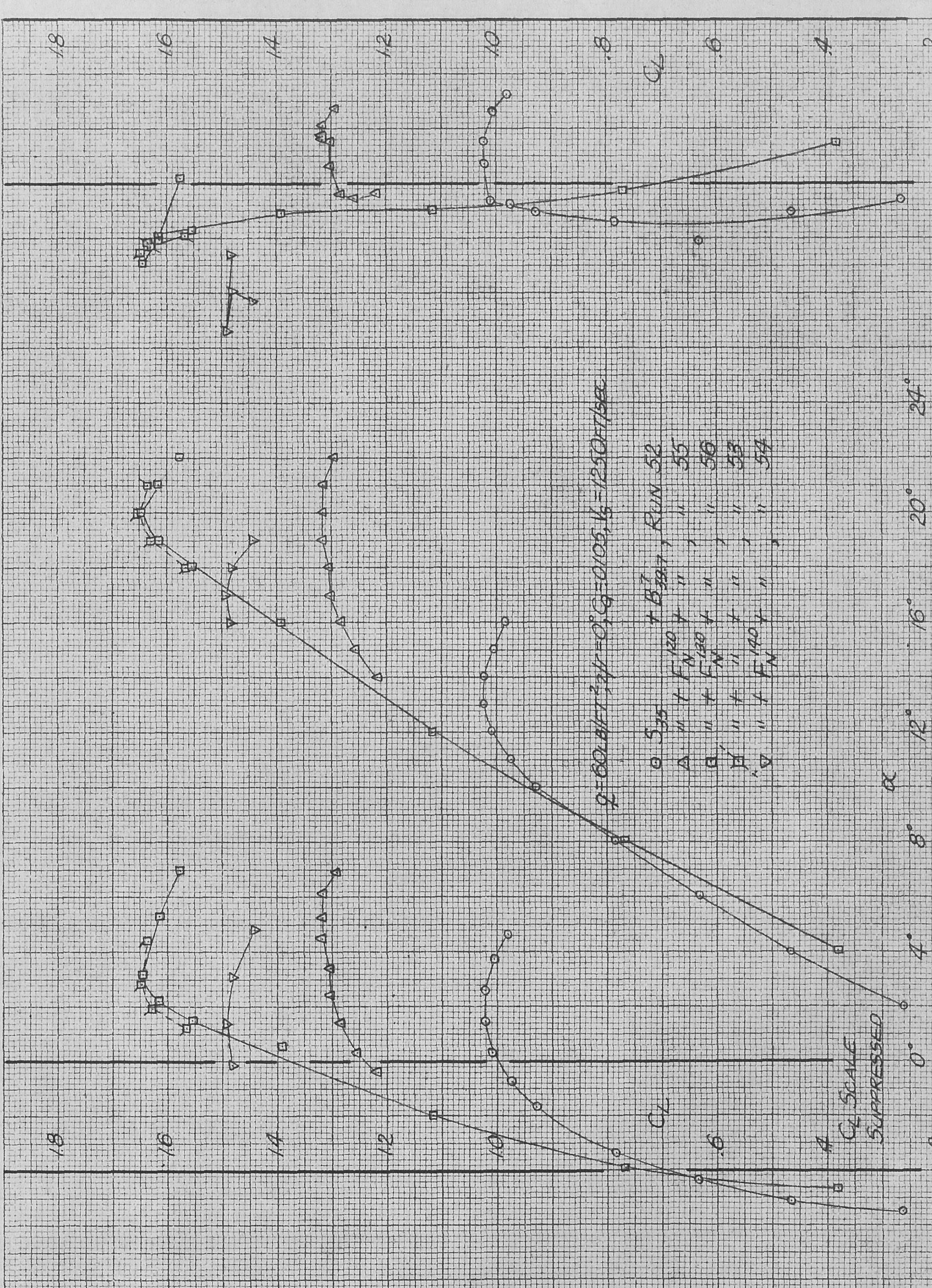


NOSE FLAP EFFECTIVENESS
WITH BLOWING, CONFIGURATION $S_{35}+F_N+B$

SPLIT FLAP EFFECTIVENESS
WITHOUT BLOWING CONFIGURATION $S_{15}+F_5$

PAGE 64
FIG. 38

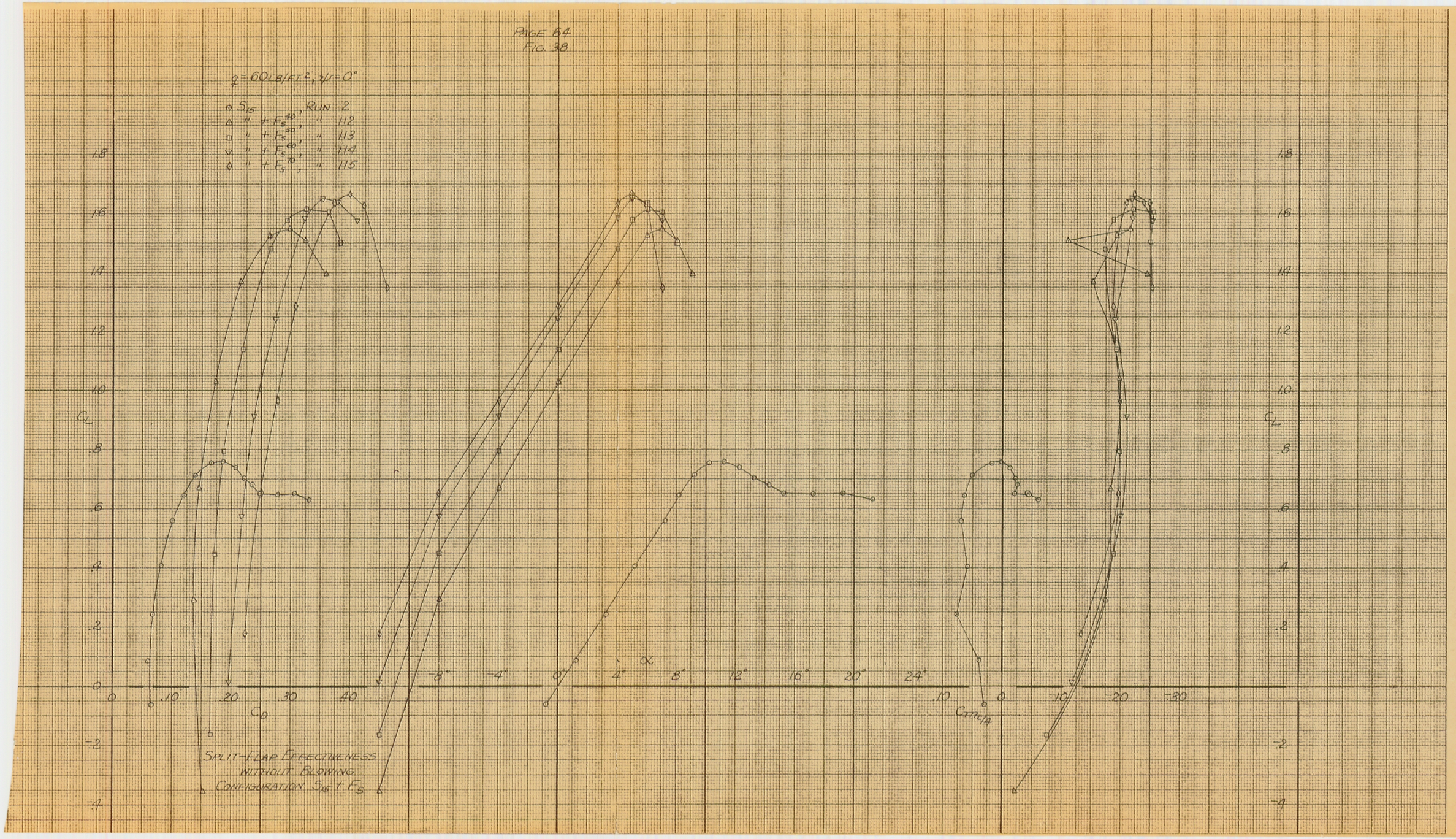


UNIVERSITY OF MINNESOTA
AERONAUTICAL ENGINEERING
SECTION

Burn-jw

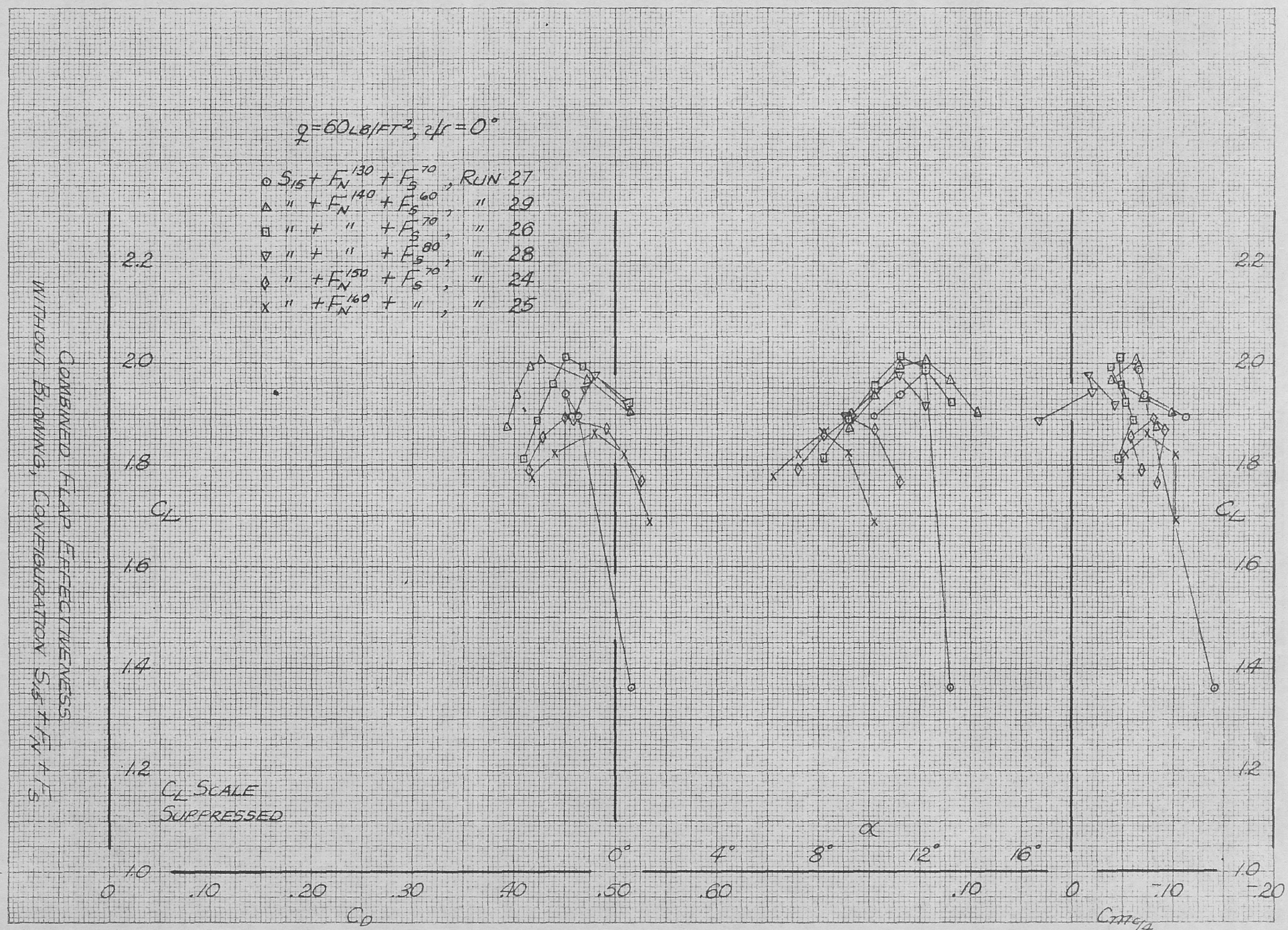
COMBINED FLAP EFFECTIVENESS
WITHOUT BLOWING, CONFIGURATION $S_{15}+F_N+F_S$
$q = 60$ LB/FT$^2$, $i_t = 0°$
$S_{15}+F_N^{130}+F_S^{70}$, RUN 27
" $+F_N^{140}+F_S^{60}$, " 29
" $+$ " $+F_S^{70}$, " 26
" $+$ " $+F_S^{80}$, " 28
" $+F_N^{150}+F_S^{70}$, " 24
" $+F_N^{160}+$ " , " 25
$C_L$ SCALE SUPPRESSED
$C_L$
$C_D$
$\alpha$
$C_{m_{c/4}}$
2.2
2.0
1.8
1.6
1.4
1.2
1.0
0
.10
.20
.30
.40
.50
.60
0°
4°
8°
12°
16°
.10
0
-.10
-.20

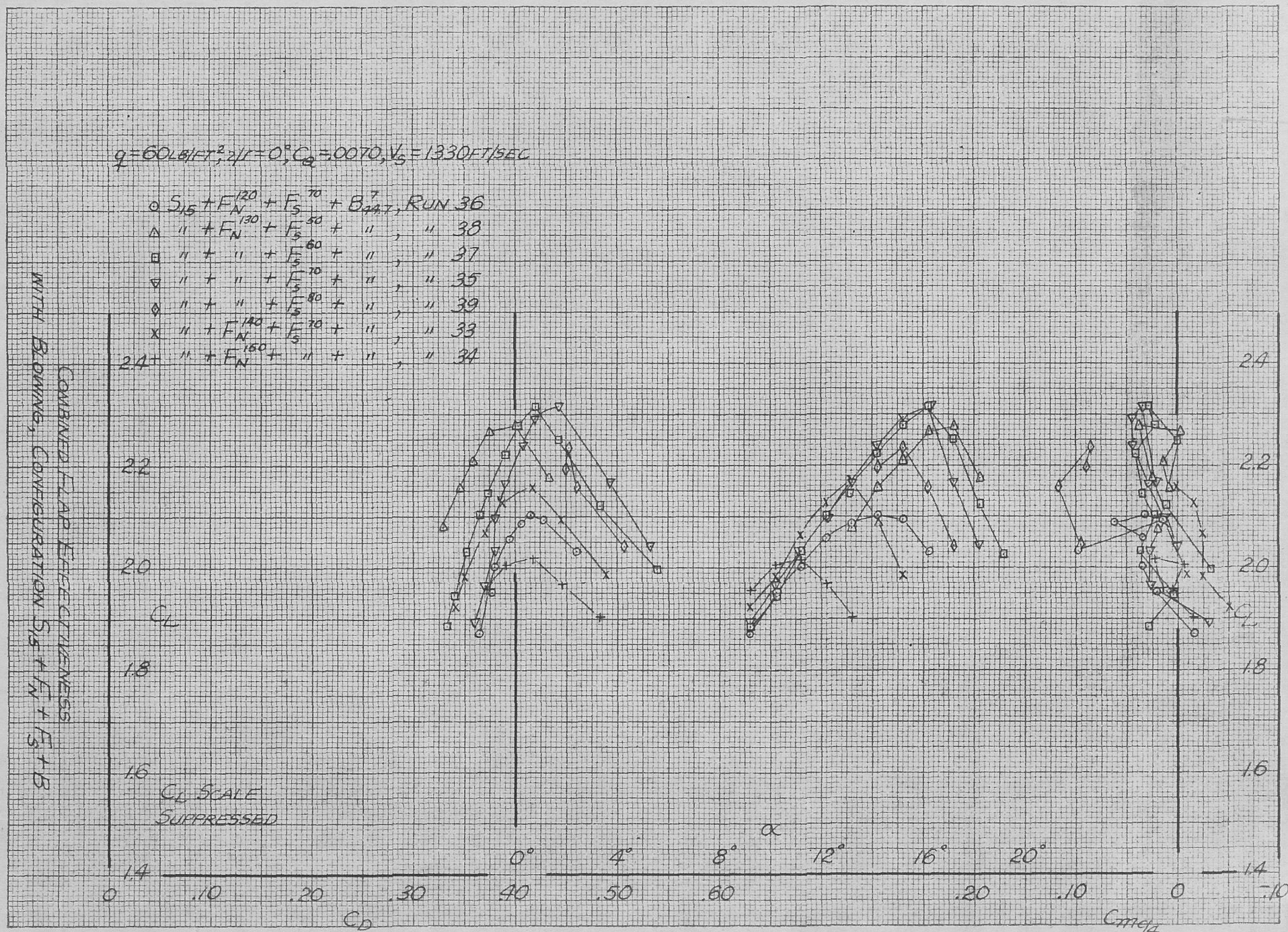
q = 60 LB/FT², a/f = 0°, C_Q = .0070, V_S = 1330 FT/SEC
⊙ S_15 + F_N^120 + F_S^70 + B_447, RUN 36
△ " + F_N^130 + F_S^60 + " , " 38
□ " + " + F_S^60 + " , " 37
▽ " + " + F_S^70 + " , " 35
◇ " + " + F_S^80 + " , " 39
× " + F_N^140 + F_S^70 + " , " 33
+ " + F_N^150 + " + " , " 34
COMBINED FLAP EFFECTIVENESS WITH BLOWING, CONFIGURATION S_15 + F_N + F_S + B
C_L
C_L SCALE SUPPRESSED
α
0° 4° 8° 12° 16° 20°
2.4 2.2 2.0 1.8 1.6 1.4
0 .10 .20 .30 .40 .50 .60
C_D
.20 .10 0 -.10
C_m/4

$q$ 60 lbs/ft² $T_j$ 540° $C_\mu$ 0105 $V_j$ 1250

○ $S_{35} + F_E^{70} + B_{70}^{7}$ RUN 61
△ " $+ F_N^{110}$ + " + " " " 57
□ " $+ F_N^{130}$ + " + " " " 60
▽ " + " + " + " " " 58
◇ " $+ F_N^{150}$ + " + " " " 59

$C_L$

$C_D$

$\alpha$

$C_{DT+A}$

Buccaneer

COMBINED FLAP EFFECTIVENESS
WITH BLOWING, CONFIGURATION $S_{35} + F_N + F_E + B$

PAGE 58
FIG. 42

$\delta_f = 0°$

○ $\delta_{LE}$ $q = 60$ LB/FT², RUN 2
△ " $+F_N^{150}$ " " 102
□ " $+F_N^{140} + B_{447}^{7}$, $q = 80$ LB/FT², $C_D = .0090$, $V_0 = 1830$ FT/SEC. " 103

$C_L$

$C_D$

$\alpha$

$C_{PROFILE}$

NOSE FLAP BUILD-UP, CONFIGURATION $S_{15}$

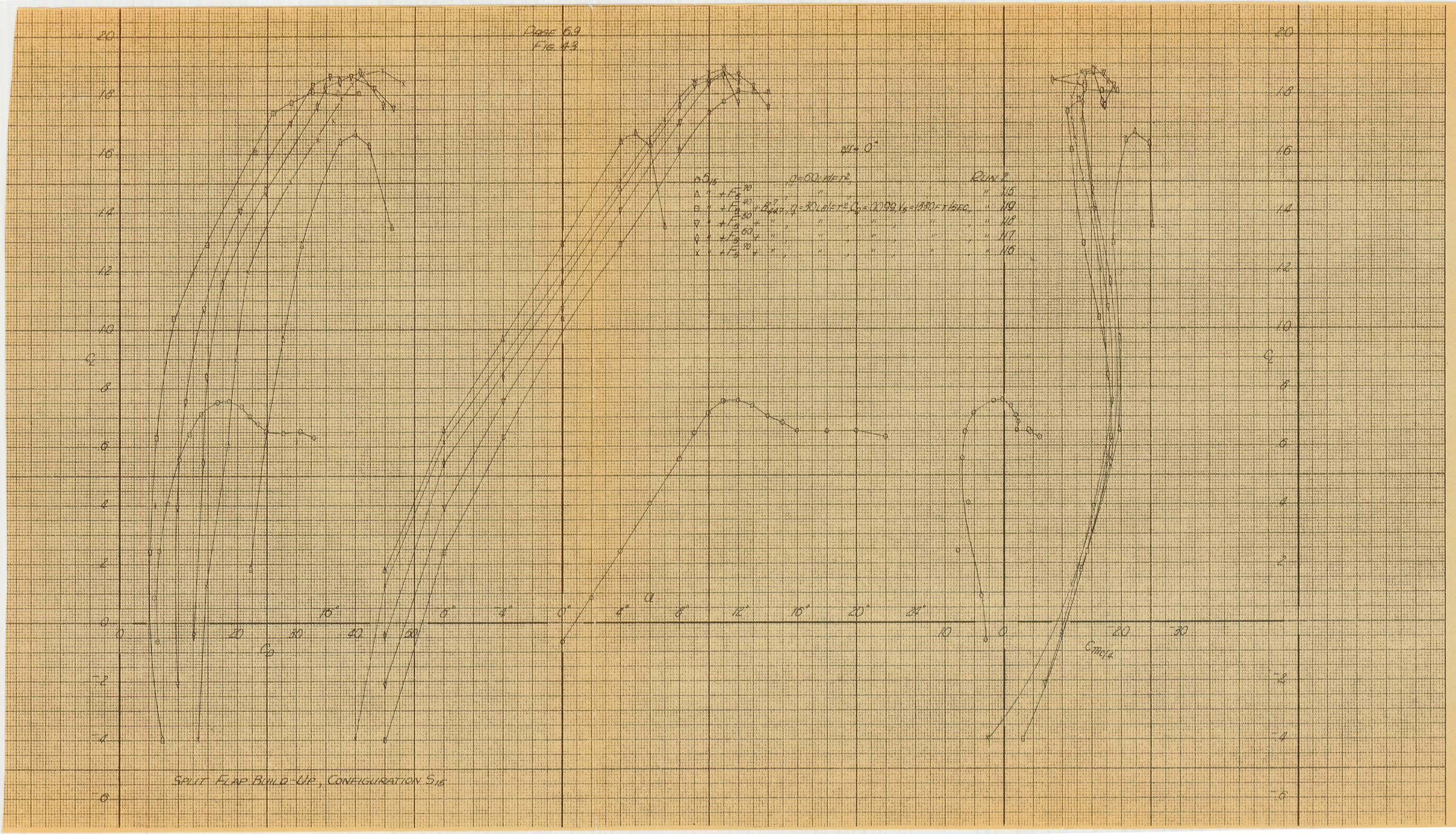


SPLIT FLAP BUILD-UP, CONFIGURATION $S_{16}$

CROSS SECTION MILLIMETER
CHARLES BRUNING COMPANY

Bacon jr

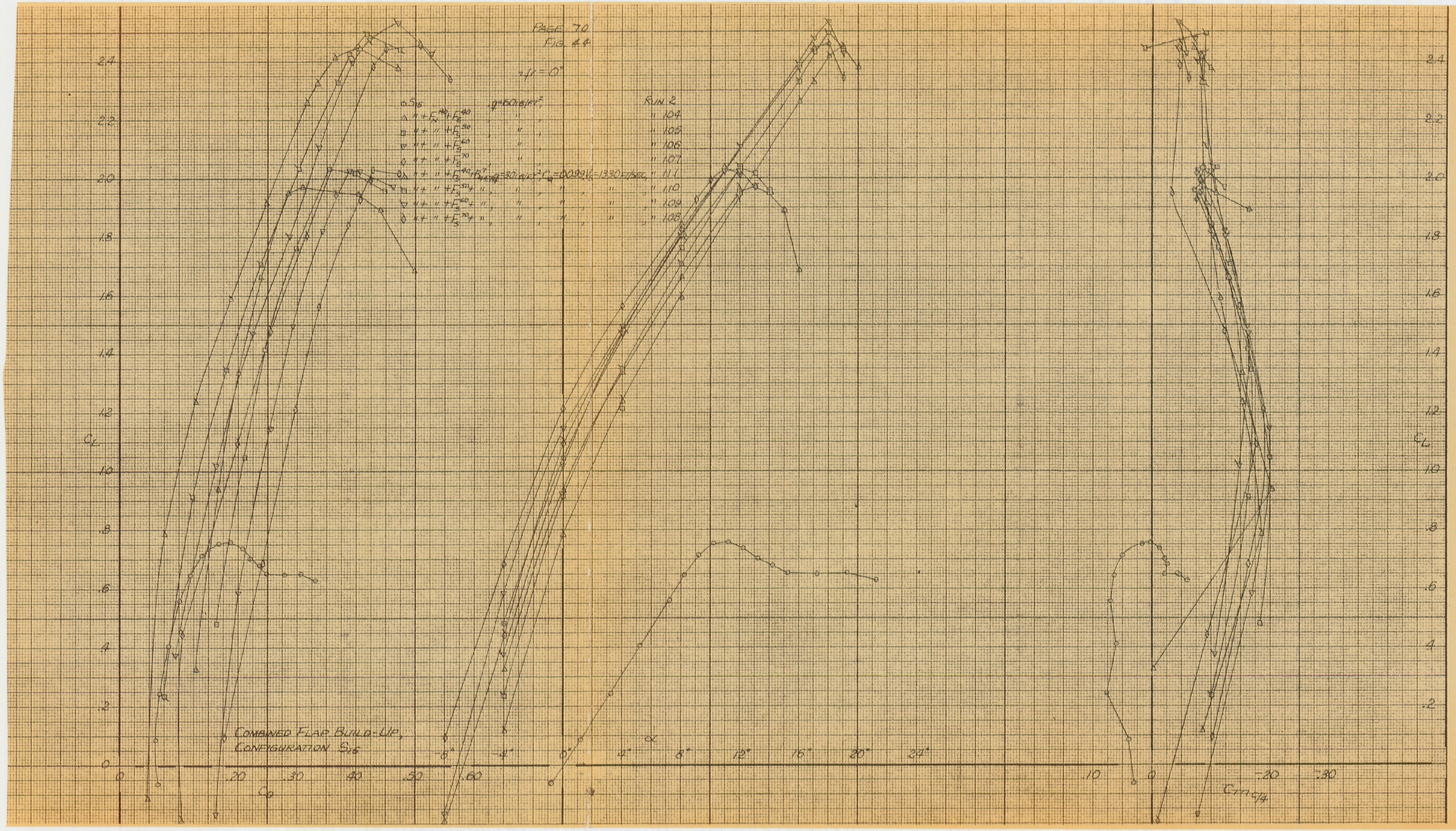
$i_t = 0°$
$q = 60.1 \text{ lb/ft}^2$
RUN 2
104
105
106
107
111
110
109
108
$R = 30.0 \times 10^6$
$C_q = .0099$
$V_t = 1330 \text{ FT/SEC}$
$C_L$
$C_D$
$\alpha$
$C_{m\,c/4}$
COMBINED FLAP BUILD-UP,
CONFIGURATION $S_{16}$

BELCOM_JVW

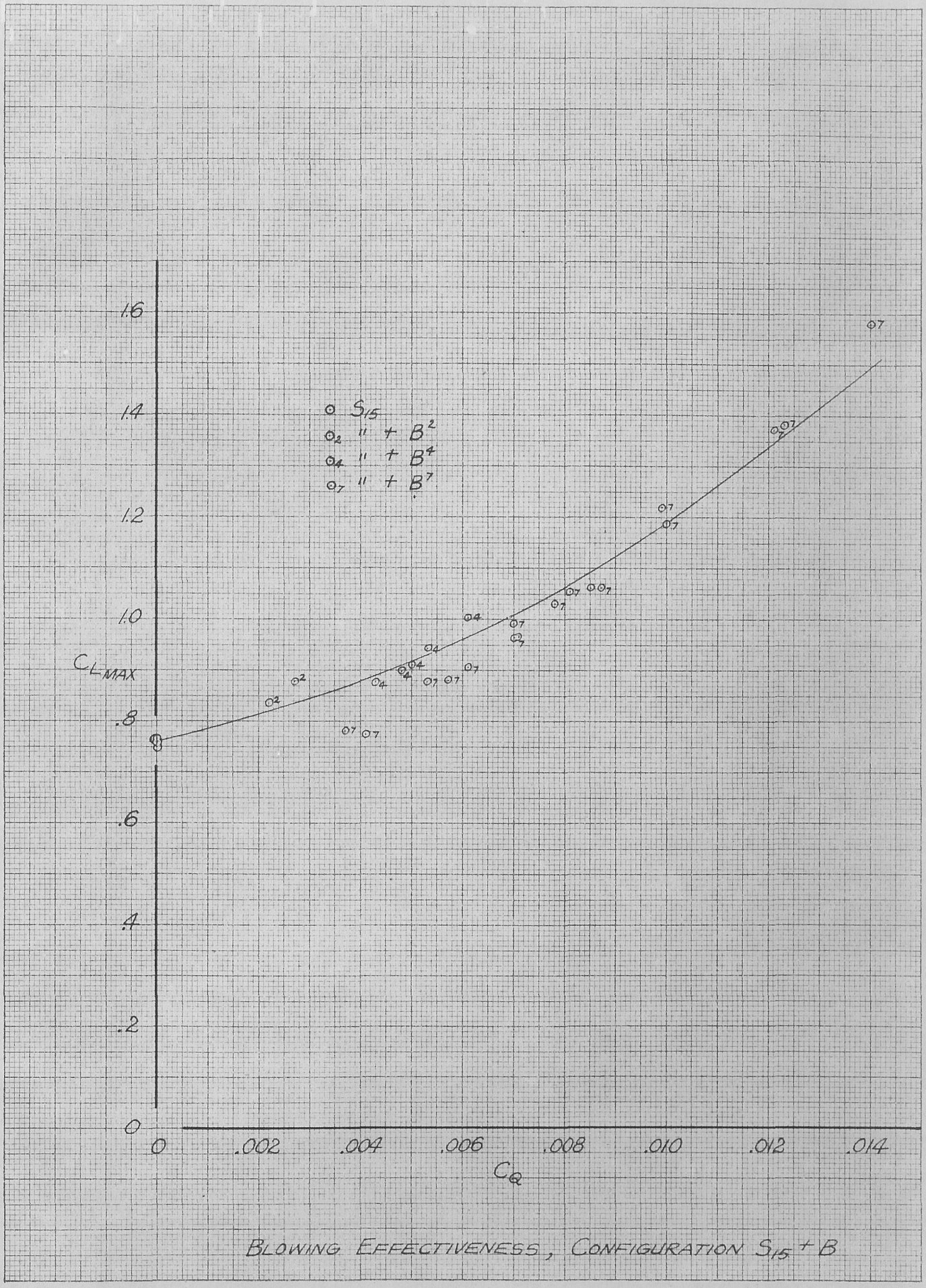


BLOWING EFFECTIVENESS, CONFIGURATION $S_{15}$ + B

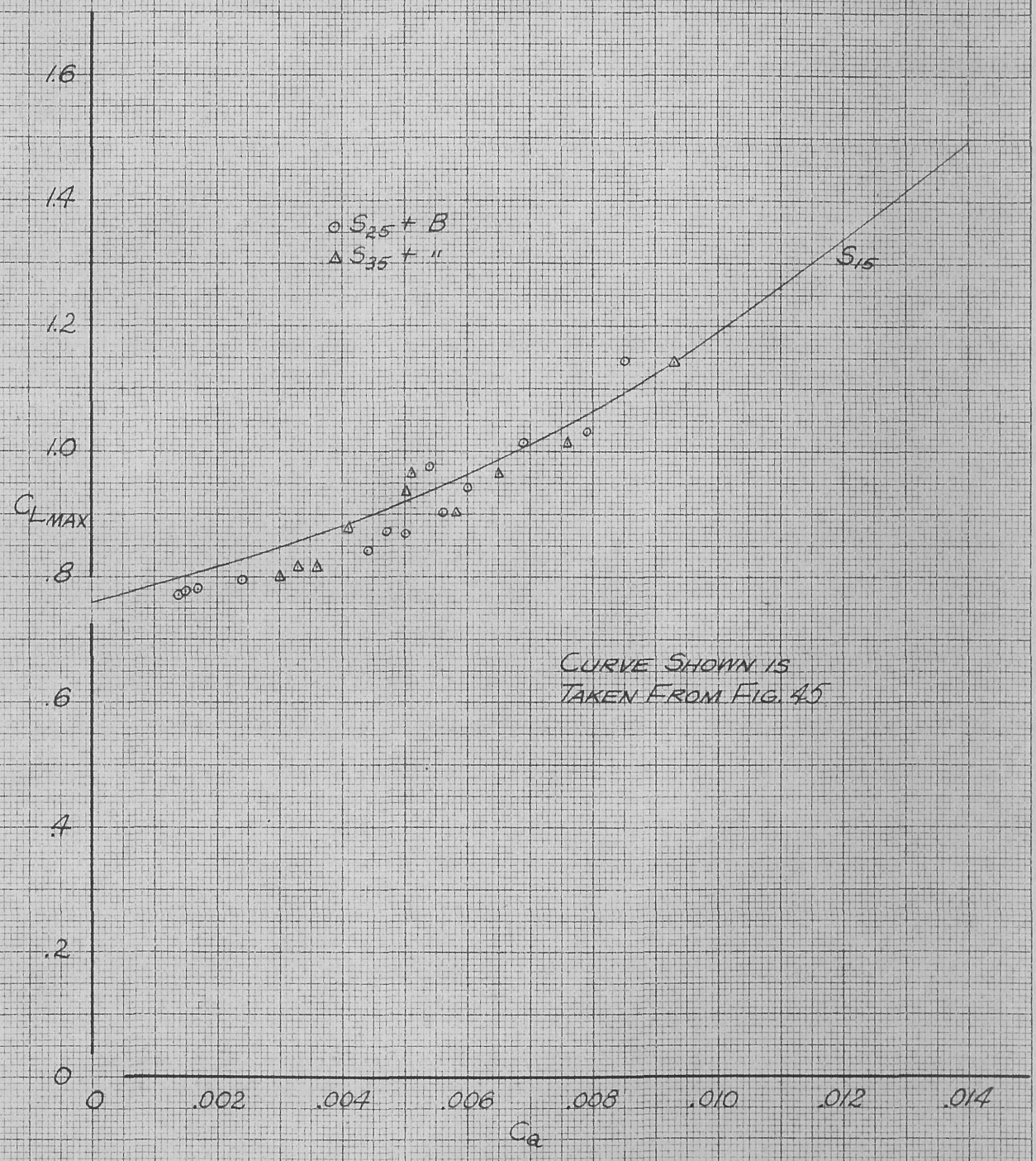


CURVE SHOWN IS TAKEN FROM FIG. 45

BLOWING EFFECTIVENESS, CONFIGURATION $S_{25}$ AND $_{35}$ + B

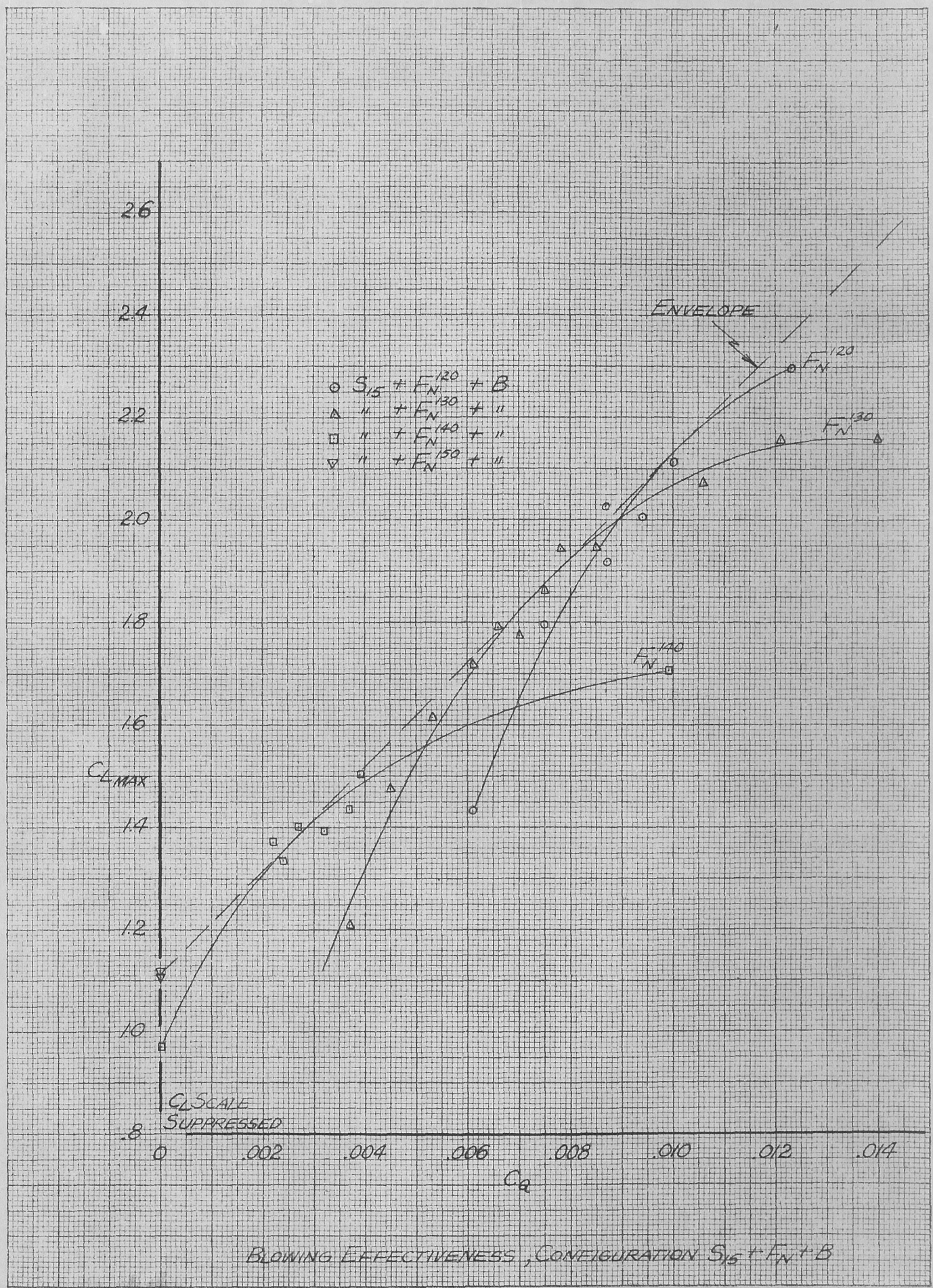


BLOWING EFFECTIVENESS, CONFIGURATION $S_{15} + F_N + B$

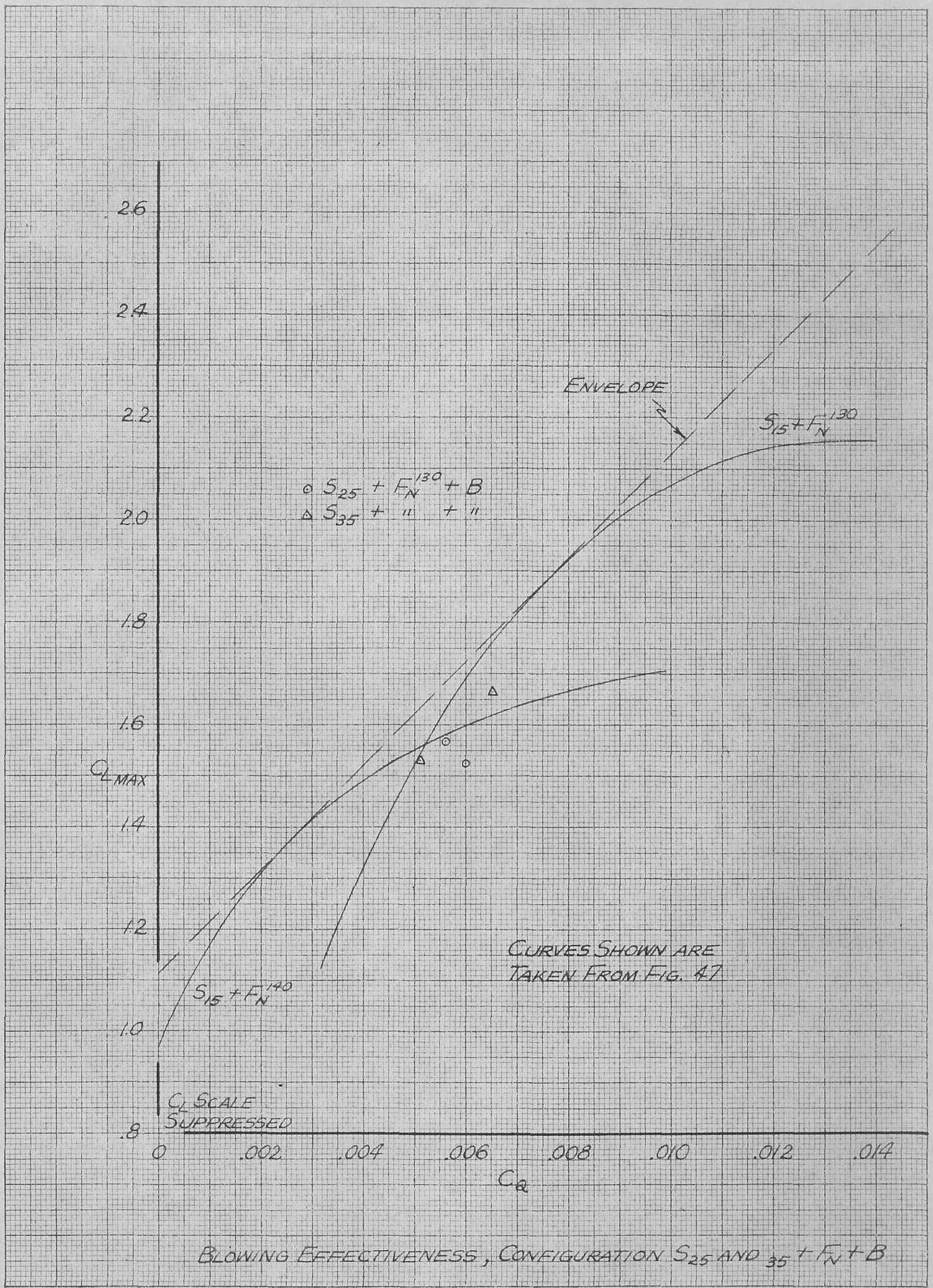


BLOWING EFFECTIVENESS, CONFIGURATION $S_{25}$ AND $_{35}+F_N+B$

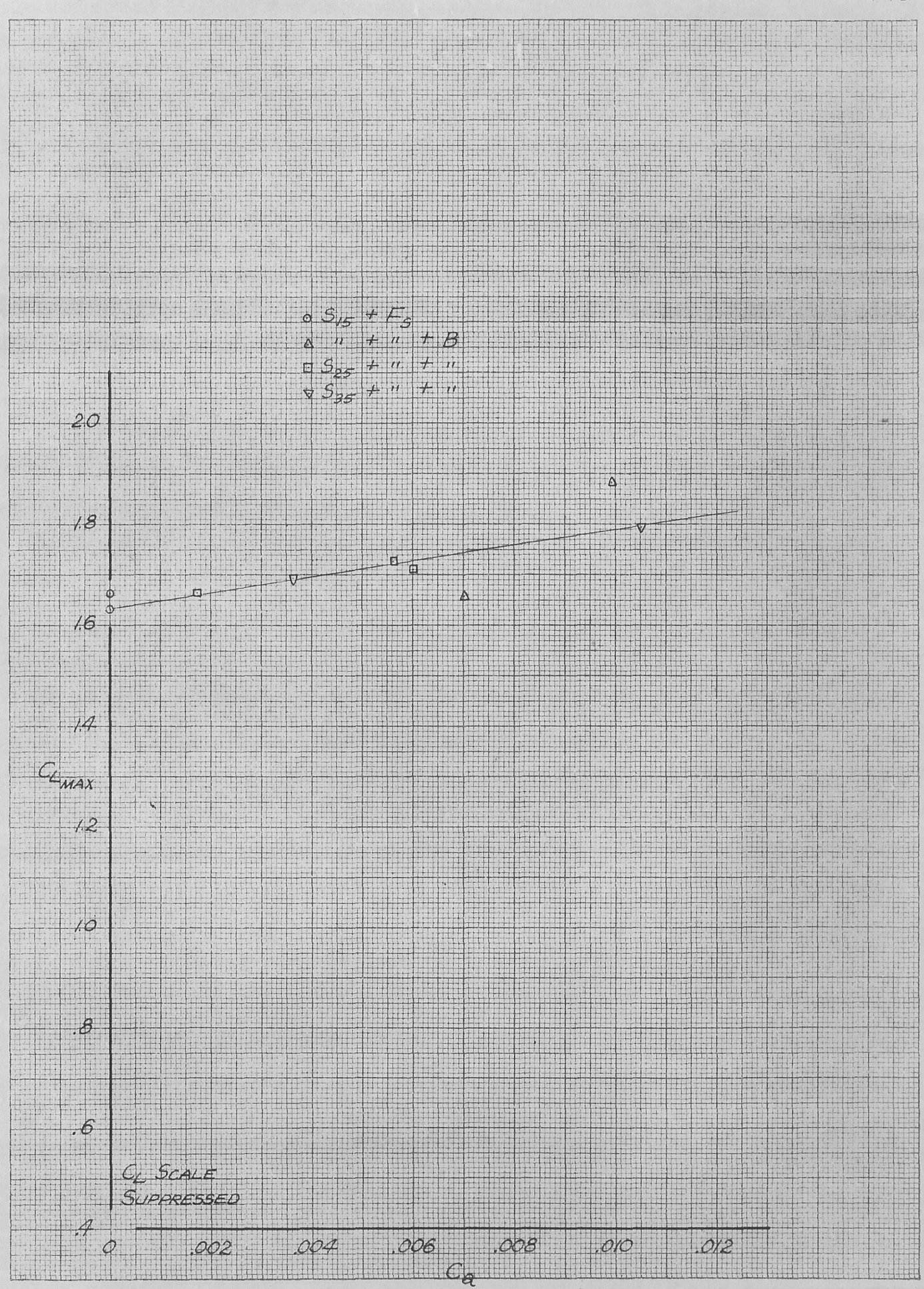


BLOWING EFFECTIVENESS, CONFIGURATION $S+F_S+B$

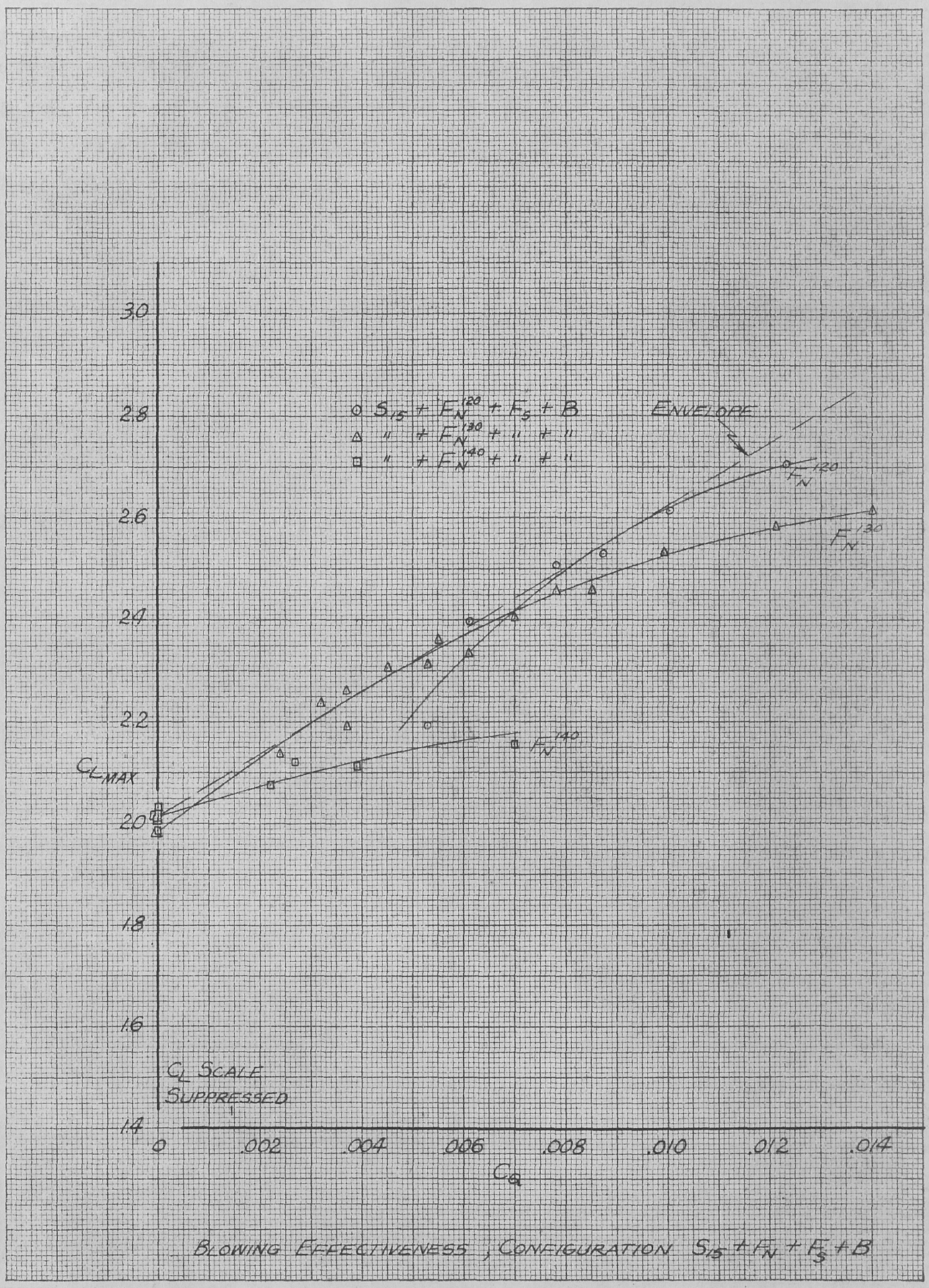


BLOWING EFFECTIVENESS, CONFIGURATION $S_{15} + F_N + F_S + B$

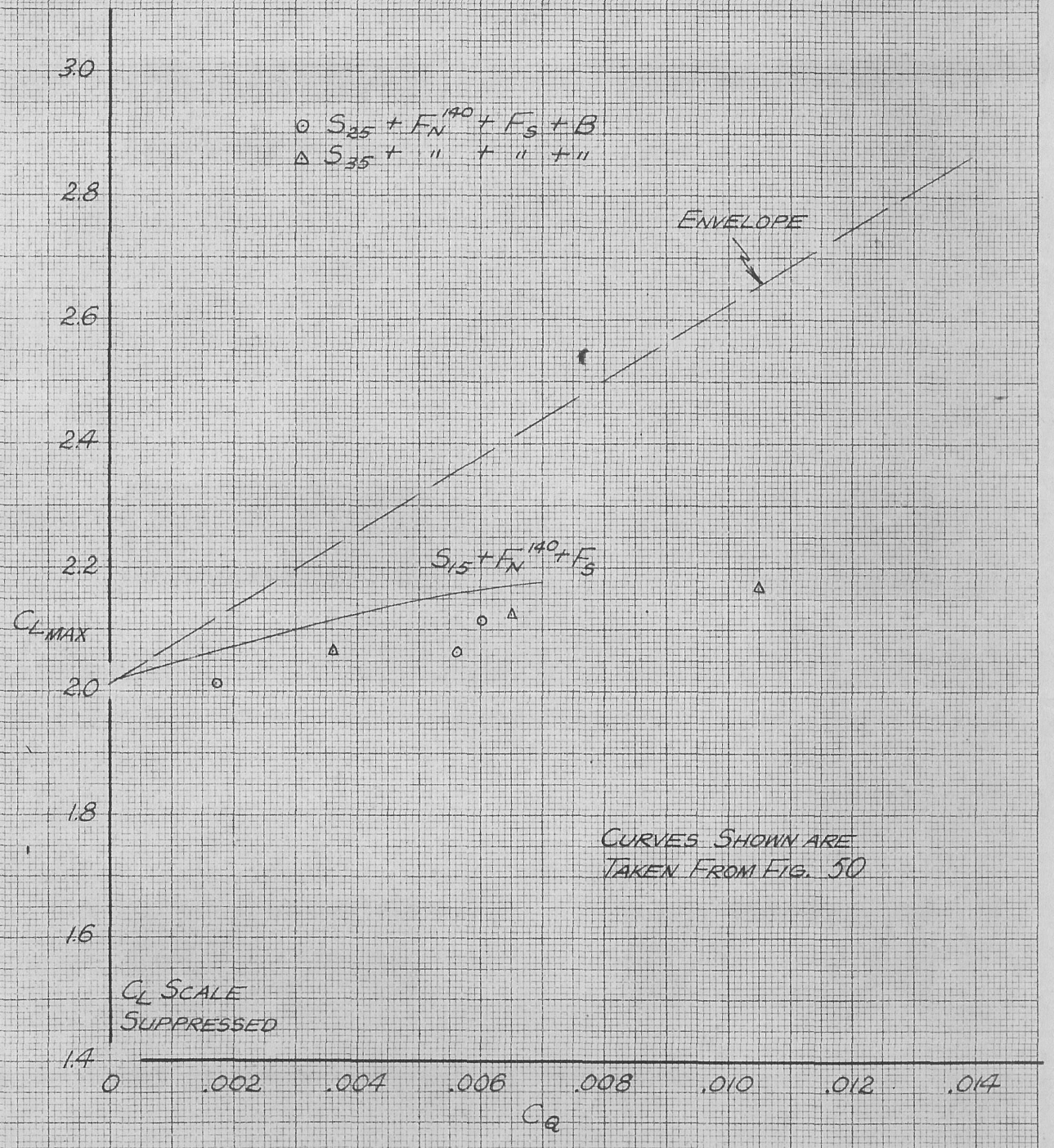


BLOWING EFFECTIVENESS, CONFIGURATION $S_{25}$ AND $_{35} + F_N + F_S + B$

INDEX OF FIGURES (Cont'd)

Tuft Photographs, Configuration $S_{15}$ + Tufts

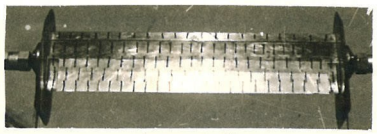

$\alpha_g = -4^\circ$

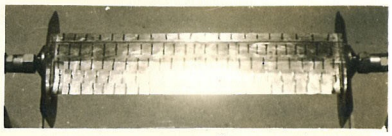

$\alpha_g = 0^\circ$

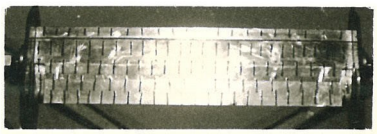

$\alpha_g = 4^\circ$

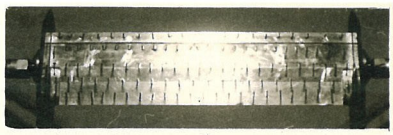

$\alpha_g = 8^\circ$

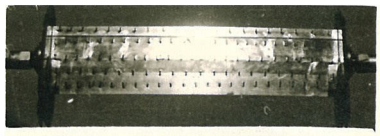

$\alpha_g = 12^\circ$

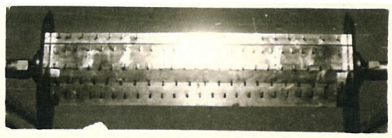

$\alpha_g = 13^\circ$

INDEX OF FIGURES (Cont'd)

Tuft Photographs, Configuration $S_{15}$ + B + Tufts

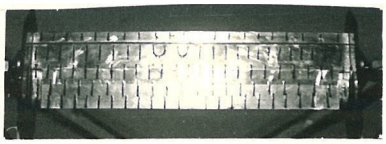

$\alpha_g = 4^\circ$

$\alpha_g = 8^\circ$

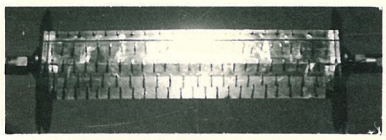

$\alpha_g = 12^\circ$

$\alpha_g = 14^\circ$

$\alpha_g = 15^\circ$

$\alpha_g = 16^\circ$

INDEX OF FIGURES (Cont'd)

Tuft Photographs, Configuration $S_{15} + F_N^{150} +$ Tufts

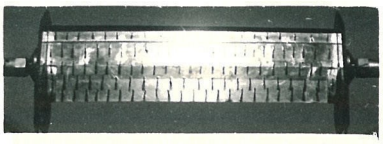

$\alpha_g = 12°$

$\alpha_g = 13°$

$\alpha_g = 14°$

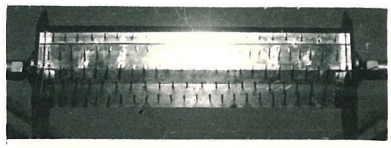

$\alpha_g = 15°$

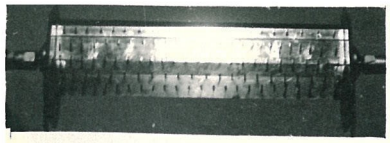

$\alpha_g = 16°$

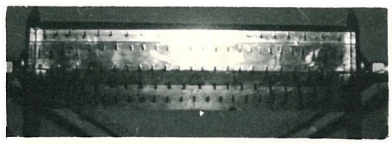

$\alpha_g = 17°$

INDEX OF FIGURES (Cont'd)

Tuft Photographs, Configuration $S_{15} + F_N^{120} + B + Tufts$

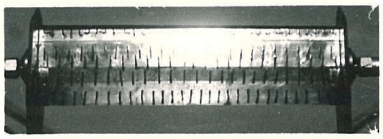

$\alpha_g = 18^\circ$

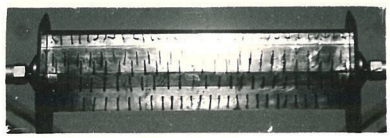

$\alpha_g = 20^\circ$

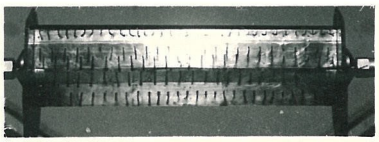

$\alpha_g = 22^\circ$

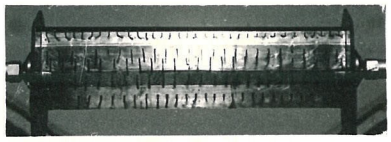

$\alpha_g = 24^\circ$

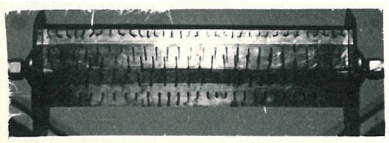

$\alpha_g = 26^\circ$

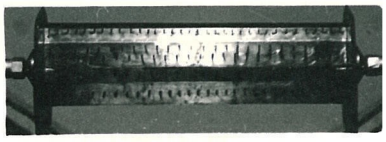

$\alpha_g = 28^\circ$

INDEX OF FIGURES (Cont'd)

Tuft Photographs, Configuration $S_{15} + F_S^{70} +$ Tufts

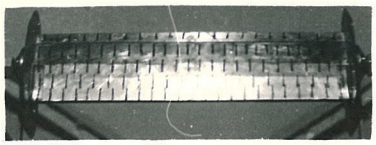

$\alpha_g = -4^\circ$

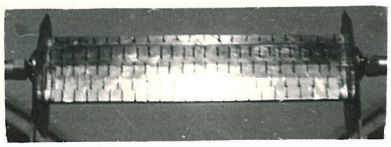

$\alpha_g = 0^\circ$

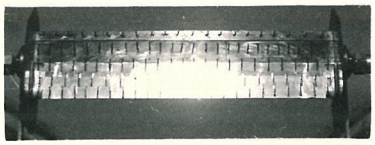

$\alpha_g = 4^\circ$

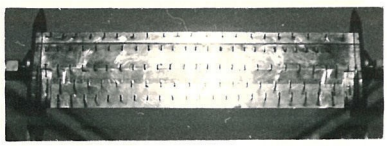

$\alpha_g = 5^\circ$

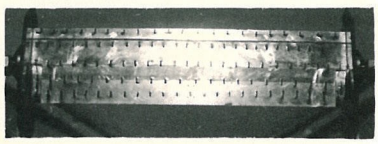

$\alpha_g = 6^\circ$

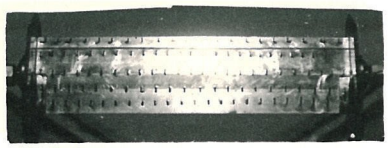

$\alpha_g = 7^\circ$

INDEX OF FIGURES (Cont'd)

Tuft Photographs, Configuration $S_{15} + F_S^{70} + B + Tufts$

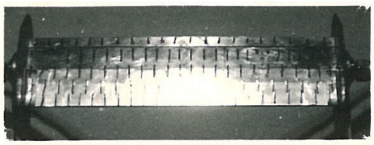

$\alpha_g = -4^\circ$

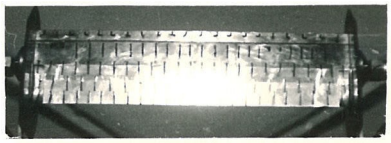

$\alpha_g = 0^\circ$

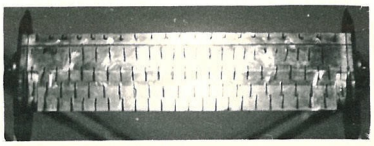

$\alpha_g = 4^\circ$

$\alpha_g = 6^\circ$

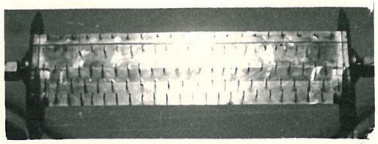

$\alpha_g = 8^\circ$

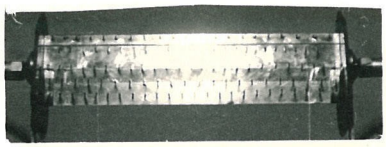

$\alpha_g = 10^\circ$

INDEX OF FIGURES (Cont'd)

Tuft Photographs, Configuration $S_{15} + F_N^{140} + F_S^{70} + \text{Tufts}$

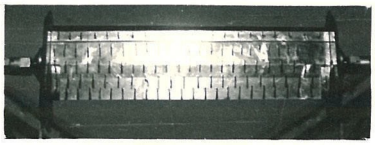

$\alpha_g = 8^\circ$

$\alpha_g = 12^\circ$

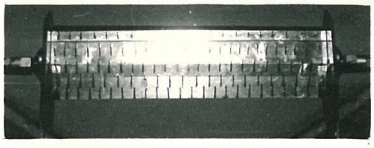

$\alpha_g = 10^\circ$

$\alpha_g = 12^\circ$

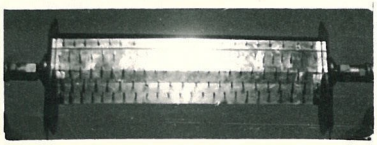

$\alpha_g = 13^\circ$

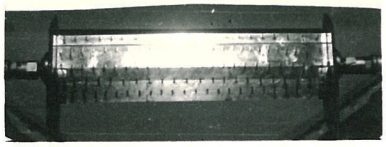

$\alpha_g = 14^\circ$

INDEX OF FIGURES (Cont'd)

Tuft Photographs, Configuration $S_{15} + F_N^{120} + F_S^{60} + B + Tufts$

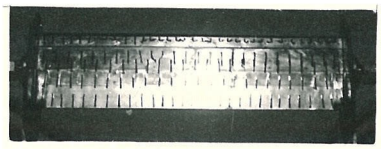

$\alpha_g = 4^\circ$

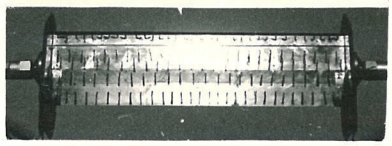

$\alpha_g = 16^\circ$

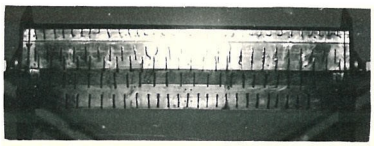

$\alpha_g = 17^\circ$

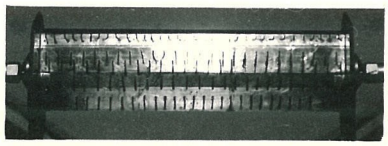

$\alpha_g = 20^\circ$

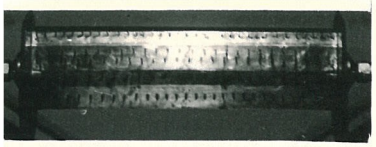

$\alpha_g = 22^\circ$

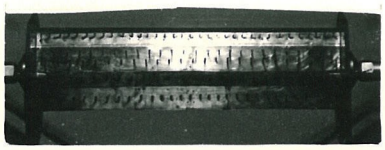

$\alpha_g = 24^\circ$

INDEX OF FIGURES (Cont'd)

Model Photos

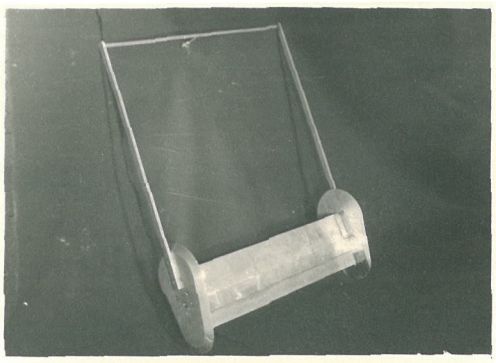

Photo 1. Top View Showing Model

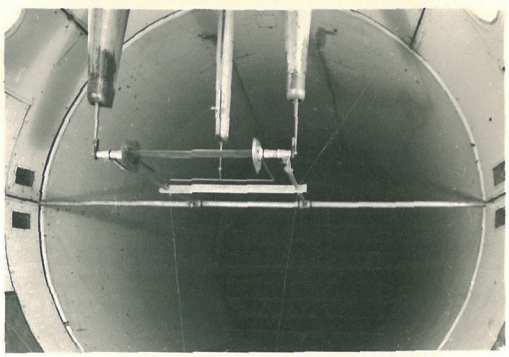

Photo 2. Front View Showing Model Mounted in Tunnel

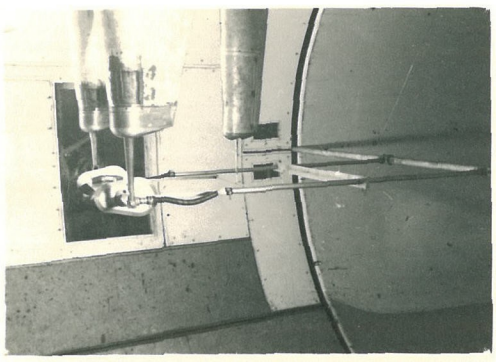

Photo 3. Side View Showing Model Mounted in Tunnel

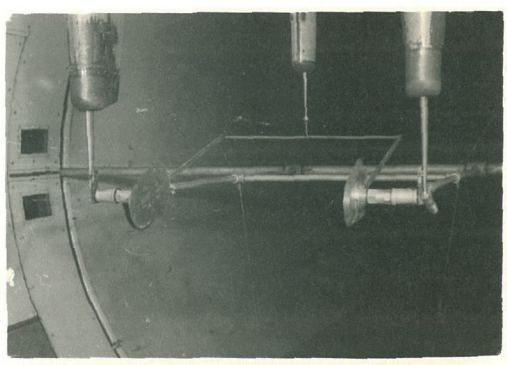

Photo 4. Front View Showing End Plates and Tail Sting with Wing Removed

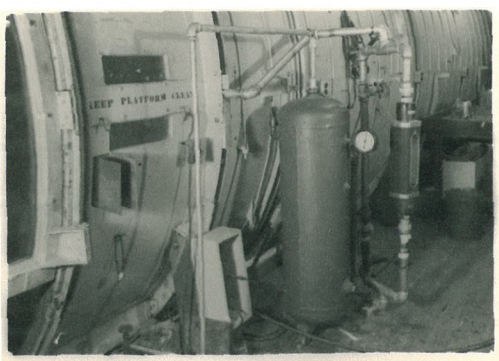

Photo 5. Front View Showing Air Supply Outside Tunnel

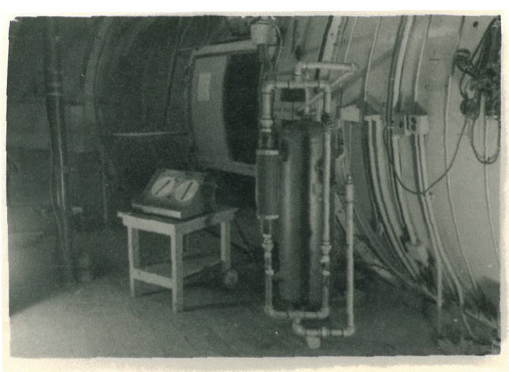

Photo 6. Rear View Showing Air Supply Outside Tunnel